November 2023

Examining paleoshorelines in the eastern Gulf of Mexico: Insights on sea level history and potential areas of interest for habitat management

Catalina Rubiano
University of South Florida

Examining Paleoshorelines in the Eastern Gulf of Mexico: Insights on Sea Level History and Potential Areas of Interest for Habitat Management

by

Catalina Rubiano

A thesis submitted in partial fulfillment
of the requirements for the degree of
Master of Science
with a concentration in Hydrography
College of Marine Science
University of South Florida

Co-Major Professor: Alastair G.C. Graham, Ph.D.
Co-Major Professor: David F. Naar, Ph.D.
Cheryl J. Hapke, Ph.D.

Date of Approval:
November 3, 2023

Keywords: seafloor geomorphology, multibeam bathymetry, mesophotic coral ecosystems, West Florida Shelf

DEDICATION

This work is dedicated to members of the LGBTQ+ community who have been made to feel less deserving or worthy than others. You are enough just as you are and are capable of anything you set your mind to. Just because others may not see how your story fits in doesn’t mean we can’t teach them.

ACKNOWLEDGMENTS

This research was made possible thanks to funding from the Bridge to the Doctorate Endowed Fellowship, the Sanibel-Captiva Shell Club/Mary & Al Bridell Memorial Fellowship, and NOAA's five-year, $9 million cooperative agreement with the Center for Ocean Mapping and Innovative Technologies (COMIT) at USF.

My personal thanks go first and foremost to my advisor, Dr. Ali Graham, who provided me with the utmost kindness and support throughout my graduate school experience. He gave me encouragement when I needed it most, and I would not be where I am now without his guidance and support. Big thanks also to everyone in COMIT who has helped me along the way – in particular, Matt Hommeyer for his help on endless technical questions and software troubleshooting, and Sherryl Gilbert for her mastery of organizational matters and her moral support and encouragement throughout.

Training and field experience in seafloor mapping would not have been possible without the support of the Florida Institute of Oceanography along with the Captains and crews of the *R/V Weatherbird II,* the *R/V Hogarth,* and the *R/V Western Flyer*. Also, fantastic at sea experience was gained with NOAA Ocean Exploration onboard the *Okeanos Explorer*, with the Alfred Wegner Institute for Polar and Marine Research onboard the *R/V Polarstern,* and with Ocean Exploration Trust onboard the *E/V Nautilus*. I thank all captains, crew, and shipmates that I sailed with for imparting their knowledge upon me and creating such incredible memories along the way.

Finally, thank you from the bottom of my heart to my family, my friends, and my partner who have been right next to me through this whole journey and who have supported me unconditionally. I love you all!

TABLE OF CONTENTS

LIST OF TABLES

LIST OF FIGURES

LIST OF ABBREVIATIONS

Abbreviations	Definitions
m	Meters
Ma	Million years
ka	Thousand years
MIS	Marine Isotope Stage
LGM	Last Glacial Maximum
SLR	Sea level rise
MWP	Meltwater pulse
WFS	West Florida shelf
MCE	Mesophotic coral ecosystem
FCMaP	Florida Coastal Mapping Program

ABSTRACT

An inventory of multibeam bathymetry containing relict drowned and lithified paleoshorelines has been compiled and analyzed in the first ever shelf-wide investigation of paleo sea level indicators on the west Florida shelf (WFS). On the largest scale, the WFS is a wide and gently sloping terrain that is characterized by a carbonate-rich sediment regime. This framework coupled with the region's tectonic stability provided a setting in which sea level changes since ~ 20 ka have been recorded to a remarkable degree of resolution in the form of paleoshorelines which formed at sea level and were subsequently drowned and preserved in place. Previously described geophysical datasets along with new unpublished datasets were compiled and analyzed in a suite of geoinformatic softwares (ArcGIS, Fledermaus, Qimera) to obtain information about the depth, geomorphology, and dispersal of paleoshoreline features. In total, 27 paleoshorelines were identified and classified based on geomorphic identifiers, and a hypothetical scenario for sea level history between 14.3 ka – 11.0 ka is put forth. Additionally, recommendations and basemaps have been laid forth regarding deep light-dependent mesophotic coral ecosystems which have been documented on the lithified ridges formed by paleoshorelines and drowned reefs across the Gulf of Mexico, particularly on the WFS between -45 to -90 m. The overarching conclusion of this work is the need for continued high-resolution mapping on the WFS in the interest of paleoclimatological, geological, hydrographical, and ecological research.

CHAPTER ONE:

INTRODUCTION

1.1 Sea Level Change and How to Measure it

Since 3 Ma, sea level has been as much as ~ 150 meters (m) apart from present levels (Fig. 1; Miller et al. 2020). Following the onset of glaciation in both the northern and southern hemispheres ~ 2.7 Ma, the Earth has cycled between glacial and interglacial periods in which the oscillation of ice sheets exerted major control on global sea levels. The most notable drop in sea level resulting from glacial expansion occurred 26-19 ka during marine isotope stage (MIS) 2, which marks the culmination of the Last Glacial Maximum (LGM). MIS 2 was preceded by incrementally decreasing low stands (~ -110 m) as a result of glaciations at ~300-130 ka (MIS 8-6), 460-380 ka (MIS 12, Railsback et al., 2015) and (~ -90 m) 600 ka (MIS 16, Bendixen et al., 2018).

Additional causes of sea level variation include fluctuation in ocean basin volume caused by changes in rate of seafloor spreading (Donoghue, 2011), and to a lesser degree, thermal expansion and contraction of the ocean (Lambeck et al., 2014). In recent decades, global eustatic sea level has been rising at an increasing rate due to accelerating melt of land-based glaciers and the polar ice sheets, in Greenland and Antarctica. The cause of this is widely attributed to rapid climate and ocean warming caused by anthropogenic fossil fuel combustion beginning in the late 19th Century which has been sustained and increased through to the modern-day (Roe et al., 2021). Coupled with climate and ice-sheet variations, sea level variability, on decadal to multimillennial timeframes, is one of the major drivers of paleogeomorphic change, and a critical environmental and societal stressor today (Hinkel et al., 2018).

Approximately 25,000 years ago, the Laurentide ice sheet occupied much of the North American continent as the most recent glacial period reached its maximum extent (Gowan et al., 2021). At the same time, continental ice covered large parts of NW Europe and high-latitude Eurasia, and Antarctica and Greenland witnessed major expansions onto adjacent continental shelves (Larter et al., 2014). The amount of water 'locked away' from the sea in Earth's ice sheets was so great that sea level in the Gulf of Mexico stood ~ 120 meters (and globally ~ 125-135 m; Pan et al., 2022) lower than today with the Pleistocene shoreline breaking near the edge of the continental shelf (Fig. 2; Donoghue, 2011). As the glaciers melted over the next 20,000 years, sea levels around the world slowly rose to modern levels, but not at a steady rate (Fig. 1). Previous work has highlighted between one and three periods of accelerated rates of sea level rise (SLR), referred to as meltwater pulses (MWP). Originally identified in reef-drowning events and coral records from the Caribbean-Atlantic (Blanchon and Shaw, 1995) the MWPs are reflected in sea level curves as steep jumps punctuated by occasional slowdowns (Leventer et al., 1982; Fairbanks, 1989; Lambeck et al., 2014; Donoghue, 2011; Joy, 2019). A general timeline of hypothesized meltwater pulses is as follows: at ~ 14.5 ka, sea level rose 24 meters in about 500 years during MWP-1A; from approximately 12.9 to 11.6 ka sea level rise slowed down during the Younger Dryas cool period, which put a pause to the warming that was occurring in the Northern Hemisphere during the broader deglaciation; warming resumed and at ~ 11.2 ka sea level rose 20 meters in about 400 years during MWP-1B; and finally, a smaller MWP-1C is hypothesized to have occurred at around 8 ka where sea level rose 10 meters in about 800 years (Donoghue, 2011; Lambeck et al., 2014; Joy, 2019).

The precise timing and sources of meltwater pulses remains contentious due to uncertainties around ice sheet dynamics, the physical response of oceans to the changing gravitational signature of the cryosphere, as well as the accuracy of sea level proxies that record the timing of these events, such as the oxygen isotope record (Shackleton, 1978; Clark et al., 2002; Lambeck et al., 2014; Joy, 2019). To address these uncertainties, many studies have attempted to improve past sea level estimates by fine-tuning interpretations of oxygen isotope records from corals and sediment cores (e.g., Fairbanks, 1989; Chappell et al., 1996), as well as looking at more direct evidence of recent sea level stands such as submerged coastal transgressional features. These tangible landform signatures can include reef terraces, beachrock outcrops, dunes and barrier islands (Passos et al., 2019). At a fast enough rate of sea level rise, it is believed that these depositional features can be overstepped and preserved without significant alteration leaving behind an intact sea level marker in the geomorphic record (Donoghue, 2011).

Shorelines submerged during deglaciation therefore have great potential to record sea level transgressions (and their rates), as well as coastal evolutionary processes at levels of detail (and scales) that are different than records from individual corals or core sites. On the west Florida shelf (WFS), drowned shoreline features have previously been identified and dated to periods of rapid sea level change during the last deglaciation (e.g., Gardner et al., 2007; Locker et al., 1996). However, a wider appreciation of how sea level change is reflected spatially and temporally on a carbonate shelf, and when, how, and why, sea level markers have been well-preserved on such a shelf, is lacking. By taking advantage of the region's relative tectonic stability, as a location of passive margin lithosphere unaffected by major glacial isostatic loading and flexure (Adams et al., 2010), coupled with the record of sea level stands recorded on the

WFS, it should be possible to resolve the Gulf of Mexico sea level history to a greater degree of accuracy than currently exists.

Joy (2019) who is cited herein as the most complete Gulf of Mexico sea level curve, studied regional sea level history in the interest of narrowing down depth zones of interest for marine archaeological studies. By identifying times of rapid sea level rise, it is possible to target depth zones in which the likelihood of preservation is high for archaeological sites and their associated sediments. According to their findings, Joy (2019) identified -100 to -70 m, -60 to -40 m, and -20 to -10 m as zones of high preservation potential due to periods of rapid sea level rise (following slow ones) that corresponded to these depths. Much like their application to archeology, these depth zones can be similarly utilized to target areas of the WFS that may contain preserved paleoshorelines. Previous studies (Locker et al., 1996; Jarrett et al., 2005; Gardner et al., 2005; 2007) have identified paleoshorelines at these depths, and existing bathymetry appears to indicate that many of the features exist beyond the extents of what has currently been mapped.

In the context of present-day coastal changes, the rate of global sea level rise is predicted to continue increasing to between 4 – 15 mm yr^{-1} by 2100 (IPCC, 2021), which means that even at the lowest emissions scenario, sea level would be rising at a faster pace than at any time over the past 6,000 years. With these predicted rates of accelerating sea level rise, it is expected that barrier islands around the world will being transitioning to a mode of retreat as sea level rise forces them into a backstepping pattern (Mellett and Plater, 2018). Donoghue (2011) estimated that a rate of 16 mm yr^{-1} could be enough to initiate the overstepping and drowning of shorelines. With a 1 m rise in sea level, Florida would experience the greatest economic loss in the United States – approximately $130 billion – due to its 3,660 km of “tidal shoreline” (Donoghue, 2011).

These forecasts do not even consider the fact that modern coastal engineering is potentially increasing the risk of barrier drowning by obstructing natural processes that allow these landmasses to migrate with changing sea levels (Nienhaus, 2019). Consequently, as we move forward into an uncertain future of climate change, it is increasingly relevant to look to the geomorphic record formed during deglacial sea level changes, including during times of rapid sea level rise (e.g., MWP-1A saw rates of sea-level rise of up to 60 mm yr^{-1}), to better understand how shorelines have responded to, and will evolve in response to coastal inundation.

1.2 Geologic Setting of Florida

The recent geologic past of Florida is dominated by the Mesozoic formation of the massive carbonate platform that expanded from the area of modern-day Florida to the Bahamas, Mexico, and up the eastern seaboard of North America. This carbonate structure has largely influenced the geomorphology of what we know today as the state of Florida. While a smaller version of the carbonate producing system is still extant in the southern reaches of the state (e.g., the Florida Keys), carbonate sedimentation has largely been replaced by a thin veneer of siliciclastic sedimentation (Hine, 2013).

The west Florida shelf is a wide, gently sloping portion of the platform that was drowned during the recent deglaciation. Today, the shelf is a low-energy, sediment-poor environment characterized by a thin layer of Holocene sediment that drapes over a limestone layer many kilometers thick (Brooks et al., 2003). Ancient coastal deposits left behind when barrier islands and shorelines were overstepped and drowned are prominent features found scattered across the shelf at the seafloor. On land, these features are elevated ridges that mark the locations of previous sea level high stands (Simms, 2021). On the seafloor, paleoshorelines are markers of where sea level was lower in the past. Submerged paleoshorelines have been identified on Florida’s continental shelf from the northwesternmost sector near the Alabama-Florida border to the southernmost sector seaward of the Florida Keys (Locker et al., 1996).

Unlike many other coastlines around the world that contain barrier islands, a large portion of Florida’s barriers are unique in that they have a much higher potential for preservation due to the capacity for rapid diagenesis and cementation of the carbonate sediment that composes them. Barrier islands formed from the reworking of siliciclastic sediments that have been eroded and transported from the continents do not contain such a potential for rapid lithification (Jarrett et al., 2005). Therefore, when eustatic sea level quickly rises due to events like the melting of glaciers, ice caps, or ice sheets, siliciclastic barrier islands are most often broken up and reshaped into offshore shoals (Swift et al., 1856; Davis and Clifton, 1987). In addition to the potential for rapid cementation, the west Florida shelf offers yet another favorable condition for shoreline preservation in that it is a low-gradient carbonate ramp (Fig. 3) which allows for rapid overstepping of barriers with even modest changes in sea level (De Falco et al., 2015). Florida is not unique in this characteristic, as other similar submerged carbonate barriers have been identified around the world, for example on the Fraser Shelf of Australia (Passos et al., 2019), Western Sardinia in the Mediterranean (De Falco et al., 2015).

1.3 Florida Paleoshorelines in the Literature

Evidence of shorelines on the west Florida shelf that are postulated to have drowned and stranded after the Last Glacial Maximum is available and has been identified using various geophysical acoustic instruments: principally, multibeam echo sounders (MBES) for seafloor bathymetry, as well as side-scan sonar for imagery along various sections of the west Florida shelf (Hine, 2013). Gardner et al. (2005, 2007) identified a suite of features (Fig. 4) along comparable isobaths west of De Soto Canyon and further southeast on the Florida shelf. Gardner et al., (2005) described a series of shelf-edge deltas between -40 and -150 m using MBES. Features such as ridges, mounds, bed forms, and moats were identified both overlaying and adjacent to the deltas. The ridges are hypothesized to be remnants of ancient barrier islands although they could also be easily mistaken for reef ridges. The study made the distinction based on two indicative features: their low seaward-facing slope and curved landward ridges that are nearly identical to beach ridge terraces found on strand plains in analogous shoreline environments. Furthermore, following a trend seen in modern subaerial barrier island formation, the submerged ridges were preserved in an orientation facing into the prevailing winds.

In a similar study nearby, Gardner et al. (2007) examined another series of shelf-edge deltas and related features (Fig. 4) northwest of the 2005 study area at the head of De Soto Canyon in the northeast Gulf of Mexico (Florida panhandle area). Features included shelf-edge deltas with superimposed barrier islands, reefs, hardgrounds, bedforms, pinnacles and mounds – all of which are attributed to shoreline environments. Ridges along the northern side of De Soto Canyon are interpreted to be drowned barrier islands as they have nearly identical morphology to modern ones. They are long, narrow shore-parallel ridges that fall within depth ranges of other submerged paleoshorelines on the west Florida shelf. Other shore-related features in Gardner et al. (2007) included: low-relief hardgrounds, which are believed to have formed in the intertidal zone; structures which, based on their steep seaward-facing morphology, are presumed to be reefs; and large, smooth mounds which are interpreted to be bioherms built by the stony coral *Oculina*. Interestingly, Gardner et al. (2005, 2007) proposes these paleoshorelines formed while sea level was regressing not transgressing.

Continuing southeast along the west Florida shelf, Brizzolara et al. (2020) investigated areas within the Madison-Swanson and Steamboat Lumps Marine Protected Areas (Fig. 4), regions also examined by Gardner et al., (2005). The focus of Brizzolara et al. (2020) was to optimize substrate classification schemes by using a combination of multibeam bathymetry and backscatter data in conjunction with a towed-camera system to ground truth interpretations.

Southeast of Steamboat Lumps (Fig. 4), approaching the interior of the west Florida shelf, two areas, informally named the Southwest Florida Middle Grounds and the Elbow, contain long, narrow ridges that resemble those found along the northwest edge of the shelf (Stanley Locker, *pers. comm., 2019*). These features, like those in Brizzolara et al. (2020) have been studied for benthic habitat mapping purposes (Ilich et al., 2021). Additionally, the Elbow, was targeted for geologic sampling, subbottom profiling, and sediment grain size analysis, which enabled a preliminary interpretation of the feature as a coastal spit structure (Stanley Locker, *pers.comm., 2019*).

Further south along the west Florida shelf, Pulley Ridge (Fig. 4) is an ~ 200 km long ridge system whose main crest lie near -65 m (Jarrett et al., 2005), with deeper ridges near -80 and -90 m. This region is located ~ 250 km west off the coast of Florida (Allee et al., 2012; Reed et al., 2019) and ~95 km west of the Dry Tortugas. It is a well-known spot for fishing as the ridge system is home to a deep photosynthetic coral reef. It is believed to the deepest light-dependent reef in the United States fed by the warm, nutrient-poor waters of the Loop Current (Jarrett et al., 2005). Because of its unique status as a deep-water reef habitat, Pulley Ridge has received significantly more attention by academic, private, and federal agencies in an effort to understand the ecosystem and its underlying geology, as well as to preserve and manage it.

Jarrett et al. (2005) mapped Pulley Ridge and surveyed it with an array of geophysical tools (300 kHz multibeam and seismic systems) to understand the underlying geology that the modern coral reef sits upon. Allee et al. (2012) extended the 300 kHz multibeam bathymetry and backscatter coverage significantly, which was subsequently used by Reed et al. (2019). Jarrett et al. (2005) discovered that the reef only formed a thin layer over a limestone ridge. Based on seismic reflection profiles and geomorphic features seen in multibeam bathymetry, Pulley Ridge was determined to be a system of submerged barrier islands. Evidence included horizontal, layered bedding patterns as well as rectilinear jointing characteristic of beachrock formation – both of which are apparent in video footage (Cross et al., 2005). Subsurface seismic reflection profiles also confirmed the interpretation based on the presence of high-amplitude, parallel bedded reflectors, a pattern characteristic of a barrier island depositional environment, and seaward inclined reflectors that are consistent with a subtidal or aeolian setting.

It has been highlighted in the Continental Shelf Characterization, Assessment, and Mapping Project (C-SCAMP) technical report (Murawski, 2020) that areas of interest along the -50 to -60 m isobaths between The Elbow and Pulley Ridge may contain new paleoshoreline features that have yet to be mapped, therefore certain regions along these isobaths could be suitable targets for future mapping. Considering the pattern of known paleoshorelines on the west Florida shelf and the high preservation potential that characterizes the region, it is probable that new features will be uncovered by future mapping missions to the area. Furthermore, some of the existing datasets that have identified shoreline features on the seabed (e.g., Allee et al., 2012) have not been fully examined in detail, especially framed within the context of former sea level change and processes.

Finally, the southernmost group of identified submerged shorelines on the west Florida shelf lies along the margin southwest of the Marquesas Keys (Fig. 4). These features were surveyed by Locker et al. (1996) who identified distinct linear tracks of ridges at the seabed. The features were interpreted to be shorelines based on subsurface characteristics from seismic reflection data, side-scan sonar imaging, and submersible observations. The ridges, like many of the others previously mentioned, lie in a depth range between -50 and -140 m and are interpreted to be subtidal shoal complexes and beaches that formed during the meltwater pulses following the sea level lowstand at the end of the Last Glacial Maximum. The ridges here standout from the others in that they contain oolitic grainstones, indicative of a highly productive carbonate system.

This system consists of four features that lie in parallel succession with the oldest feature, the 'S1' shallow marine shoal complex, lying in the deepest water in the -80 to -124 m depth range; and the ensuing features at -71 to -80 m, -64 to -71 m, and -58 to -65 m. The S1 shoal only extends 4 km, while the other shorelines, S2-S4 extend longer, up to 24 km. Radiocarbon dating of oolites in these ridges, including the shoal complex, gave 14C ages of approximately 18.9 ka to 13.7 ka, age ranges which are comparable to many of the estimated ages of the previous ridge complexes mentioned. To date, these ridges are the only features to have been directly dated using absolute methods. Similar to the interpretations Jarrett et al. (2005) made from seismic reflections southwest of Pulley Ridge, Locker et al. (1996) observe similar well-sorted, layered reflectors along with low-angle seaward facing reflectors that are consistent with the beach and aeolian environments that would be found on a barrier island.

1.4 Habitats of Importance – Mesophotic Coral Reefs

In addition to being a subject of interest to geologists, submerged paleoshorelines are of great interest to ecologists who focus on the study and management of mesophotic coral ecosystems (MCEs). MCEs are defined by the presence of light-dependent corals and their associated communities of sponges, algal communities, and reef dwellers; and they are found along rocky seafloor ridges in the depth range of -40 to -150 m in tropical and subtropical regions (Puglise et al., 2009). The understanding that lithified paleoshoreline ridges form suitable substrate for these ecosystems is a well-documented one (Koenig et al., 2000; Jarrett et al., 2005; Locker et al., 2010; Sherman et al., 2010; Khanna et al., 2017; Murawski, 2020). However, despite this knowledge of MCEs, these ecosystems are still poorly understood due to limited technology that allows scientists to study them. Lying just beyond the depth limit for conventional scuba diving, MCEs are only accessible by remote means or submersibles (NOAA, 2023).

Analysis of bathymetry in the northern and eastern Gulf of Mexico indicated that this region has a high potential for hosting MCE communities, particularly along the WFS (Locker et al., 2010). The gentle slope of the shelf provides an ideal location for MCEs to colonize in comparison to the steep slopes found in many other places. With the knowledge that certain Florida paleoshorelines already support MCEs (e.g., Pulley Ridge), the work presented in this thesis can serve as a guide to future researchers who are interested in the exploration and protection of these ecologically important habitats.

Archeologists, geologists, and fisheries ecologists alike have noted the importance of further exploring the seafloor on the WFS. It has been estimated that more than 15,000 km^2 of unmapped “high-priority habitat,” as defined by their underlying paleo-coastal geologic framework, exists on the WFS (Murawksi, 2020). Additionally, gap analyses performed by the Florida Coastal Mapping Program (FCMaP) found that less than 20% of Florida's coastal waters have been mapped using modern survey techniques (Hapke et al., 2022). Therefore, following this work, scientists, industry and government stakeholders can move ahead with the continued exploration of the west Florida shelf particularly now that $100 million has been awarded by the Florida Department of Environmental Protection with the sole purpose of mapping the state's surrounding seafloor (Florida DEP, 2022).

1.5 Aims and Hypotheses

The overarching aim of this study is to improve our understanding of the geomorphological evolution of the WFS in relation to sea level changes over the past ~20,000 years as well as understand how that geologic framework relates to modern ecosystems. The goals of the project are framed around two central hypotheses:

Hypothesis 1: Based on the locations of previously described paleoshorelines on the WFS and the expanse of seafloor that has not been examined, more geologic features of interest will be discovered in similar depth ranges (-45 to -90 m).

Objective 1. To test this hypothesis, the project will compile an inventory of existing and new shorelines imaged in multibeam swath bathymetry datasets synthesized across the WFS. The geomorphology of paleoshorelines as seen in bathymetric data will be studied and interpreted, both individually and as a collective, to indicate what types of environments characterized the ancient coastline of Florida and to draw out regional geomorphological trends in shoreline topography and characteristics.

Hypothesis 2: Paleo-sea level indicators (i.e. paleoshorelines) mapped as part of Objective 1 will be able to provide a new assessment of the extent and significance of sea level signatures on the WFS. In particular, we hypothesize that patterns in the shoreline depths will reveal concentrated periods of formation that correlate to periods of lower rates of sea level rise.

Objective 2: To test this hypothesis, we will correlate newly mapped shorelines and their depths to regional sea level curves for the WFS. Building off of the assumption that WFS paleoshoreline features in the -45 to -90 m depth range are all of a post-LGM age (e.g. Locker et al. 1996), new data points will be able to build upon a regional sea level history including improving understanding of the dynamics of the coastal environment through periods of rapid past sea level rise, such as the well-known meltwater pulse 1B (e.g. MWP-1B) which occurred approximately 11,200 years ago.

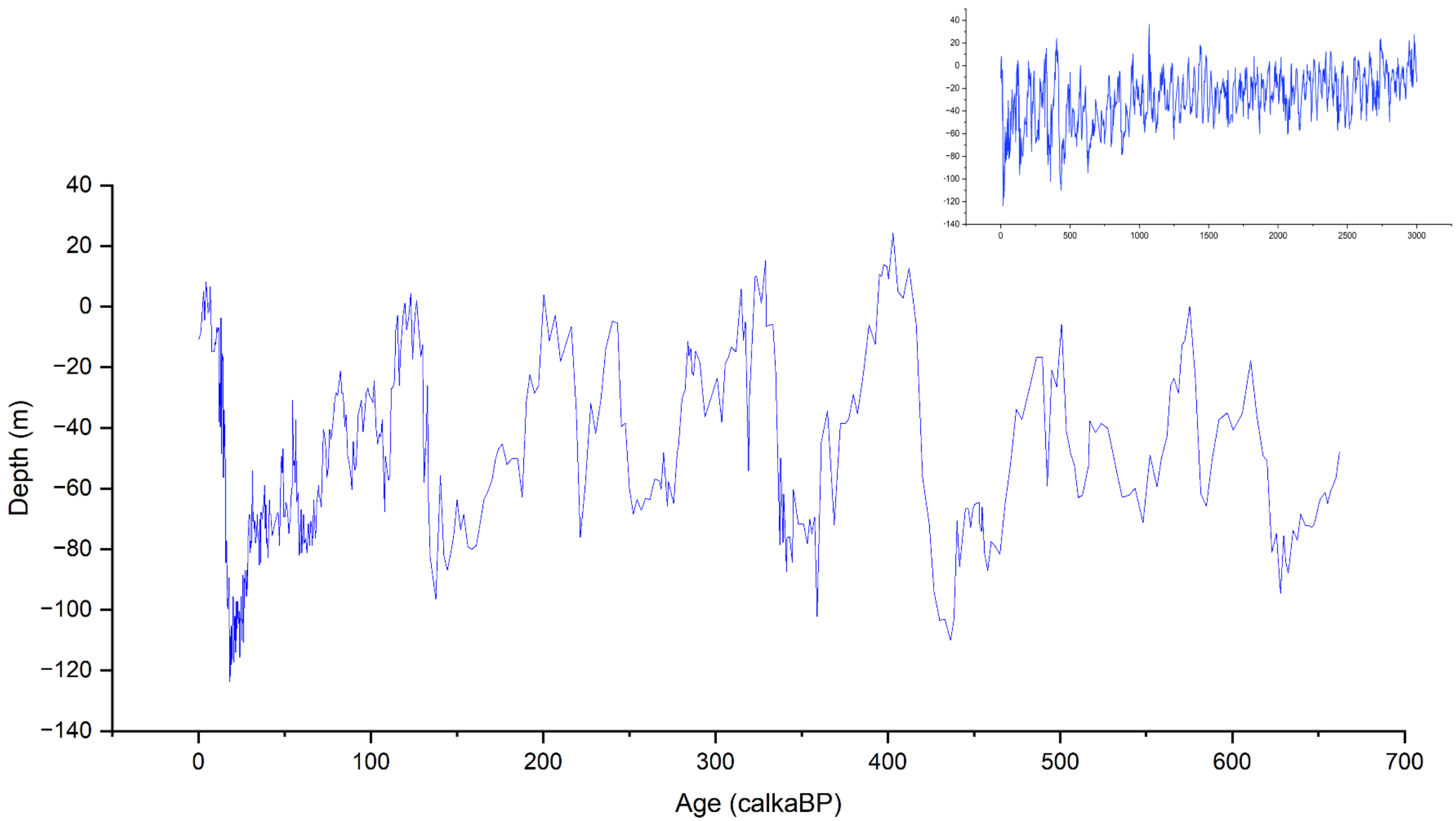

Figure 1: Smoothed sea level curve derived from Pacific benthic foraminiferal oxygen isotope data and Mg/Ca records as an estimate for global mean sea level from the past 700 Kyrs. Inset: same sea level curve for past 3 Myrs. Based on data published in Miller et al., (2020). Three recent marine isotope stages are marked illustrating the progression of sea level falls with glaciations.

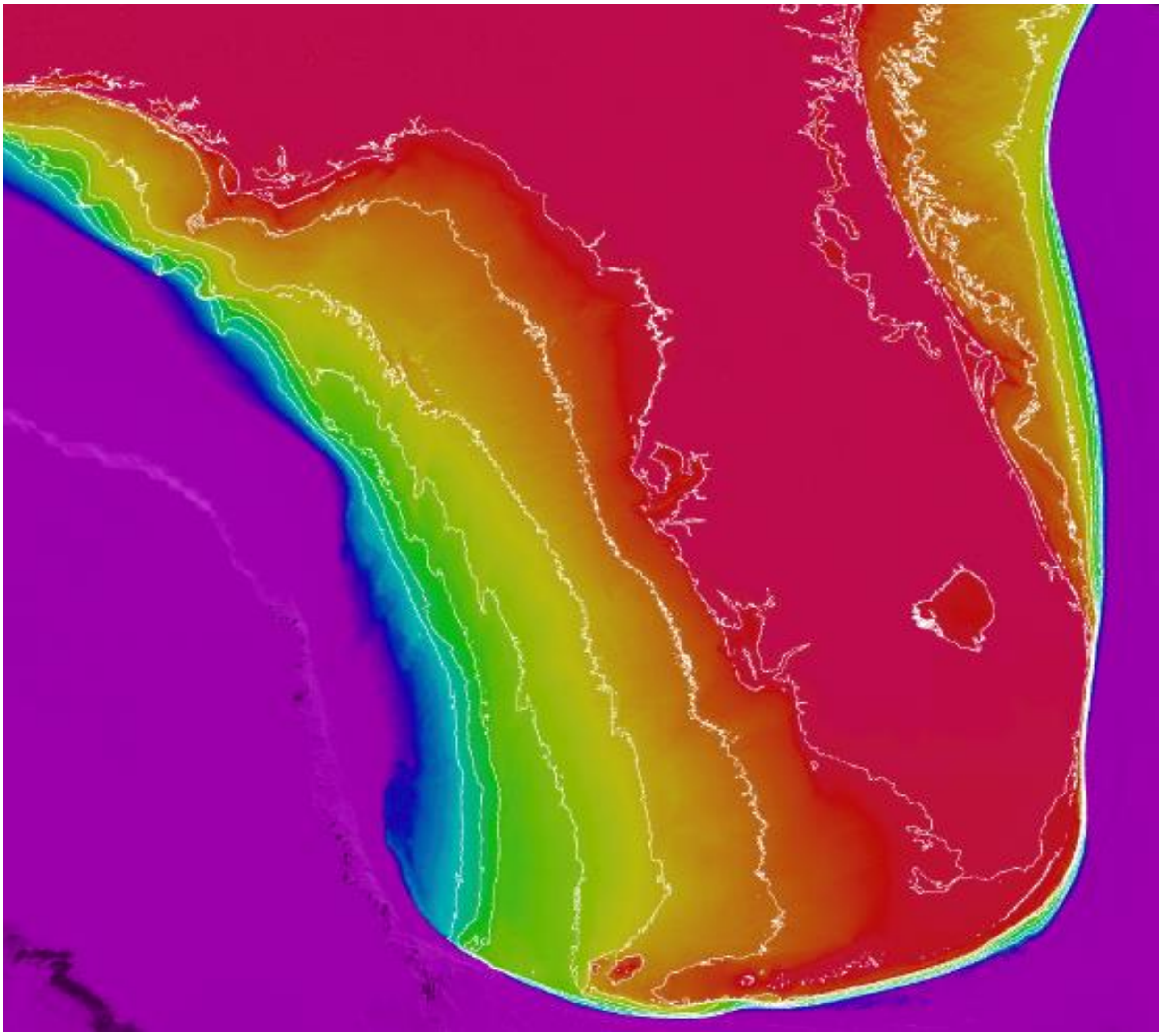

Figure 2: Bathymetric contour map of the West Florida Shelf. Intervals are 20 m, and the deepest interval marks -120 m – the LGM lowstand.

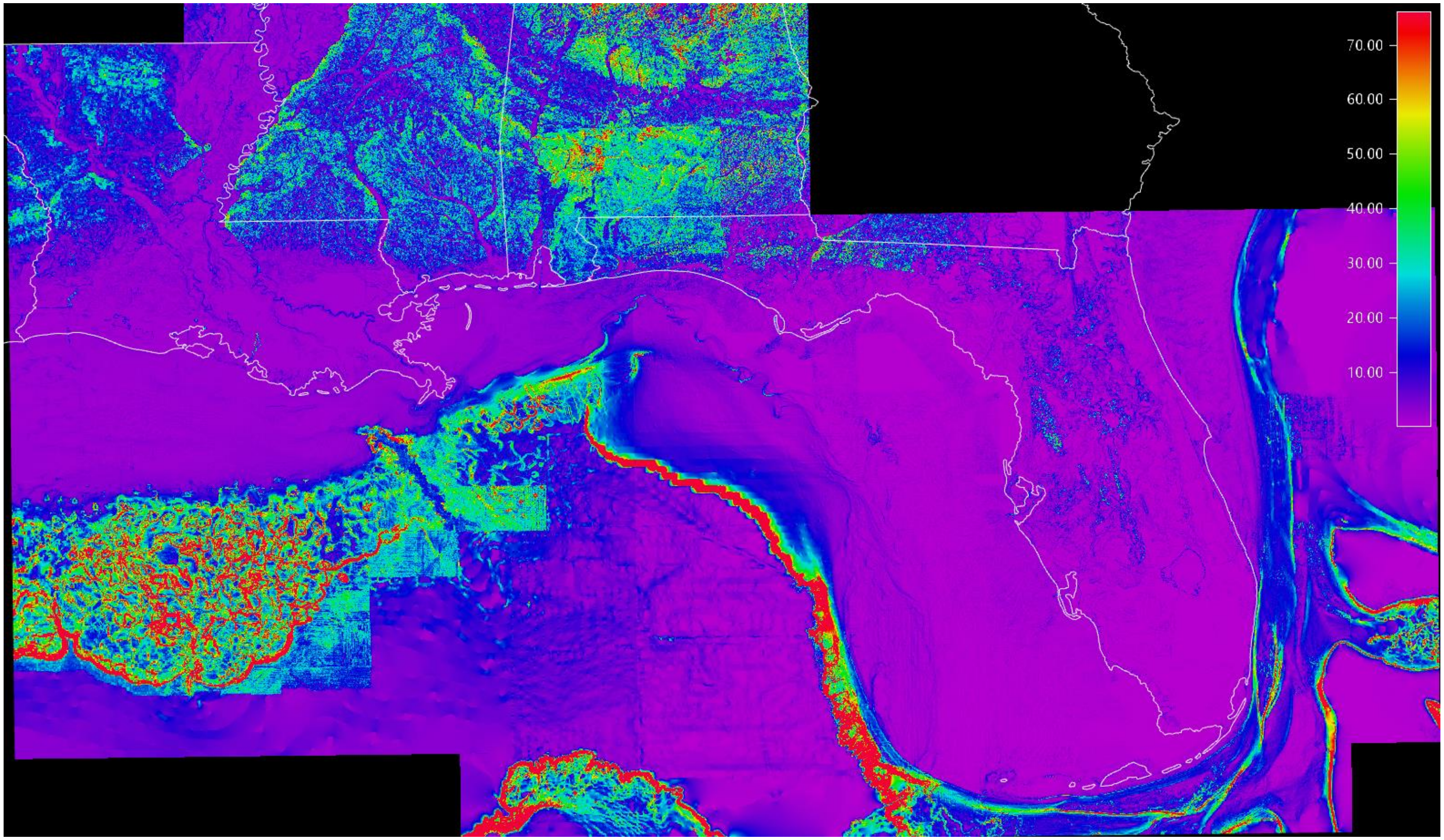

Figure 3: Slope map of the north and eastern Gulf of Mexico highlighting the extent and gradient of the West Florida Shelf. Color legend is degrees of slope. Note location of De Soto Canyon which marks the boundary between siliciclastic sediments from the Mississippi River to the west, and carbonate sediments to the east.

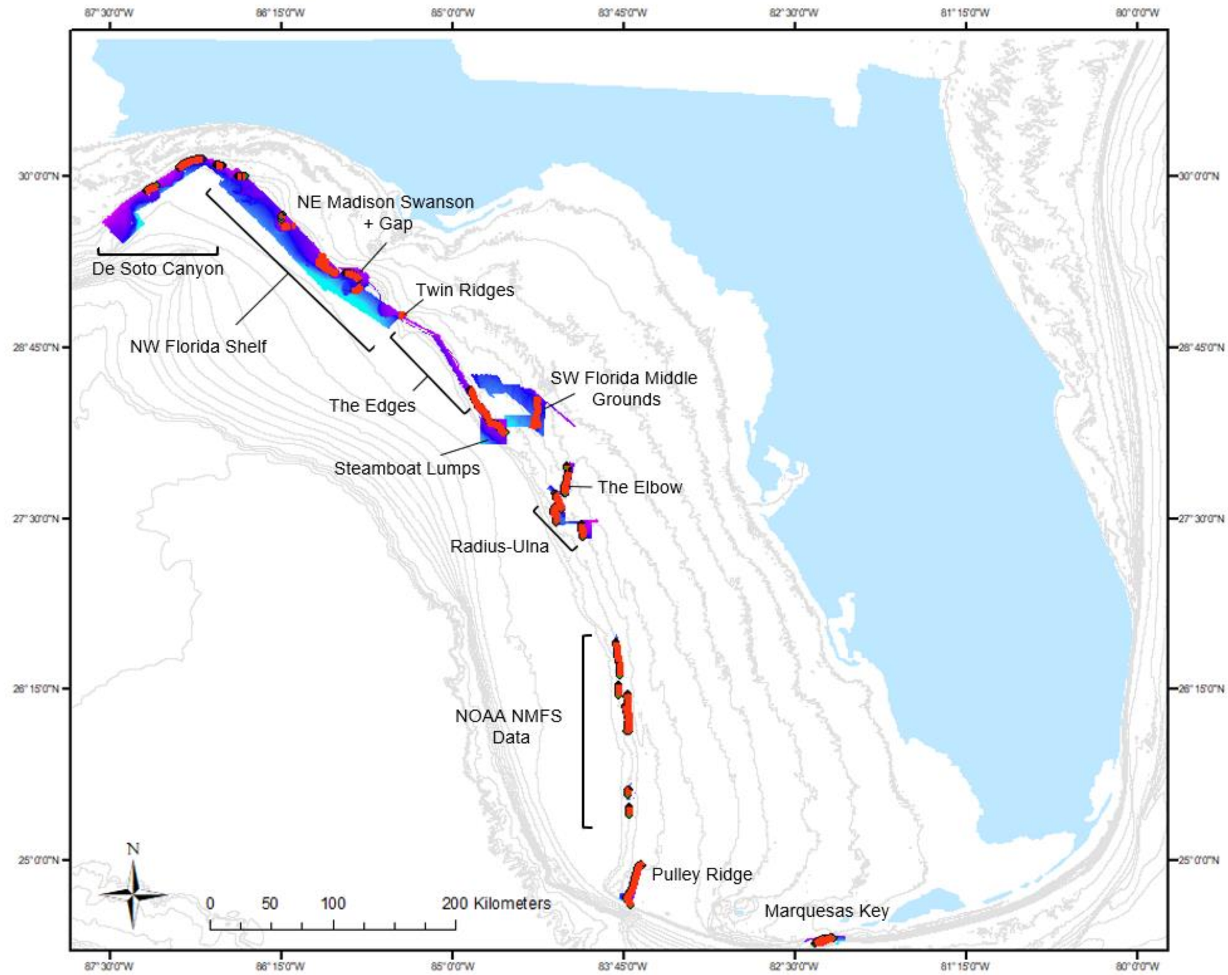

Figure 4: Location and names of bathymetric datasets collected for this project. Red lines indicate location of paleoshoreline features (1-27).

CHAPTER 2:

DATA & METHODS

2.1 Data

2.1.1 – Acquisition and Processing of Existing Data Sets

To create a shelf-wide inventory of known or suspected paleoshorelines on the west Florida shelf, high-resolution multibeam bathymetry data were collected from various sources, specifically targeting datasets that fall within the -45 to -90 m depth zone of interest. These sources included: The C-SCAMP project, the United States Geological Survey (USGS), the National Oceanic and Atmospheric Administration (NOAA), and new data that were collected on the RV *Weatherbird II* as part of a graduate level course at the College of Marine Science in 2022. Importantly, a large proportion of these data were either unpublished, or published but without description of the shoreline features contained within the data. As such, this is the first compilation of datasets explicitly targeting paleoshorelines of its kind. For a complete summary of these datasets and their associated vessel configurations see Appendix 2 and see Figure 4 for a map view of locations. In the following, we describe the acquisition and processing of existing datasets, sequentially from the north-west Florida shelf southwards to the Florida Keys. Where existing features have colloquial names in the literature (e.g., the Elbow) we retain the nomenclature of those bathymetric objects. All features, whether named or unnamed, are also assigned a numerical marker for identification and description (referred to here-in as shorelines 1 through 27).

The De Soto Canyon, NW Florida Shelf, and Steamboat Lumps datasets were acquired by the USGS between 2001 and 2002 using a 95-kHz Kongsberg Simrad EM1002 MBES for the NW Florida Shelf and Steamboat Lumps and a Kongsberg Simrad 300-kHz EM3000 MBES for De Soto Canyon (Gardner et al., 2005; 2007). The data were gridded to 8 m (De Soto Canyon, NW Florida Shelf) and 4-m (Steamboat Lumps) resolution, respectively. Subsequently, those datasets were expanded with mapping led by PI David Naar at USF in 2002. The northeast corner of the Madison Swanson Marine Protected Area (MPA), situated on the Madison Swanson shelf-edge delta, was mapped with the USF 300-kHz EM3000 MBES and data gridded to a 10 m resolution. A gap between the USGS and USF datasets at Madison Swanson was later filled in by the C-SCAMP group at USF through mapping conducted using a 400-kHz Reson SeaBat 7125 MBES, producing a grid with a 2 m resolution.

On the southeast corner of Madison Swanson delta, a feature known as 'Twin Ridges' was mapped by for NOAA Fisheries (aka National Marine Fisheries Service or NMFS) in 2006 using the USF Kongsberg Simrad 300-kHz EM3000 MBES. The resulting data were gridded to a 0.0001° resolution (equivalent to ~ 10 m grid cells at a latitude of 28.9° N). Track lines from a series of USF cruises undertaken in 2005 that ran along a corridor southeast of Twin Ridges were combined to create a ~ 10 m resolution grid by USF in an area known as The Edges Seasonal MPA.

Moving into the mid-shelf region (between approx. 28.46 – 27.35 ° N), a series of datasets were collected primarily for habitat mapping purposes by the C-SCAMP group at USF between 2015 and 2019. These offer extensive seafloor coverage of across a number of important shoreline features. Using a 400-kHz Reson SeaBat 7125 MBES, C-SCAMP mapped the Elbow in 2015 and the SW Florida Middle Grounds in 2016. Data were gridded at a resolution of 4 m in those areas. In 2018, C-SCAMP returned to the same features and acquired single-channel seismic reflection data across both sets of shorelines. The source was a Falmouth Scientific Inc. dual-plate Bubble Gun coupled with a short streamer. In 2019, a 400-kHz Teledyne Reson SeaBat T-50R MBES was used to map a feature dubbed the Radius-Ulna to a grid resolution of 3 m. Most recently in 2022, a rectangular area 14 by 2 km, connecting the two mapped portions of the Radius-Ulna, was mapped using a 200-700 kHz R2Sonic 2026 MBES. Data were gridded at 2 m resolution as part of cruise MGT22 on the RV *Weatherbird II* (a Marine Geophysical Tools field training course taught at USF's College of Marine Science). Subbottom profiler data were also gathered along portions of the newly mapped areas using an Edgetech SB-512i CHIRP system.

Further south on the shelf, NOAA NMFS mapped a series of discontinuous datasets along a corridor that runs along the 60-90 m depth range north of Pulley Ridge using a 70-100 kHz Simrad ME70 Scientific Echosounder, gridded to a resolution of 5 m. Subbottom profiler data of a feature within this area were collected by Al Hine (2008) and are used as supporting geomorphological information in the discussion. Southern Pulley Ridge was mapped by USGS in 2005 using a 300-kHz Kongsberg Simrad EM3000, gridded to a resolution of 5 m, with supplementary subbottom profiler data collected using a Huntec Boomer/Elics Delph Seismic single-channel seismic system (for additional details, see Jarrett et al., 2005).

The bathymetry data for shorelines U and V (unnamed in the literature) were retrieved from NOAA's NCEI Bathymetric Data Viewer. They are analyzed in this project as a comparison to work carried out by Locker et al. (1996) who described the same features using only subbottom seismic profiles (collected with an Elics Delph 1 single channel system) and core samples. By combining information about their stratigraphic history, their radiocarbon-dated absolute ages, and now their bathymetric expression in detail, these shorelines provide a strong baseline against which other paleoshorelines can be compared and correlated. The data were collected in 2014 on the NOAA Ship *Nancy Foster* using a dual frequency (200 and 400 kHz) Reson SeaBat 7125 multibeam echosounder (Donahue, 2014). The grid resolution for the dataset is 2 m.

2.1.2 Data – Processing Methods: This Study

For some datasets, further processing of the bathymetry was undertaken in order to produce outputs tailored for geomorphic analysis. A conceptual overview of the post-processing steps are as follows: (i) preliminary correction of survey data for inaccuracies relating to: water levels (e.g., tides, ship draft), transducer alignment and offsets, sound speed of the water body being surveyed, and vessel position and navigation. In the case of the data used in this study, this step was already performed and therefore only needed a basic visual QC check; (ii) data cleaning is performed using a combination of filters (e.g., Surface Spline filtration) and manual point removal; (iii) review of the data and comparison of results to expected depths, reference data sets, and nearby gridded products (Kazimierski and Jaremba, 2023).

To analyze the datasets containing newly identified candidate shorelines in three dimensions, ASCII XYZ and/or ESRI GRID files were brought into ArcMap as rasters and were subsequently exported as .bag files for import and viewing in Fledermaus 8.4.4 software.

In the case of the Twin Ridges, The Edges, and Pulley Ridge datasets, they were regridded from their original raw bathymetry files. The original .all files were imported into Qimera 2.5.1, processed and cleaned of apparent outliers, and finally regridded to 10 m grid cell resolution for export into .bag files for use in ArcMap. The assembly of the Pulley Ridge data set similarly required reconstruction from the raw .all and .mb56 files. In post-processing we applied weak spline filters across much of the surface and then undertook manual point cleaning to eliminate any remaining outliers in the data in order to produce a cleaned product.

2.2 Methods

2.2.1 – Identification of candidate shoreline landforms

Using the assembled dataset described above, an initial analytical step involved the reconnaissance and identification of features as ‘candidate’ paleoshorelines. Some of these were already suspected from description in the literature; for others, we used a combination of slope, contours, and visual inspection of the bathymetry to identify likely features for further investigation. Due to the late acquisition of new high-resolution data for “the Edges”, the naming scheme for the shorelines that were identified within the expansive NW-SE running dataset was modified to account for this change. Rather than being considered its own unique shoreline, “the Edges” was split in two due to the separation and differences in depth of the ridges that were identified within the expansive bathymetric footprint (Fig. 10,11).

The data were assembled into map format in ArcMap for 2D visualization (Fig. 4), and simultaneously in Fledermaus for 3D visualization. The first analysis that was performed was to create axial and ridge-perpendicular profiles in ArcMap to determine profile morphology for each of 27 known or suspected shoreline features identified in the above step. This was achieved using the ArcMap 3D Analyst Profiling Tool. Drawing these profiles in combination with analyzing specific features in the bathymetry allowed us to determine if the data contained paleoshorelines based on the following criteria: (i) evidence of a prominent and contiguous seafloor ridge, (ii) inflexions in the seafloor profile drawn perpendicular to the shoreline (Fig. 5),

(iii) the presence of terrace or terrace-like features that many indicate sea level erosional platforms, and (iv) preserved strand plains or spit-like features abutting ridges.

The Fledermaus Profiler tool was used to build on initial ArcMap profile investigations, because it allows for manipulation of the vertical exaggeration as well as precise drawing of profile lines within the 3D geometry of the shorelines. The use of highly vertically exaggerated grids in this analysis (i.e., applying a multiplying factor to the depth, thus exaggerating or attenuating variations in relief – in this case, we typically used an exaggeration of 10:1) is important because many of the paleoshoreline features on the west Florida shelf are relatively difficult to pick out from the surrounding bathymetry at normal exaggeration (Fig. 6). The features have either been eroded down or buried in sediment to the point that there is only a subtle expression of the geomorphology at the seabed. Moreover, compared to their surrounding swaths of flat sea bed, the shoreline landforms are inherently small-scale geological structures that would be difficult to identify visually in situ, and thus are only captured adequately using the sonar imaging techniques described in this thesis. While some may argue that such a degree of exaggeration might distort the morphology of the features, it is useful in this case because it has allowed us to capture features that otherwise might be missed and which have not been described before until now. For the sake of characterizing the geomorphology, the true expression of the bathymetric features has been considered, and vertical exaggeration is used only as a second derivative subsequently to point out specific features. We combined the z-value exaggeration of data with multi-angle light shading, to best image the shorelines identified within the data, following typical practices in geomorphological analysis (e.g., see Rolland et al., 2022).

2.2.2 – Geomorphic Characterization

To characterize the paleoshoreline features that we identified, the next step was to collect basic metrics on them which included morphometric parameters (lengths, depths) and geographic position (latitude and longitude). To measure the length of shoreline features, the bathymetric rasters were imported into ArcMap. We were consistent in using the WGS84 Geographic datum as our reference, with the data projected in UTM Zone 16N or 17N respectively, with the choice of projection appropriate to the location of the exact dataset in question, given that the WFS spans more than one UTM zone. We chose to use UTM projections since, within their 6-degree zones, they provide very little aerial distortion meaning over-ground measurements are true and accurate. With the bathymetry accurately mapped in a regional coordinate system, the lengths of each feature were calculated using the Measure tool and the latitude and longitude were obtained using a center point for each feature. To accurately describe the depths at which the shorelines are found, the following procedure was used: (i) polylines were drawn along each shoreline ridge creating a unique shapefile for each feature, (ii) the polylines were populated with vertices that occurred every 500 meters using the Densify and Feature Vertices to Points tools, (iii) z-values were calculated for each vertex along the shoreline using the Feature to 3D tool and the resulting attribute table was exported for analysis. The result of the polyline characterization process was a complete geomorphological map of recognized paleoshorelines for all available multibeam data from the west Florida shelf. Interpretations and preliminary speculation on the origin of these features are presented later in the discussion.

2.2.3 – Age Estimation using the Joy Curve

Having mapped and analyzed shoreline features on the shelf, the approximate/anticipated ages for paleoshoreline features were estimated based on their distribution of depths. In doing so, it is necessary to establish a standard for the terminology used from here forth. Conventions for describing the depth of submerged shoreline features vary throughout literature; for example, whether a sea level stand relates to a ridge crest, ridge base, or other geomorphic indicator for former shore position (Allee et al., 2012; Salzmann et al., 2013). In this study we adopt the estimated base of a shoreline – or the foreshore – as the most likely depth value for former sea level (Bird, 2000). The depths of ridge crests – assumed in many cases to be dunes based on their presence throughout much of the modern Florida coastline – were tabulated for the purpose of quantifying shoreline depths because they were easiest to distinguish from sun-illuminated bathymetry and provided a distinctive feature that could be easily measured. A relative sea level value was assigned to each feature based on a reasonable location for the foreshore within a 5-meter range from the top of the ridge (Fig. 7). In some instances, this location is easier to discriminate than others. When it was less obvious, for example, due to apparent erosion or flattening of the feature, a sea level position was assigned within the 5-meter window from the ridge and chosen from the nearest well-established sea level stand. For example, shoreline 11 which lies between -67 and -75 m and has an average ridge depth of -74 m, was assigned a RSL value of -75 m based on a) the location where the base of the shoreline appears to reasonably fall in cross-section, and b) by association with other known regional features; for example, where a corresponding sea level stand has been established in other locations at a matching depth range. The sea level curve produced by Joy (2019) is utilized in this study as the most accurate and up-to-date sea level curve for the Gulf of Mexico. The Joy curve is a synthesis of data from 32 publications, and it includes samples – dated by varying methods – of corals, peats, mangroves, wood, charcoal, and oysters (Fig. 8A). Due to the wide range in ages and dating methodologies (and the potential errors associated with those methods) used across the original datasets, corrections of proxy ages were necessary and are spelled out in complete detail in Joy (2019). The original Joy curve utilized a linear regression model that was separated into four depositional environments; therefore, it was difficult to assign an estimated age from it. For this reason, we chose instead to use the 95% chronology range for sea level rise that the author produced using the Bchron age/depth Bayesian modeling program (Fig. 8B).

Two different sea level curves were derived as the basis of our comparison: (i) a nine-point moving average calculated from the edited legacy data set provided by Joy, 2019 and (ii) a 95% chronology range for sea level rise introduced by the author using the Bchron age/depth Bayesian modeling program with the same legacy data set. The nine-point moving average was chosen to reduce the data set compiled by Joy (2019) to a more practical sea level curve for cross referencing depth to estimated age, reducing the effect of some very obvious age outliers and spread of noise in the original data. The original Joy curve utilized a linear regression model that was separated into four depositional environments; therefore, it was difficult to assign an estimated age from it. The nine-point moving average provided an appropriate simplified fit to the data that also eliminated the separation based on depositional environment and allowed for a simpler depth-to-age correlation. In comparison, the 95% Bchron chronology is a model designed to estimate unknown age/depth by using dated strata to determine the probability distribution of the estimated age of undated strata (Fig. 8B). By applying the Law of Superposition, the model restricts the probability distribution of age ranges by excluding any that pre- or post-date samples lower or higher in the sediment core (i.e., shallower or deeper along the

Gulf of Mexico seafloor.) It is typically applied to sediment cores, but in this case, the entire Gulf of Mexico was treated as a single core. The resulting curve provided a more statistically robust age range probability to serve as a comparison to the age estimate produced from the nine-point moving average. Importantly, the following age estimates assume that all shorelines on the shelf are approximately 20,000 years of age or younger, having formed during the major sea level transgression following the Last Glacial Maximum described in the introduction (and was not formed prior to that time during the preceding regression as was postulated by Gardner et al., 2005). Further discussion of our reasoning for this is provided in sections 3.2 and 4.2, but we acknowledge the assumption here and retain the possibility of other interpretations with the future addition of more dating information.

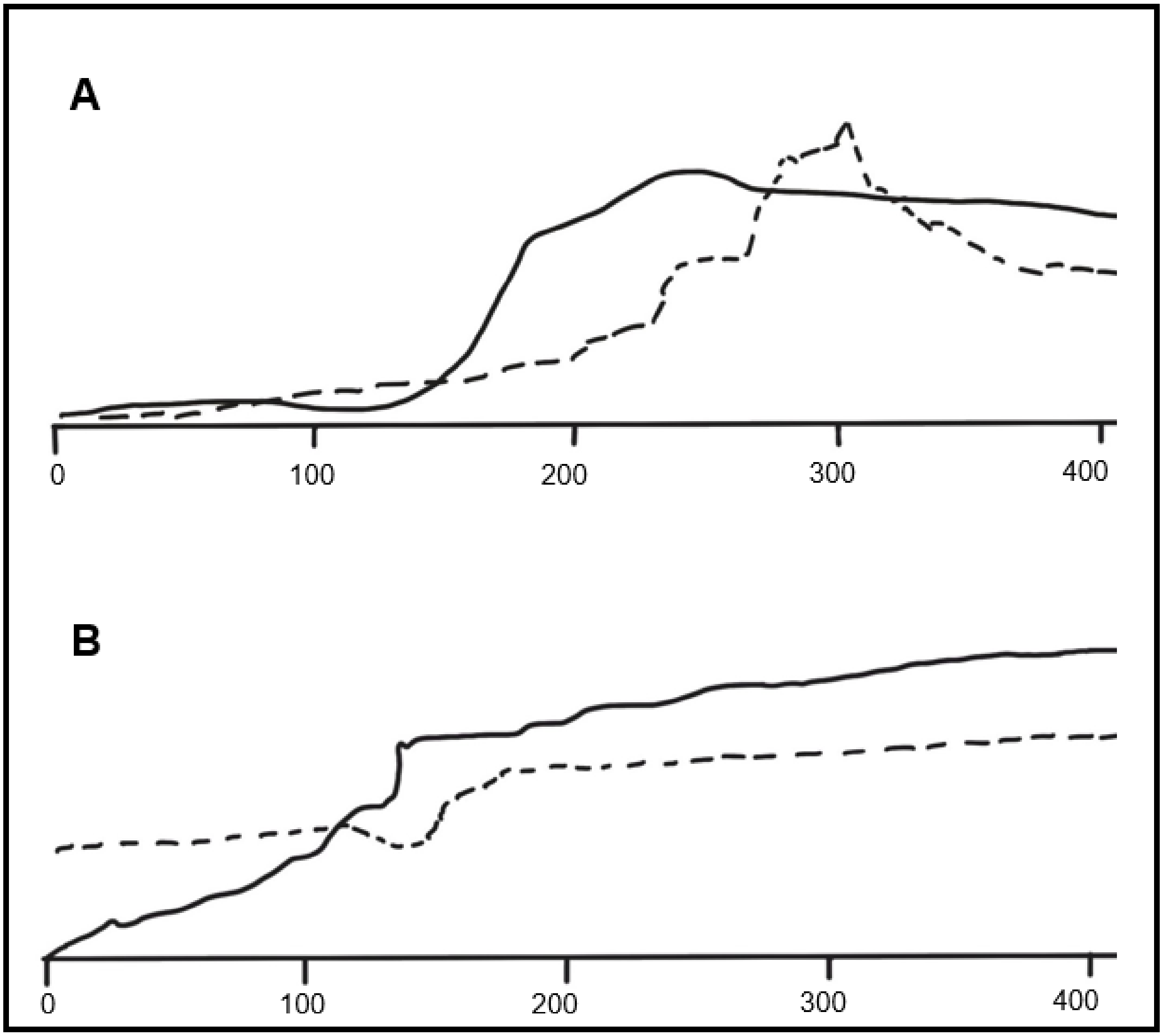

Figure 5: Conceptual cross-sectional profiles of candidate shorelines (10x vertical exaggeration). Bottom axis is distance in meters. (A) Various beach ridge morphologies: from more rounded ridge-to-sea drop offs to peaked inflections of well-preserved shoreline ridges. (B) Terrace-type profiles expected from suggested reef terraces and/or mangrove platforms.

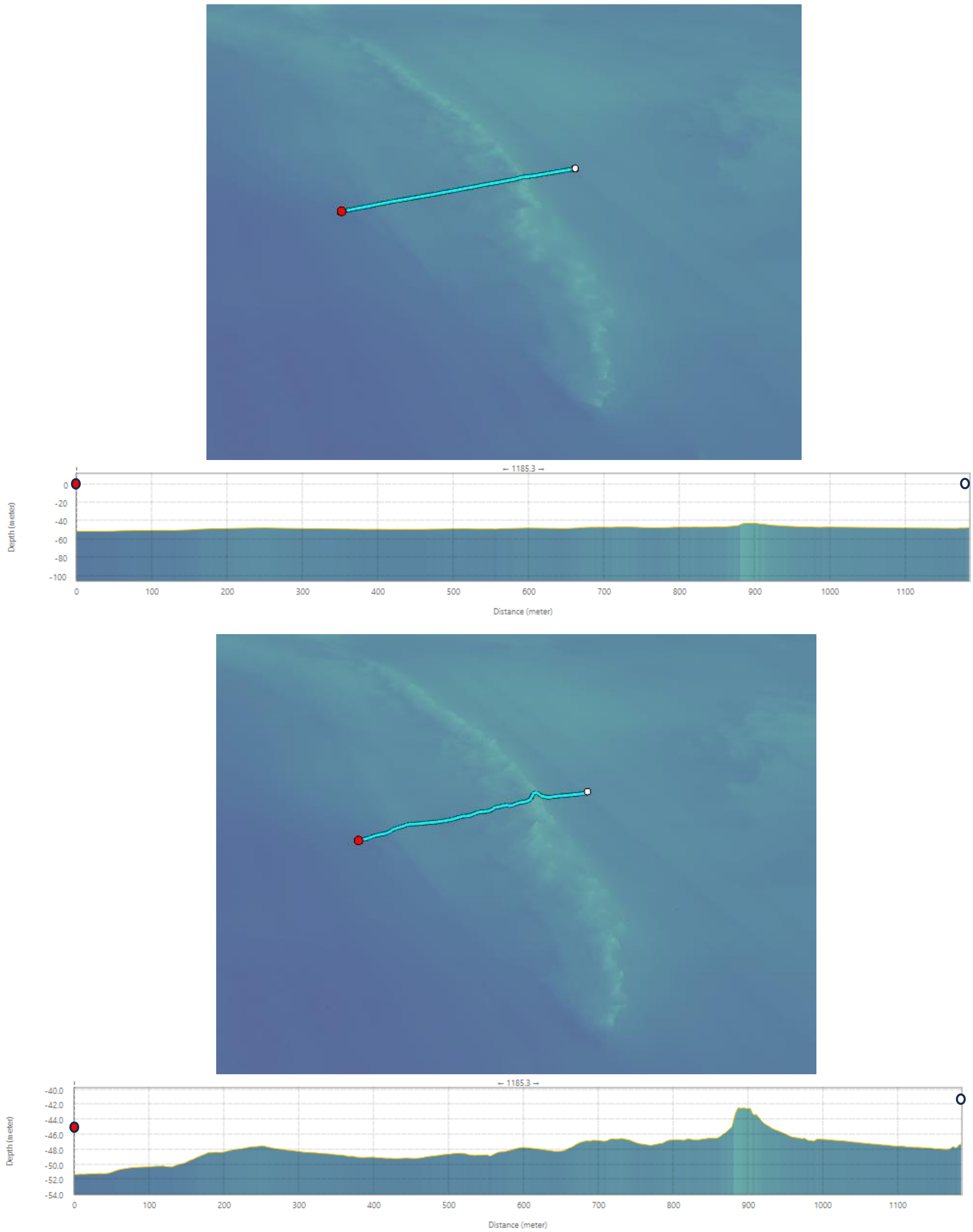

Figure 6: An example of the same paleoshoreline feature (from the SW Florida Middle Grounds) with no vertical exaggeration (A) and using 10x vertical exaggeration (B) to illustrate the usefulness of this technique in identifying subfeatures that would otherwise be indiscernible due to the subtlety of their seafloor expression.

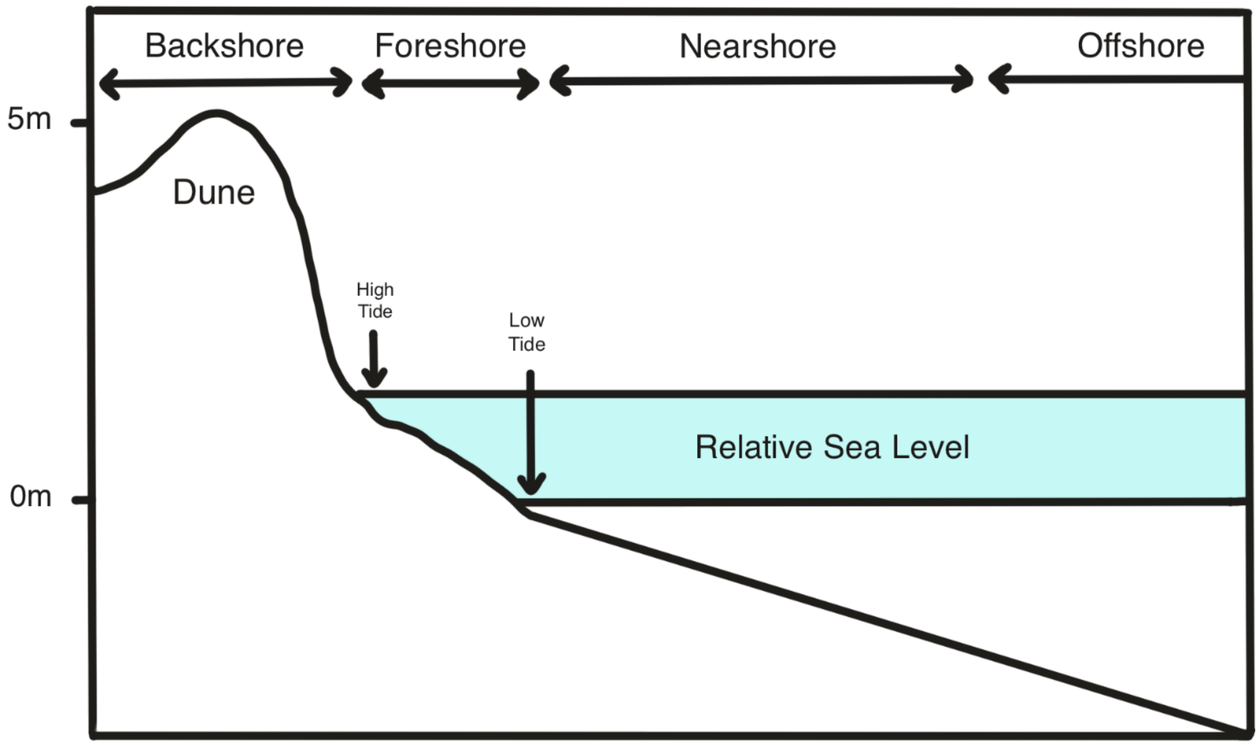

Figure 7: Beach profile highlighting foreshore and dune crest from which a window for deriving relative sea level values was based on (derived from Bird, 2000).

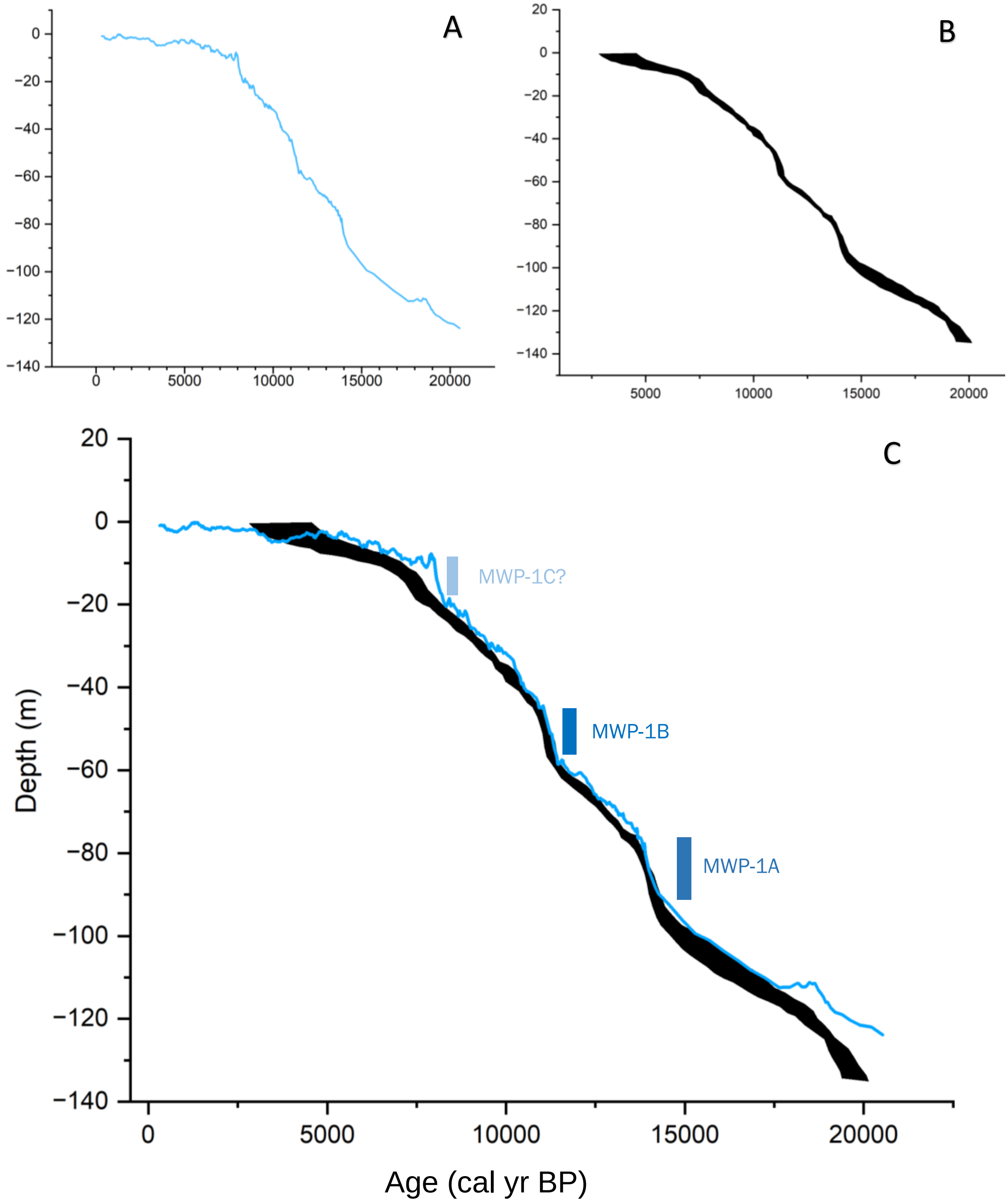

Figure 8: (A) The nine-point moving average Gulf of Mexico sea level curve (derived from Joy, 2019) and (B) 95% chronology for post-LGM sea level history replicated from Joy (2019). (C) Comparison of plots A and B showing timing and magnitude of meltwater pulses 1A and 1B. (D, *below*) The original Joy (2019) Gulf of Mexico sea level curve.

CHAPTER 3:

RESULTS

In the following results, we first describe the detailed morphology of new paleoshoreline features on the WFS individually, using their geometries to interpret likely depositional origin, and assign ages to the newly-mapped features based on age-depth relationships. We then consider the geomorphological characteristics of the shorelines together as a regional assemblage. Figures 9-22 contain plan view imagery of each of the newly described shoreline features with specific subfeatures highlighted per the results below. Additionally, cross-sectional profiles, shoreline delineations (see for precise call outs), and modern analogs are listed for all 27 paleoshorelines in Appendix 3.

3.1 Descriptions of New Paleoshoreline Features: observations, origins, and ages

Analysis of the bathymetry that was collected between -45 and -90 m yielded a total of 27 paleoshoreline features forming a new inventory of shoreline features for the entire WFS spanning over 5 degrees of latitude and more than 8 degrees of longitude (Fig. 4). Shoreline length, average depth to ridge crest, estimated age, and relative sea level were tabulated for each shoreline providing geomorphological details for each newly-identified and existing feature (Tab. 1 and 2). Some features, like the shoreline complexes in the Edges dataset, were considered a single feature if the group of ridges making up the complex were at the same depth and geographically close enough that their identification as a single unit could be reasonably made (e.g., Fig. 10A). Others that contained a series of more distantly separated features, like the

Radius-Ulna (Figs. 15-17), were subdivided due to differences in depth range and proximity that indicate they were not part of the same, contemporary coastal feature.

Some of the preserved shorelines included in this inventory have previously been described either explicitly as paleoshorelines (Shorelines 1-9 from De Soto Canyon through the Madison Swanson delta, plus shoreline 22 at Pulley Ridge) or indirectly as part of a larger study on habitat areas of interest (Twin Ridges). Therefore, the following detailed descriptions only include information and observations on structures and features that have not been described yet explicitly as paleoshorelines. Nevertheless, a summary of descriptions is provided for all previously examined paleoshorelines is included in our inventory, which has allowed for new comparisons and interpretations of the shoreline inventory as a whole (Appendix 1 and section 3.2).

3.1.1 – Shoreline 8 – NE Madison Swanson

Shoreline 8 is an 11 km-long arcuate ridge curling from the NW to the SE at -85.73 W, 29.28 N at the NE sector of the feature known as the Madison Swanson delta (Fig. 9A). The base of shoreline 8 lies at -65 m with the ridge cresting at an average depth of -63 m. The deeper ridge lying at -80 m (shoreline 9), previously described by Gardner et al. (2005), Allee et al. (2012), and Brizzolara et al. (2020), has been linked to the most recent deglaciation and it is speculated that it could share a common formational age to the ridges at Pulley Ridge and Marquesas Key at the same depth. Despite appearing (partially) in the bathymetry published by Allee et al., shoreline 8 has never been fully examined and described in the context of a paleoshoreline. Based on an approximate relative sea level estimate of -65 m, shoreline 8 is estimated to be between 12.3 – 12.5 ka in age.

3.1.2 – Shoreline 10 – Twin Ridges + The Edges North

Shoreline 10 initiates near -85.38 W, 28.99 N, about 40 km southeast of shoreline 9 (at the limit of some previously described landforms) on the Madison-Swanson delta. Although the feature known as Twin Ridges was described by Koenig et al. (2000), it has since been treated as an isolated feature. With the introduction of new bathymetry, presented here, we now describe these ridges as part of a much larger shoreline complex made up of 9 discontinuous ridge segments that lies between -59 and -74 m (Fig. 10A, B). Shoreline 10 is a feature made up of a series of discontinuous ridges totaling 26.2 km in length and runs in a NW to SE trend. The ridges, although discontinuous, lie no more than 4 km apart from one another – with one exception, discussed below. Twin Ridges lies at the northwesternmost portion of this shoreline complex and consists of two prominent, near-parallel ridges lying between -59 and -72 m. To the southeast, the ridge(s) making up shoreline 10 remain visible within a narrow corridor of bathymetry that was previously mapped in this region. If the bathymetric footprint was expanded just slightly to its north and south, it is likely many of the ridges could be traced beyond the current extent of the bathymetry based on their abrupt termination at the edge of the bathymetry. Towards the middle of the dataset, where the bathymetric dataset bends southwards, there is an area of ~ 13 km^2 containing what appears to be a lithified series of low ridges, or hardgrounds, emerging from the surrounding, smooth seafloor (Fig. 11A). Similar hardgrounds can also be seen scattered throughout the southern portion of the shoreline (Fig. 10C).

The term ‘hardground’ is based on similar classifications made by Gardner et al. (2001, 2005, 2007) of features with matching morphological characteristics on the NW Florida Shelf and which contain a strong backscatter response. While this project does not include an analysis of the primary sonar backscatter, there is evidence to corroborate the claim of widespread hardground across the depth zone of interest. Ilich et al. (2021) performed a backscatter analysis of the feature known as ‘the Elbow’ (our shoreline 11), which is recognized as containing a paleoshoreline ridge. The backscatter data analysis, supported by video ground-truthing, confirms the presence of extensive rocky substrate throughout the area. About 24 km south of the Elbow, subbottom data collected over an area of low-relief, rugged seafloor in the area known as the Radius-Ulna contain chaotic subbottom reflectors which indicates the feature is a much stronger reflector than the surrounding seafloor sediment. Based on usage in Schroeder et al. (1998), Riggs et al. (1996), and Benson et al. (1997), hardgrounds are defined as ‘lithified surfaces, regardless of origin or relief.’ Gardner et al. (2005) specifically refer to a classification of rough-topped, low hardgrounds that are pertinent to this study.

Returning to shoreline 10, just south of the bend, shown in Fig. 11B, a shoreline segment is seen running along the northern edge of the dataset, and it is accompanied by a nearby, parallel ‘offshore’ feature that contains a rugged topography unlike that of the smooth, arcuate shorelines. Its morphology resembles that of similar nearby limestone outcrops or hardgrounds that trend parallel to shore which have been described by Obrachta et al. (2003) on the west-central Florida shelf. The feature in shoreline 10 has a relief of ~5 m which, unlike some lower relief (<2 m) features correlated to the Miocene Hawthorn Group (Obrachta et al., 2003), has not been linked to a formational unit. There are two things to note of this hardground feature: (i) it is flanked by a ~100 m wide x 1 m deep depression on its seaward edge, and (ii) what could be described as a lower-relief expression of it – perhaps buried by sediment – can be traced southeast along the bathymetry data for 28 km.

A final feature to note within this complex and varied shoreline is a short, ~2 km-long ridge at the southern end of shoreline 10 that stands apart from the other ridges by nearly 17 km. (Fig. 10C). This ridge lies between -68 and -74 m and is deeper than those ridges to its north by 3-4 m, but shallower than the large ridge running through shoreline 11 just south of it (-70 to -75 m). This lone ridge is flanked by seaward-trending projections on either end superficially resembling a pocket beach; however, the presence of pocket beaches along the Florida coast today is rare so this interpretation does not fit well into the scheme of expected beach morphology on the WFS, based on modern analogs. A more likely explanation is that the ridge is a beach that formed along a tidal marshland much like the modern-day shoreline near Ochlockonee Bay, on the panhandle of Florida, with the projections likely being tidal-shaped shoals (Appendix 3). This interpretation would fit in well to the overall pattern of coastal zonation found along the WFS. Like the modern Florida coastline, the paleocoastline between -45 and -65 m transitions from long, arcuate barrier islands in the northwest to smaller, discontinuous beaches bordering tidal marshlands as you move southeastwards.

Using an age-depth correlation to the 95% chronology Gulf of Mexico sea level curve (or Bchron) that Joy (2019) produced and an approximated relative sea level estimate of -65 to -68 m, shoreline 10 is estimated to have formed between 12.3 - 12.8 kyrs ago.

3.1.3 – Shoreline 11 – The Edges South + Steamboat Lumps

Shoreline 11 is a 24 km-long feature that lies between -70 and -76 m running NW to SE through the southern portion of the Edges and onwards into the Steamboat Lumps MPA. In addition, it appears to continue beyond the limits of the currently available bathymetry (Fig. 12). The ridge in Steamboat Lumps had previously been identified in a cursory description by

Gardner et al. (2005), but those authors were unable to draw any conclusions about its character due to a lack of data coverage and information. With the addition of new bathymetry adjacent to Steamboat Lumps, the ridge is seen to clearly extend beyond its original footprint and has the appearance of a continuous shoreline ridge. In cross section, the ridge can be seen cresting at ~ -70 m at the northern end and then plateauing off into a flattened ridge in the south at ~ -72 m. In the northern section of the shoreline, a prominent trough – approximately 100 m wide and 2 m deep – runs parallel to and just seaward of the ridge (Fig. 12B). There is also a patch of hardgrounds just landward of the northern section of the shoreline. These hardgrounds differ from those farther north, as described for shoreline 10, in that rather than being a series of well-defined ridges, these are patchier and vaguely linear features. Based on an approximate relative sea level estimate of -70 to -74 m, shoreline 11 is estimated to be between 12.9 - 13.6 ka in age.

3.1.4 – Shoreline 12 – SW Florida Middle Grounds

Approximately 40 km due east of shoreline 11, shoreline 12 makes up the area known as the SW Florida Middle Grounds (Fig. 13A). Shoreline 12 comprises of a 19.3 km-long ridge running north to south between -47 and -59 m depth that contains a main central ridge, which bifurcates on its southern end. This bifurcation likely represents a time-transgressive segment of the shoreline that evolved with multiple changing sea levels. The most prominent ridge segment in the north rises 5 meters above the surrounding seafloor to a depth of -47 m and then deepens towards the south to -55 m. The northern end of shoreline 12 is accompanied by an additional ridge less than a kilometer to its east which peaks at -42 m. Based on the close proximity and matching depth to the high-relief carbonate reefs found at the Florida Middle Grounds just to the north, we remove this shallower ridge from consideration in the analysis of paleoshorelines as it is likely a biohermal processes led to its formation rather than the coastal processes that were most likely responsible for the formation of shoreline 12 (S. Locker, *pers. comm.*, *2019*). In the south, the ridge becomes less prominent, however remains clearly visible in the sun-illuminated bathymetry (Fig. 13B). The ridge system in the south lies between -54 and -59 m and bifurcates into four north-south oriented ridges spread out >3.5 km.

Seismic reflection data of the shoreline feature assigned to shoreline 12 revealed onlapping and downlapping strata that indicate it was part of a coastal depositional system that went through multiple phases during its evolution (Fig. 14B, C). Beginning as a beach environment that was cemented through carbonate diagenetic processes, it later expanded via the progradation of spits and shallow offshore shoals into the broad, low-relief seafloor feature that we see today (Dr. Stanley Locker, *pers. comm.*, *2019*). Along with the ridges running north to south, there is also evidence of additional patches of hardground west of the feature and ridge and runnel-like features just west of the northern portion of the feature (Fig. 13C). Based on an approximate relative sea level estimate of -48 to -60 m, shoreline 12 is estimated to be between 11.0 - 11.8 ka in age.

3.1.5 – Shoreline 13 – The Elbow

About 40 km southeast of shoreline 12 lies the feature known as the Elbow, or shoreline 13 (Fig. 14A). Although this feature was described as a shoreline by Ilich et al. (2021) we include it with the newly described group herein because of unpublished subbottom seismic data that we present as evidence of the timing and formation of this feature (Fig. 14B, C). Shoreline 13 is a 16 km-long ridge between -47 and -57 m that peaks at a depth of -47 m in the north and -57 m in the south and exhibits a similar morphology to the SW Florida Middle Grounds. Due to the following observations (list the characteristics), like shoreline 12, the Elbow is interpreted as a coastal depositional system formed by spit progradation. We show modern analogs that resemble closely the overall spatial shape and form of the Elbow, with erosional cuts, small delta-like features, and sedimented back-bay regions all visible in the submerged topography (Appendix 3). The well-preserved system contains traces of what can be interpreted as a beach and dune system with the dune forming the highest points on the ridge. Based on an approximate relative sea level estimate of -50 to -56 m, shoreline 13 is estimated to be between 11.0 - 11.4 ka in age. Thus, the depth range, similarly to shoreline 12, indicates formation during the Younger Dryas cool period between 11,000-12,000 years ago.

3.1.6 – Shorelines 14, 15, 16, and 17 – Radius-Ulna

Nearly abutting the Elbow is a group of features that was previously mapped for habitat studies and named the Radius-Ulna (unpublished). It is comprised of 4 ridges, each assigned their own number and shoreline characteristics, that lie in an east to west succession with a slight NW to SE offset from one another. Shoreline 14 is the farthest east and the shallowest of the four ridge features lying between -59 and -64 m (Fig. 15A, B). It is 7.5 km-long curving from the NE to the SW, and from 0.5-1.0 km in width, it is also the widest of the features making up the Radius-Ulna. It shows a much more pronounced topography compared to the other shorelines in the area potentially indicating different sedimentary depositional conditions during formation. It can be ruled out as a potential dune of shoreline 15 just to its west because of the separation of more than 4 km between the two landforms. Based solely on its surficial expression, which consists of multiple parallel ridges, we interpret the ridge as a shoreline-parallel depositional feature. Based on an approximate relative sea level estimate of -60 to -64 m, shoreline 14 is estimated to be between 11.5 - 12.5 ka in age.

Several kilometers west of shoreline 14, shoreline 15 is a 12.6 km-long feature oriented north to south (Fig. 15A). Shoreline 15 is deeper and lies between -67 and -72 m. In cross-section, shoreline 15 does not have a strong inflexion point correlating with a dune ridge (Appendix 3). Instead, it exhibits a terrace-like profile rising above the neighboring seafloor and plateauing in a landward direction. This profile shape is consistent with mangrove terraces that occur in tropical climates, like Florida, and which have been built up by entrapment of sediments in their root structures (Bird, 2005). Its smooth, curved seaward facing front and the presence of shore-parallel ridges on its northern and southern ends are consistent with a shoreline bordering the seaward margin of a mangrove platform – much like those of the modern central west coast of Florida. It is also noted that just landward of the shoreline front, scattered along much of shoreline 15, there are additional patches of hardground. At the northern end of the shoreline, a field of bedforms <0.5 m in height with wavelengths between 100 and 300 m are scattered across an area of ~27 km^2 (Fig. 15C). Their orientation and superposition overlying the shoreline suggests (a) they were formed after the shoreline was submerged and (b) they may have been formed by an east-west moving current as this type of transverse bedform forms perpendicular to the direction of water flow (Smillie et al., 2019). Based on an approximate relative sea level estimate of -68 to -71 m, shoreline 15 is estimated to be between 12.7 - 13.2 ka in age.

Just northwest of shoreline 15, lying between -67 and -74 m depth, we mapped a new feature labeled shoreline 16. Extending 12 km, shoreline 16 consists of a relatively straight edged 6-m high terrace trending NW to SE with a ~2 m depression (moat) running parallel to and just seaward of it (Fig. 16A, B). The terrace stands prominently in the central 7.5 km portion of the shoreline and gradually loses relief towards the south. In the north, the terrace loses it definition in a similar fashion, but then reemerges as three smaller sections totaling 2 km in length. Considering shoreline 16 has a similar morphology to 15, falls within a similar depth range, and lies just 14 km from where shoreline 15 begins, in addition to the fact that the relief map of the WFS shows the -70 m isobath following along and connecting the two terraces where bathymetry is absent, it is reasonable to assume that the two were part of the same contemporary shoreline and therefore share a genetic origin. Based on an approximate relative sea level estimate of -69 to -71 m, shoreline 16 is also estimated to be between 12.7 - 13.2 ka in age.

Finally, just southwest of shoreline 16, newly-mapped shoreline 17 is a 16.4 km-long feature trending north to south between -75 and -80 m depth (Fig. 17A). Unlike the neighboring shorelines 15 and 16, shoreline 17 exhibits the characteristic ridge that is more common to submerged beach and dune systems (Gardner et al., 2007). Shoreline 17 is moderately sinuous, winding from north to south and what appears to resemble an embayment – similar to the modern-day Snake Bight on the Everglades coast - can be seen in the well-preserved outline of the feature (Appendix 3). The northern half of the ridge is narrow and is only backed by a small patch of hardgrounds where the embayment begins in the north. The southern end is more complex with a pair of rugged ridges intersecting the lower end of the shoreline at a low angle, perhaps representing a dune system or a series of prograding beach ridges (Fig. 17B and Appendix 3). Surrounding shoreline 17, are fields of bedforms both to its east and west, as well as a patchy area of hardgrounds spread out over ~ 8 km^2 (Fig. 17C). Based on an approximate relative sea level estimate of -77 to -79 m, shoreline 17 is estimated to be between 13.6 - 13.9 ka in age.

3.1.7 – Shorelines 18, 19, 20, and 21 – Northern Pulley Ridge

Shoreline 18 is a 33 km-long feature trending north to south with a pronounced ridge found between -79 and -87 m depth 85 kilometers southeast of the Radius-Ulna (Fig. 18A). Shoreline 18 comprises of an extremely well-developed and well-preserved shoreline trace with segments of either built-up dunes or mangrove platform behind a relict beachfront as well as what appear to be former tidal inlets cutting through the shoreline (Fig. 18 B, C). The shoreline is 3 to 5 m high, in profile, and the platform is at least 500 m wide at its maximum. Given the setting, we consider it more likely that the shoreline sections represent a swamped mangrove platform, based on the absence of any dunes of this size anywhere else on the modern or paleo-Florida coastline. The shoreline is mapped across two adjacent data sets that are proximal to one another (~ 8 km distance apart) and over which the continuity of the ridge is clear (the ridge is oriented in the same direction and found at the same depth on both datasets). Based on an approximate relative sea level estimate of -80 to -85 m, shoreline 18 is estimated to be between 13.8 - 14.2 ka in age.

Almost directly adjacent to shoreline 18 at its southern end, shorelines 19 and 20 are nearly parallel features that lie between 1-2 km of one another (Fig. 19A). The crest of shoreline 19 lies between -77 and -79 m, and shoreline 20 a little deeper, between -82 and -87 m. Both trend generally north to south. The ridge comprising the dominant sea-floor structure of Shoreline 19 is not as prominent as 20; it is 1 to 2 m high, whereas shoreline 20 is 2 to 5 m high. In some spots the feature is subdued so that it almost appears to be ‘washed out’ – in other sea-floor settings this is a common characteristic of a sedimented sea bed or sediment-filled basins (e.g. Dowdeswell et al., 2016). In contrast, shoreline 20’s ridge can be followed continuously almost through the entire dataset. However, the shoreline expression does appear to fade towards the northernmost section.

A likely connection can be made between shorelines 20 and 18 due to their very similar depth interval occurrence, between -80 and -87 m. While the continuity between the two is not as apparent in the bathymetry, their proximity makes it plausible enough to speculate that they were part of the same system. Based on an approximate relative sea level estimate of -77 to -80 m, shoreline 19 is estimated to be between 13.6 – 14.0 ka in age. By contrast, at -83 to -87 m, shoreline 20 is estimated to be between 13.9 - 14.3 ka in age.

The only additional feature to point out in this dataset is an area of apparent scoured out seafloor forming a cluster of bathymetric highs and lows at the southern end of shoreline 20. The scours form depressions that cover an area of approximately 2.5 km^2 just landward of the shoreline. Coinciding with a break in the shoreline ridge that would be consistent with a tidal inlet, we suggest that the depressions may be scour holes associated with the water movement that would have occurred in such a channel (Fig. 19B).

The final shoreline identified in the NOAA NMFS data sets is shoreline 21 (Fig. 20A). Shoreline 21, like shoreline 18, was mapped between two separate, but adjacent data sets, and assumed to be connected due to their similar depth range and apparent continuity. Shoreline 21 totals 11.9 km in length and lies between -86 and -94 m, forming one of the deepest features documented in our inventory. This shoreline contains two notable landform elements: the first being a hairpin-like bend at the northern end of the shoreline, and what resembles a recurved spit in the southern data set (Fig. 20B, C). The hairpin consists of two ridges that bifurcate – one in a N-S trend, and the other at a NW-SE trend. The ridge in the N-S portion has a greater relief from the surrounding seafloor and has a steeper front than the NW-SE trending ridge. The recurved spit is expressed as a curved and widened sediment body at the end of a narrow, straight and segmented ridge. While there are no scour marks behind the ridge at any of the breaks like in shoreline 20, it is possible that some of the discontinuity could be due to cross-cutting tidal inlets or perhaps simply post-depositional erosion related either to subaerial processes (e.g., wind, storms) or reshaping by subsequent sea level rise. Nearly identical morphologies can be found on the modern coasts of Cayo Costa, FL and Cape Henlopen, DE (Appendix 3). Based on an approximate relative sea level estimate of -85 to -88 m, shoreline 21 is estimated to be between 13.9 - 14.3 ka in age.

3.1.8 – Shorelines 22, 23, and 24 – Southern Pulley Ridge

Although the bathymetric expression of Pulley Ridge has previously been described by Jarrett et al. (2005), Allee et al. (2012), and Reed et al. (2019), the full extent of the feature has not been analyzed in detail in the context of paleoshorelines or the geological formation of the seafloor structures in the region (Fig. 21). Allee et al. (2012) previously stated there were paleoshorelines at -65, -70, and -80 m. These rounded depth values are based on the ridge height of the shorelines. In this study, we reanalyzed the shoreline features and suggest they can be more accurately and completely described as follows: shorelines 22, 23, and 24 are sequentially stepping shorelines that span >900 km^2 in the -65 to -88 m depth zone at the southwestern edge of the WFS. Shoreline 22 lies on the eastern side of Pulley Ridge and is a 35 km-long feature located between -65 and -73 m depth. It's resemblance to the modern-day barrier island 'drumstick' morphology has previously been described by Jarrett et al. (2005), and using seismic subbottom data they confirmed the stratigraphic history of the feature indicates it was a former shoreline. Based on an approximate relative sea level estimate of -62 to -67 m, shoreline 22 is estimated to be between 11.8 - 12.7 ka in age.

Shoreline 23 is a 22.2 km-long feature running between -70 and -76 m just 2 km west of shoreline 22. Shoreline 23 is not marked by a pronounced ridge like many other paleoshorelines, however its presence is made apparent in cross section by a low-relief inflexion in profile that can be traced from -72 m at the northern end of the feature, deepening to -75 m at the southern end. Just landward of shoreline 23 leading to the base of shoreline 22, the seafloor is comprised of a series of low-relief ridges presumed to have formed at intermediary sea levels between shorelines 22 and 23. Despite its lack of a prominent ridge, we suggest that shoreline 23 is linked to the same sea level stand that created shorelines 11, 15, and 16, documented previously, and shoreline 27 described beneath (Marquesas Key). Based on an approximate relative sea level estimate of -74 to -77 m, shoreline 23 is estimated to be between 13.2 - 13.8 ka in age.

Shoreline 24 is 15.8 km long and lies between -80 and -88 m at the western edge of Pulley Ridge 15 km west of shoreline 23. The ridge crest lies at -80 m at the northern end and -83 m at the southern end. Landward of shoreline 24 and stretching as far back as 13 km, are a multitude of beach ridges that have been remarkably well preserved. Cross-cutting this ridge plain are several ~ 1 m deep channels that resemble meandering river channels, as well as a series of parallel, north-south oriented streaks that we suggest may be a result of sediment reworking by the north-south flow of the Loop Current in this area (Fig. 22). It has been shown that the Loop Current interacts with the southern edge of the WFS, which could explain the sediment patterns seen (Weisberg and He, 2003); moreover, it is believed to be one of the reasons that a uniquely deep hermatypic reef exists at Pulley Ridge because it pumps clear, nutrient-poor waters over the region where more turbid, nutrient-rich waters would otherwise reside and inhibit a coral reef from thriving (Jarrett et al., 2005). The expanse of ridges seaward of shoreline 24 all fall within the same 4 m depth range centered around 81 m which indicates that some time ~13.8 - 14.2 ka sea level must have been stable for long enough to allow for extensive progradation of this shoreline.

3.1.9 – Shorelines 25, 26, and 27 – Marquesas Key

The last and most southerly set of paleoshorelines observed on the WFS are shorelines 25, 26, and 27. Shorelines 25, 26, and 27 are parallel, sequentially stepping landforms that become deeper with every step, and are found offshore of Marquesas Key on the southern edge of the shelf (Fig. 23A). Shoreline 25 is the shallowest of the shorelines lying between -62 and -64 m. A further 1.5 km downslope, shoreline 26 lies between -65 and -69 m depth. Finally, separated by just 0.5 km from shoreline 26, shoreline 27 lies between -69 and -73 m. Shoreline 25 notably has the most well-defined ridge of the three shorelines. It consists of the main ridge front, 3-m high and 100-m wide. On its landward side, the sea floor is composed of closely spaced parallel ridges (Fig. 23B). Shoreline 26 is defined by a distinct ridge that we suggest has been partially covered with sediment on its western half (Fig. 23B), and completely buried by sedimentation on its eastern half (Fig. 23C). Shoreline 27 was either completely inundated with sediment or was eroded down after its formation into a shallow shoal. Considering the adjacent shoreline 26 shows evidence of burial, it is reasonable to assume that this is also the case for shoreline 27. Based on an approximate relative sea level estimates of -62 to -72 m, shorelines 25, 26, and 26 are estimated to be between 11.8 - 13.3 ka in age.

3.2. Shoreline Inventory: Spatial and Geomorphological Characteristics

The description and collation of the new shoreline features as described previously, with existing observations of submerged shorelines on the shelf, allows for a wider view of WFS former sea level markers to be quantified and assessed.

As a single population, the mapped shoreline features show a broadly bi-modal distribution (Fig. 24B) The landforms break apart into two apparent clusters with peaks in modern water depths at approximately -60 and -80 m respectively. Although we have assessed bathymetry from a wide range of depths in this study, the clustering of shorelines appears relatively narrow. Our deepest shorelines are found at ~ -90 m, and are relatively few.

We plotted the shorelines together, northwest to southeast, depicting a view of the individual depth distribution of landforms across the entire WFS (Fig. 25). There are three phases of shoreline evolution evident in this visualization: (i) an initial zone of shorelines, located spatially towards the SE, found in a depth range of ~ 75-90 m (Fig. 25, green), (ii) an intermediary, relatively barren zone of shelf that contains only a few shorelines from 65-75 m (Fig. 25, white), and (iii) a shallow 50-62 m zone of shorelines, dominantly clustered in the NE of the shelf (Fig. 25, blue). Overall, there is a notable north to south deepening trend in the shoreline inventory, with the deepest shorelines existing in surveys farther south on the shelf.

Fig. 26 shows similar data, with individual median depths of ridges plotted as a function of latitude. There is a correlation between the two parameters (R-squared = 0.284), with the exception of a few slightly shallower shorelines that are located to the far south of the study region.

Table 1: Paleoshoreline metrics including: length, average ridge depth, inferred relative sea level, and location. Italicized names are common names associated with paleoshorelines or datasets.

	Shoreline	Length (km)	Average ridge Depth (mbsl)	Relative Sea Level (mbsl)	Latitude	Longitude
DeSoto Canyon	1	8	56	55-60	29.915	-87.203
	2	20	55	55	30.118	-86.894
	3	5.2	59	57-60	30.080	-86.706
Destin Ridges	4	5.5	60	57-62	29.998	-86.514
	5	16.6	63	60-64	29.714	-86.246
	6	9.3	55	53-58	29.387	-85.948
	7	15.8	65	64-68	29.315	-85.896
	8	11	63	65	29.281	-85.725
	9	7	80	80-85	29.165	-85.715
Twin Ridges + The Edges (North)	10	26.2	66	65-68	28.984	-85.369
The Edges (South)	11	36.7	72	70-74	28.350	-84.827
The Mustache	12	19.3	54	48-60	28.320	-84.348
The Elbow	13	16	53	50-56	27.750	-84.180
Radius-Ulna	14	7.5	61	60-64	27.456	-84.001
	15	12.6	70	68-71	27.415	-84.053
	16	12	70	69-71	27.625	-84.224
	17	16.4	77	77-79	27.350	-84.249
Northern Pulley Ridge	18	24.6	83	80-85	26.502	-83.791
	19	11.9	79	77-80	26.136	-83.719
	20	19.4	84	83-87	26.088	-83.725
	21	11.9	88	85-88	25.363	-83.705
Southern Pulley Ridge	22	35	66	62-67	24.842	-83.676
	23	22.2	75	74-77	24.825	-83.695
	24	15.8	82	80-87	24.882	-83.831
The Florida Keys	25	8.7	63	62-64	24.423	-82.304
	26	9.5	66	65	24.415	-82.293
	27	6.2	71	70-72	24.437	-82.208

Table 2: Estimated shoreline ages based on depth, comparing results from a Bchron 95% chronology (derived from Joy, 2019).

Shoreline		Relative Sea Level (mbsl)	Age based on Bchron 95% chronology (ka)
DeSoto Canyon	1	55-60	11.1 – 11.9
	2	55	11.1 – 11.4
	3	57-60	11.3 – 11.9
Destin Ridges	4	57-62	11.3 – 12.2
	5	60-64	11.5 – 12.5
	6	53-58	11.0 – 11.6
	7	64-68	12.2 – 12.8
	8	65	12.3 – 12.5
	9	80-85	13.8 – 14.2
Twin Ridges + The Edges (North)	10	65-68	12.3 – 12.8
The Edges (South)	11	70-74	12.9 – 13.6
SW Florida Middle Grounds	12	48-60	11.0 – 11.8
The Elbow	13	50-56	11.0 – 11.4
Radius-Ulna	14	60-64	11.5 – 12.5
	15	68-71	12.7 – 13.2
	16	69-71	12.7 – 13.2
	17	77-79	13.6 – 13.9
Northern Pulley Ridge	18	80-85	13.8 – 14.2
	19	77-80	13.6 – 14.0
	20	83-87	13.9 – 14.3
	21	85-88	13.9 – 14.3
Southern Pulley Ridge	22	62-67	11.8 – 12.7
	23	74-77	13.2 – 13.8
	24	80-87	13.8 – 14.2
The Florida Keys	25	62-64	11.8 – 12.4
	26	65	12.3 – 12.5
	27	70-72	12.9 – 13.3

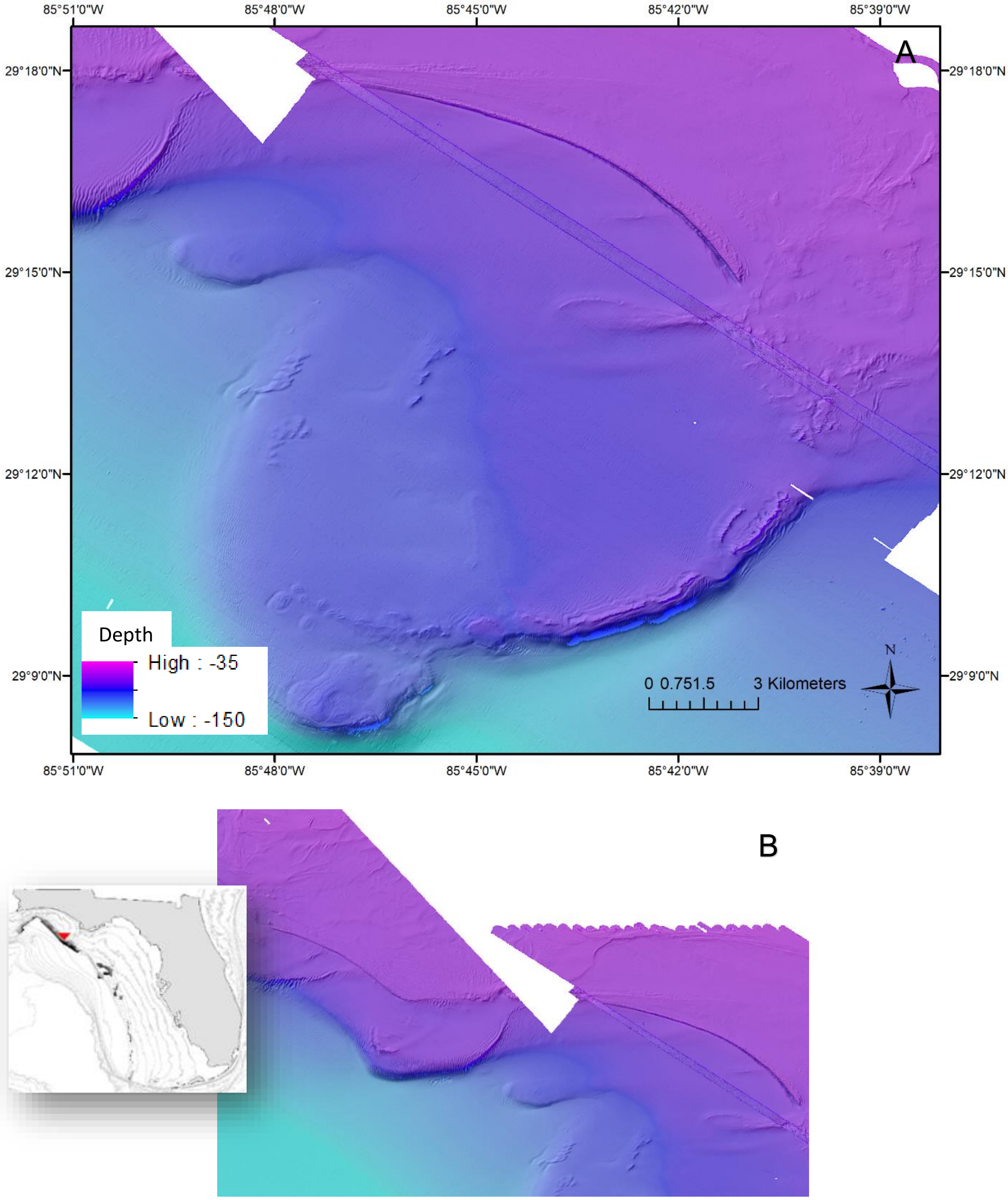

Figure 9: (A) The Madison Swanson shelf-edge delta with shoreline 8 (top) running NW to SE, and shoreline 9 (bottom) running SW to NE. (B) Zoomed out perspective (showing data outside of box A) illustrating that shoreline 8 is most likely an eastern continuation of shoreline 7 to it's west; data gap obscuring the connection; location shown with red arrow on WFS map, *left*.

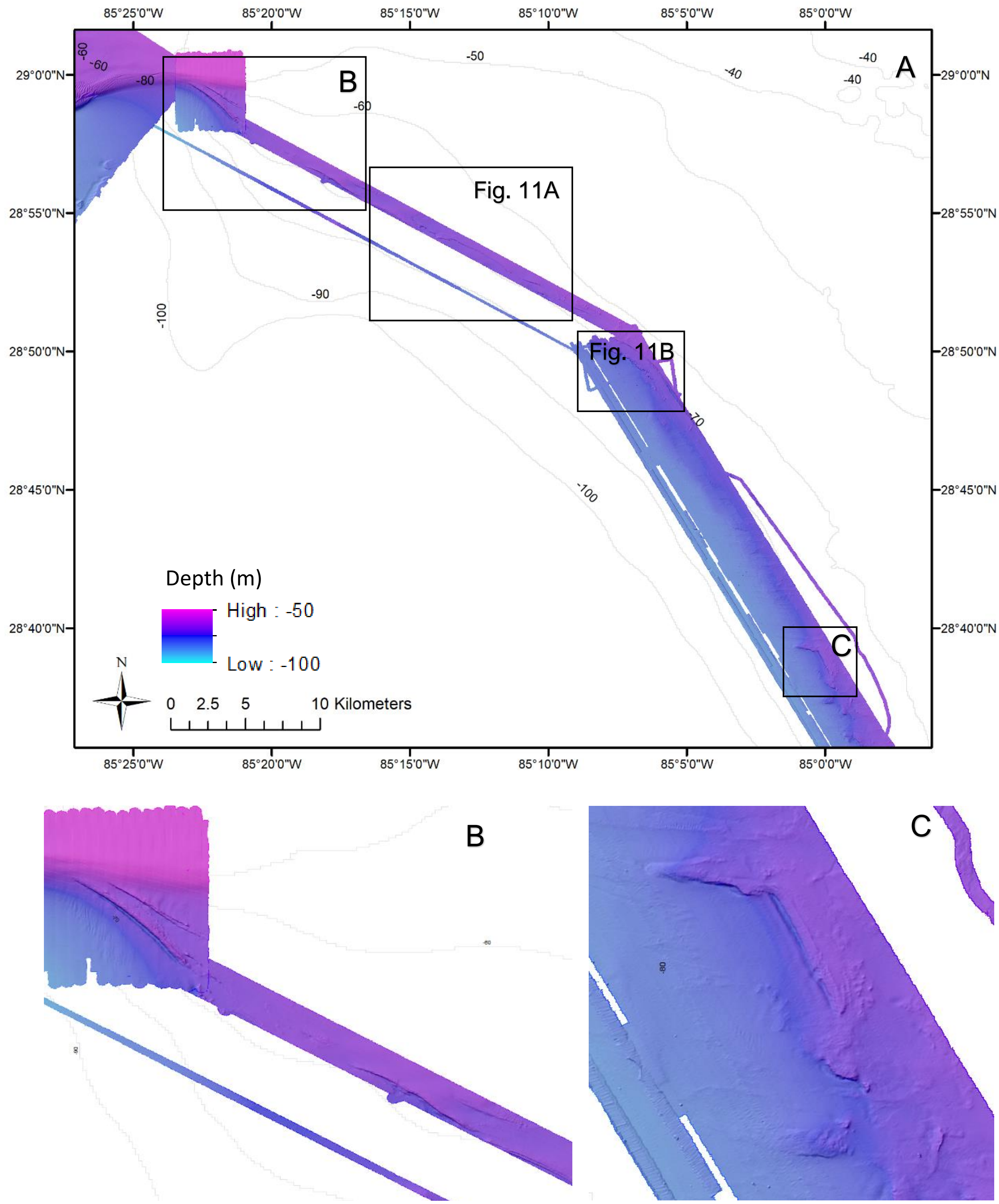

Figure 10: (A) Segments along the narrow corridor making up Shoreline 10. (B) Close-up showing the alignment between Twin Ridges and new, neighboring bathymetry along the 65 m isobath. (C) Pocket beach-like feature (Following figure) Close up of segments of shoreline 10.

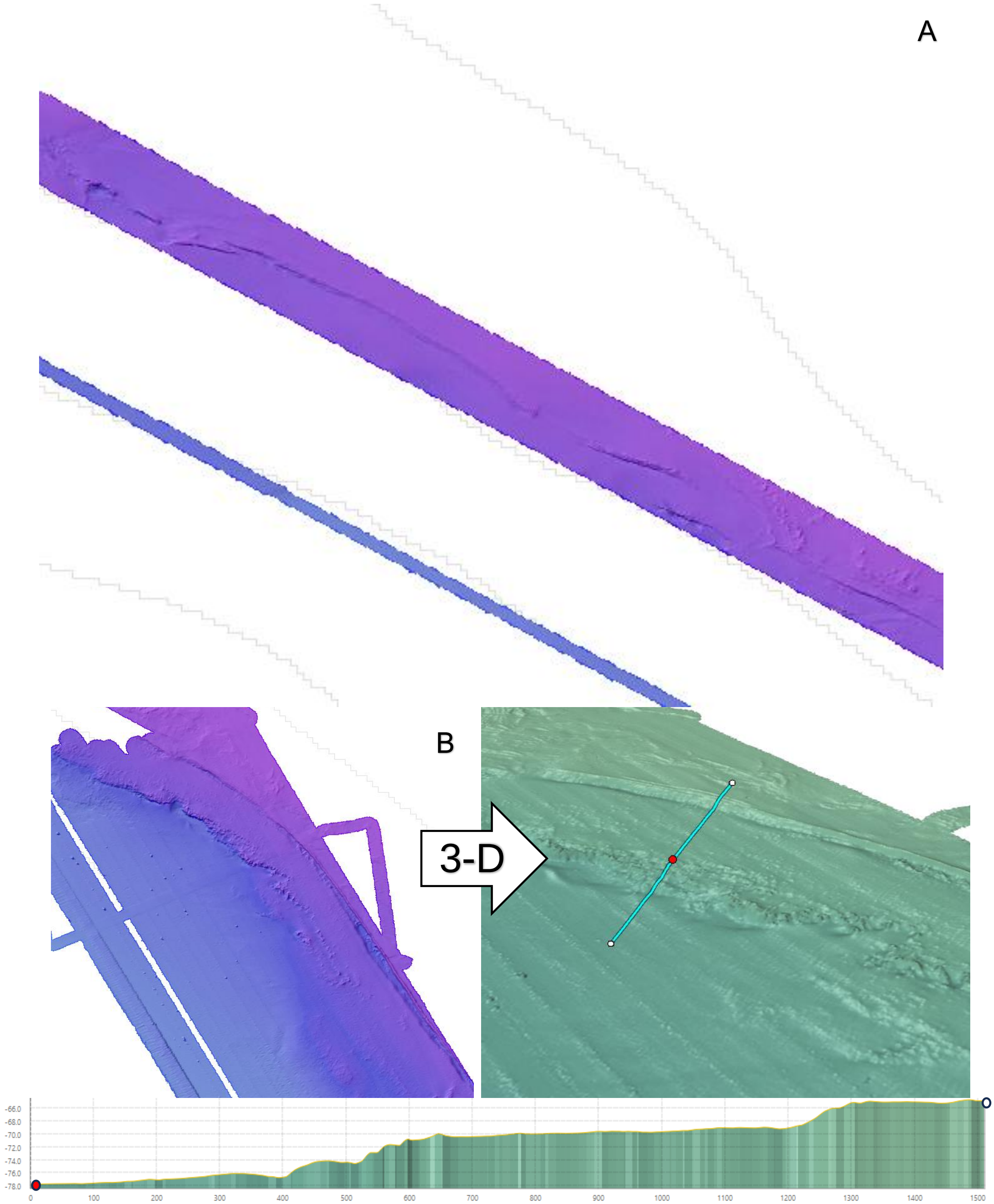

Figure 11: (A) Shoreline 10 ridge segments and hardgrounds. (E) An arcuate shoreline running along the eastern edge of the bathymetry with an adjacent 'offshore' feature ~5 meters deeper and just over half a kilometer away. Rugged topography suggests it could be similar to hardgrounds described by Obrachta et al. (2003). Blue profile = cross-section, *below*.

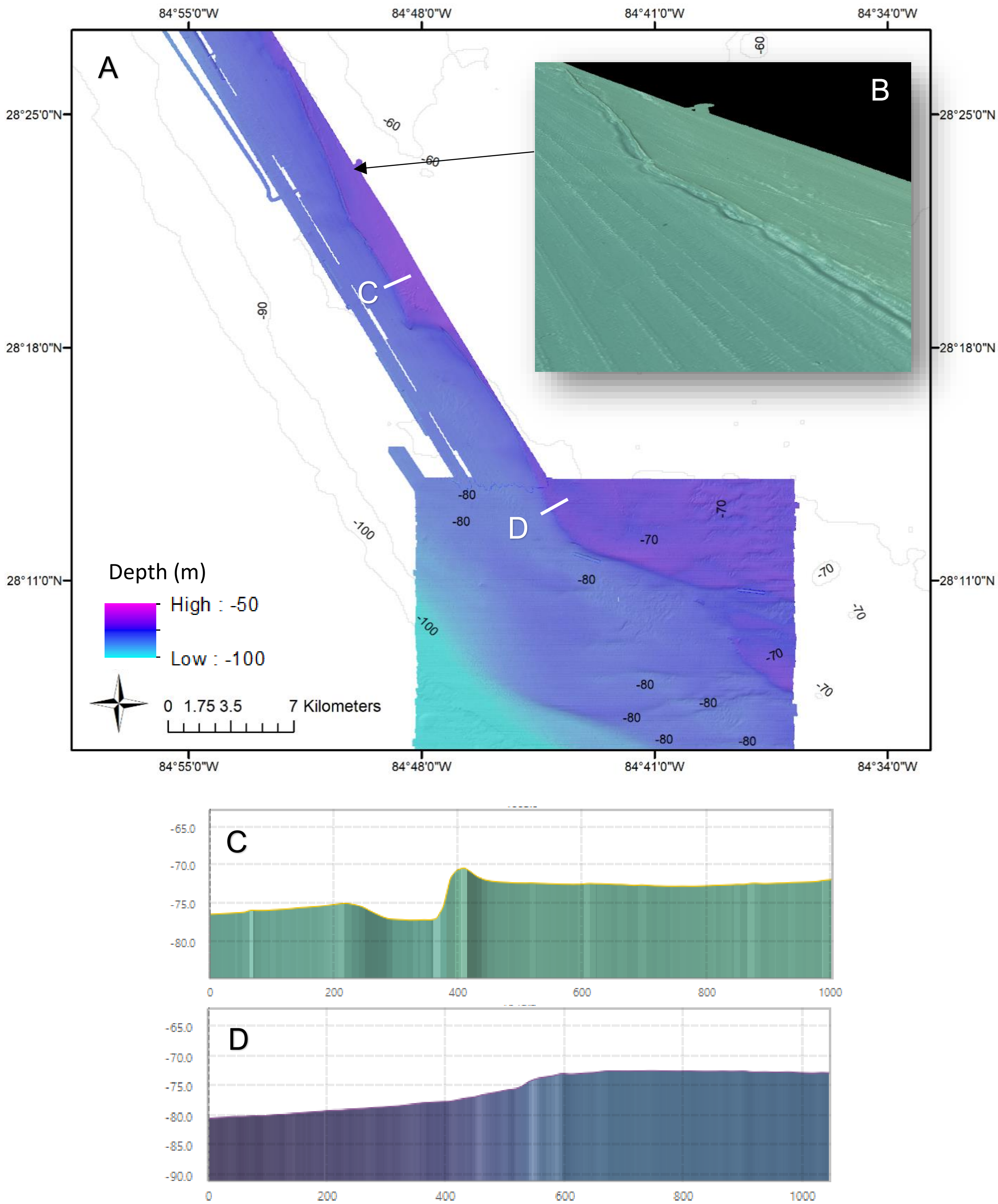

Figure 12: (A) Shoreline 11 – The Edges and Steamboat Lumps MPA's. (B) 3D close-up of trough running parallel to ridges on seaward side. (C,D) Cross-sections (10x exaggeration) through shoreline 11 showing a prominent ridge and seaward depression in the north which becomes more rounded and smooth to the south.

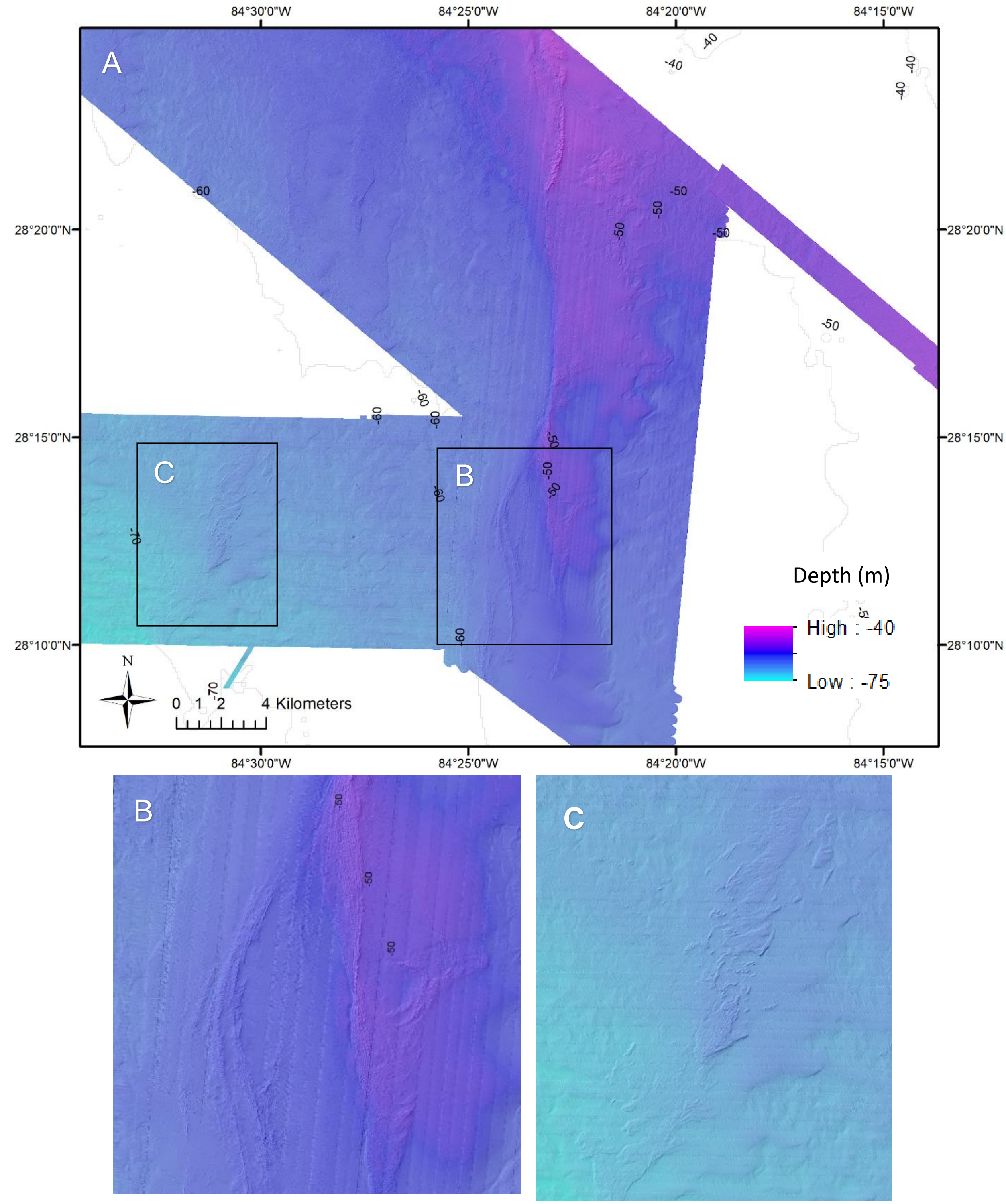

Figure 13: (A) Shoreline 12 – SW Florida Middle Grounds. (B) Close-up of the spit-like structure on shoreline 12. (C) Previously undescribed hardground features.

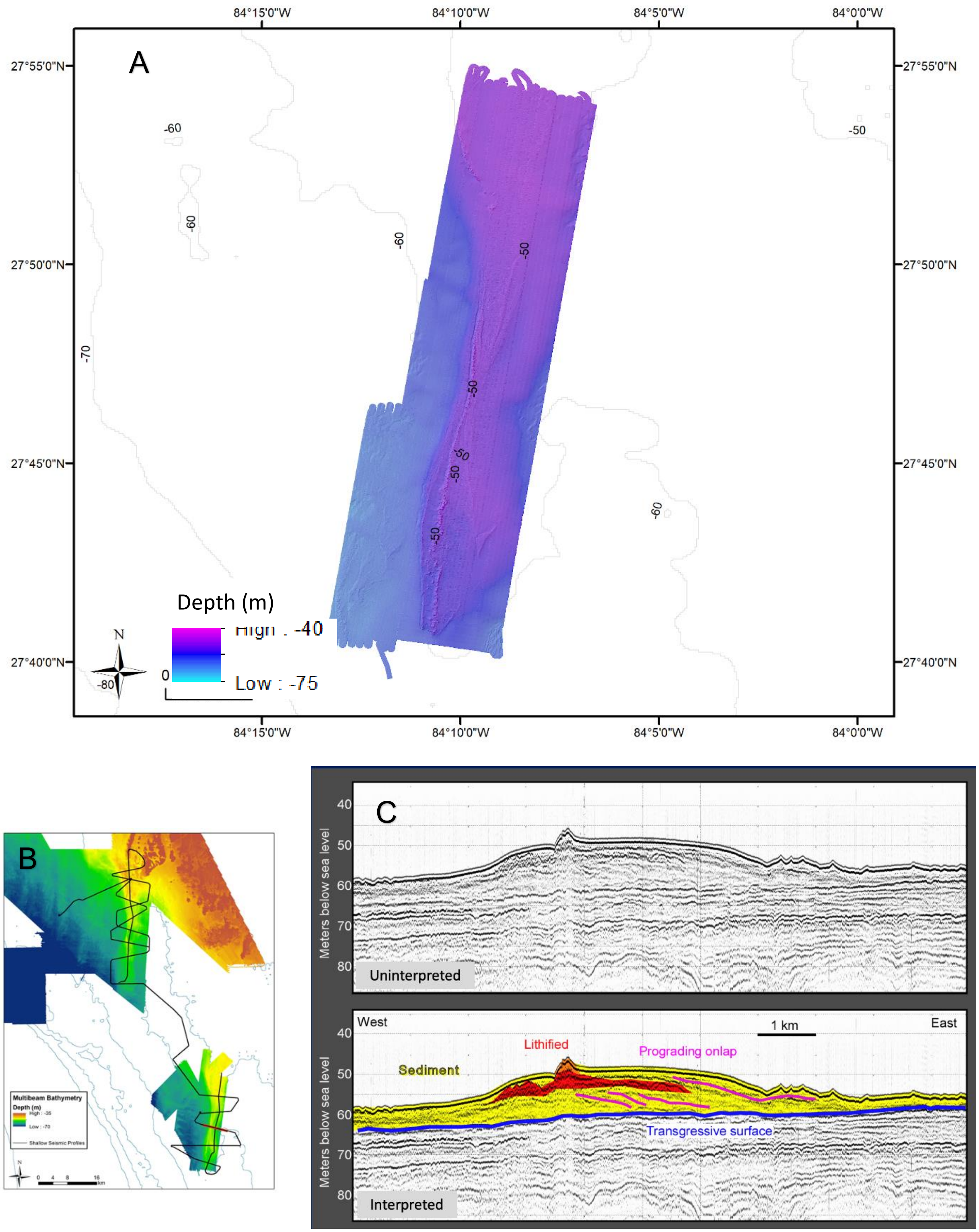

Figure 14: (A) Shoreline 13 – The Elbow. (B) Seismic profile track line over the SW Florida Middle Grounds and The Elbow from July-August 2018. (C) Interpretation of subbottom profile of The Elbow indicates the feature is a coastal spit structure containing probable beachrock and non-marine beach deposits (Dr. Stanley Locker, pers. comm.).

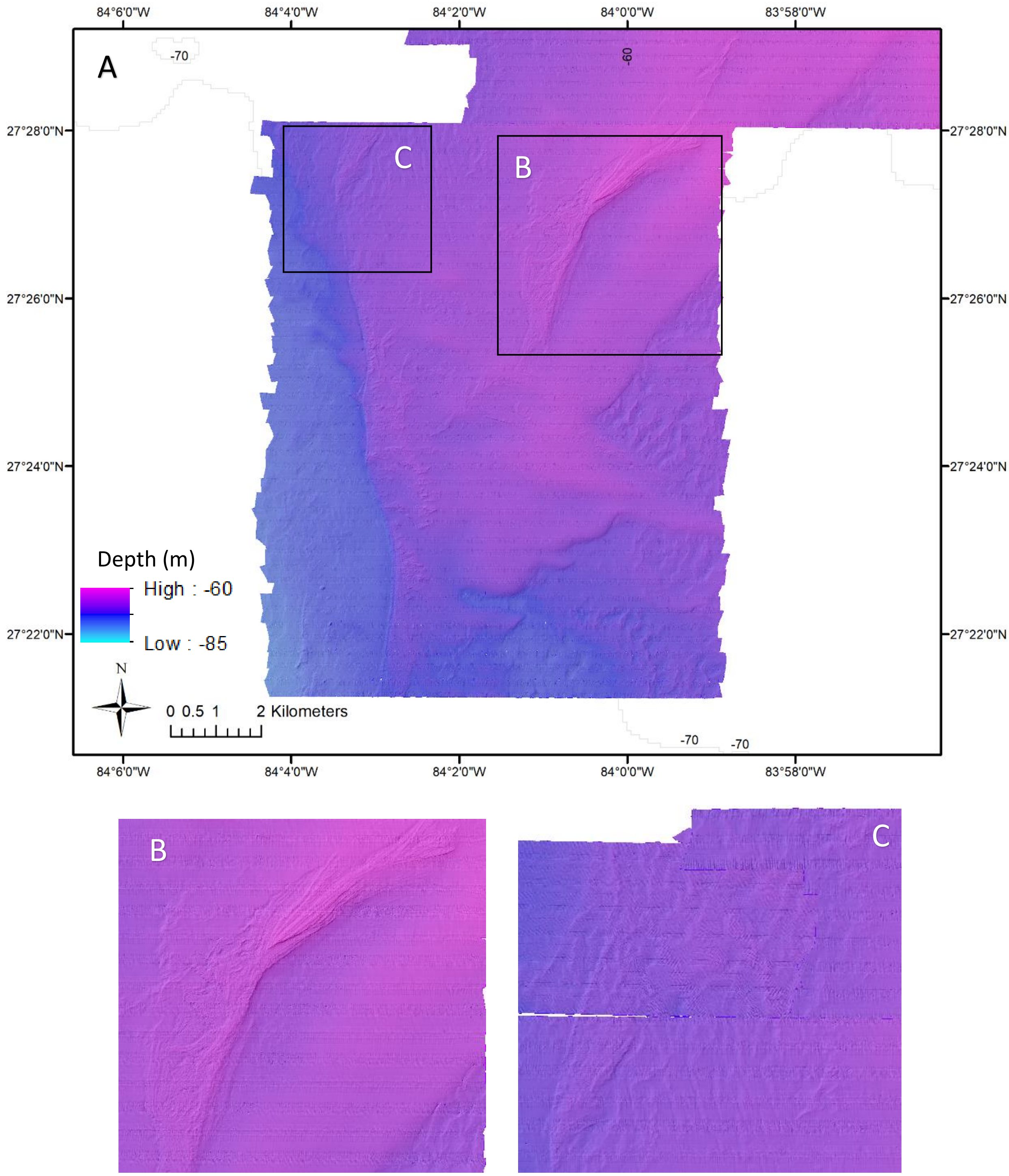

Figure 15: (A) From east to west: Shorelines 14 and 15 – The Radius-Ulna. (B) Close-up of the ridge in shoreline 14. (C) Bedforms surrounding the northern end of shoreline 15.

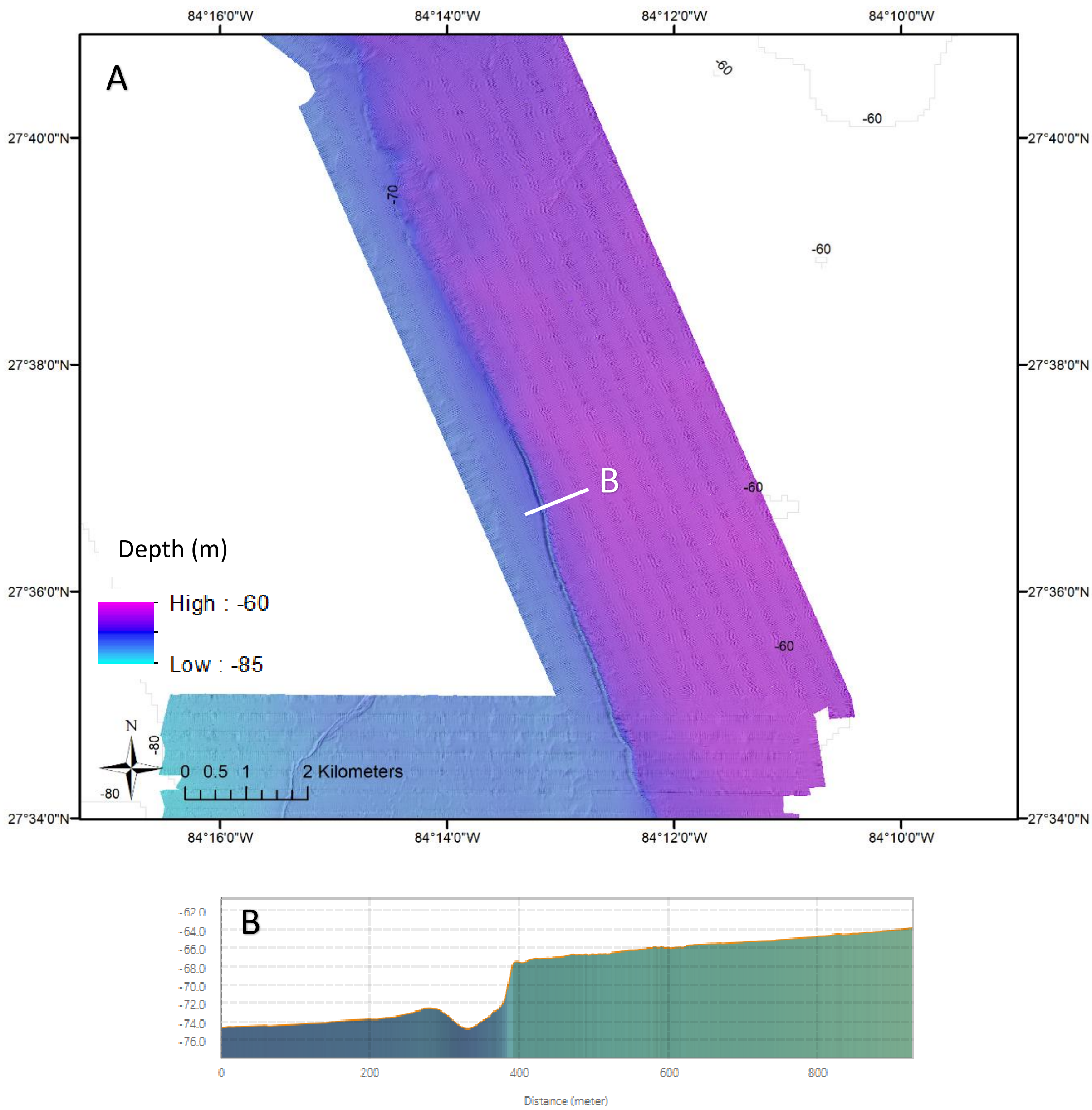

Figure 16: (A) Shoreline 16 – Radius-Ulna. (B)Cross-section showing the terrace that is speculated could be a former mangrove platform.

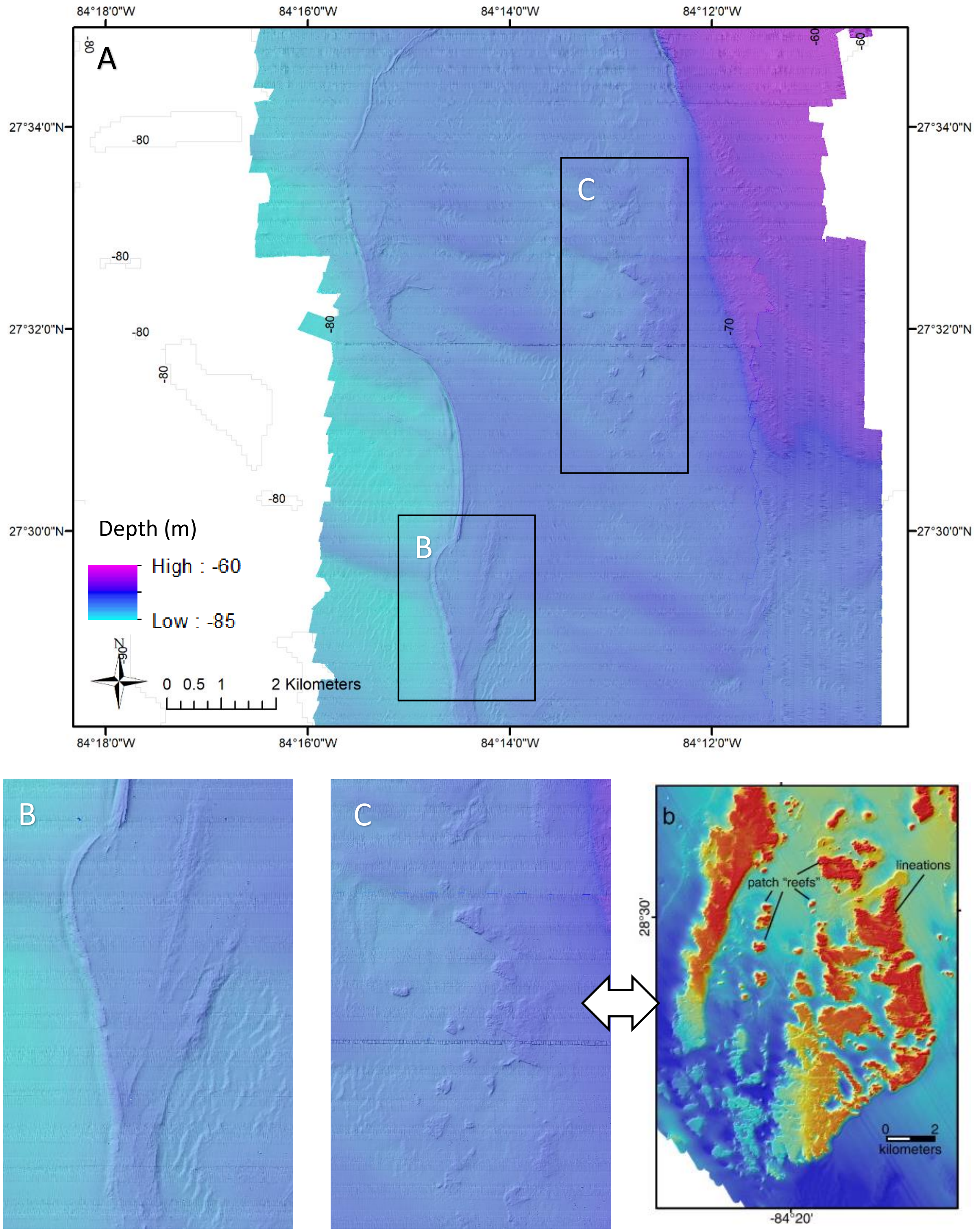

Figure 17: (A) Shoreline 17 - Radius-Ulna. (B) Back ridges intersecting the main front of Shoreline 17 plus some of the surrounding bedforms. (C) Patchy hardgrounds landward of shoreline 17 (*left*); comparison to features identified as "patch reefs" in the Florida Middle Grounds (*right*, figure from Mallinson et al., 2014).

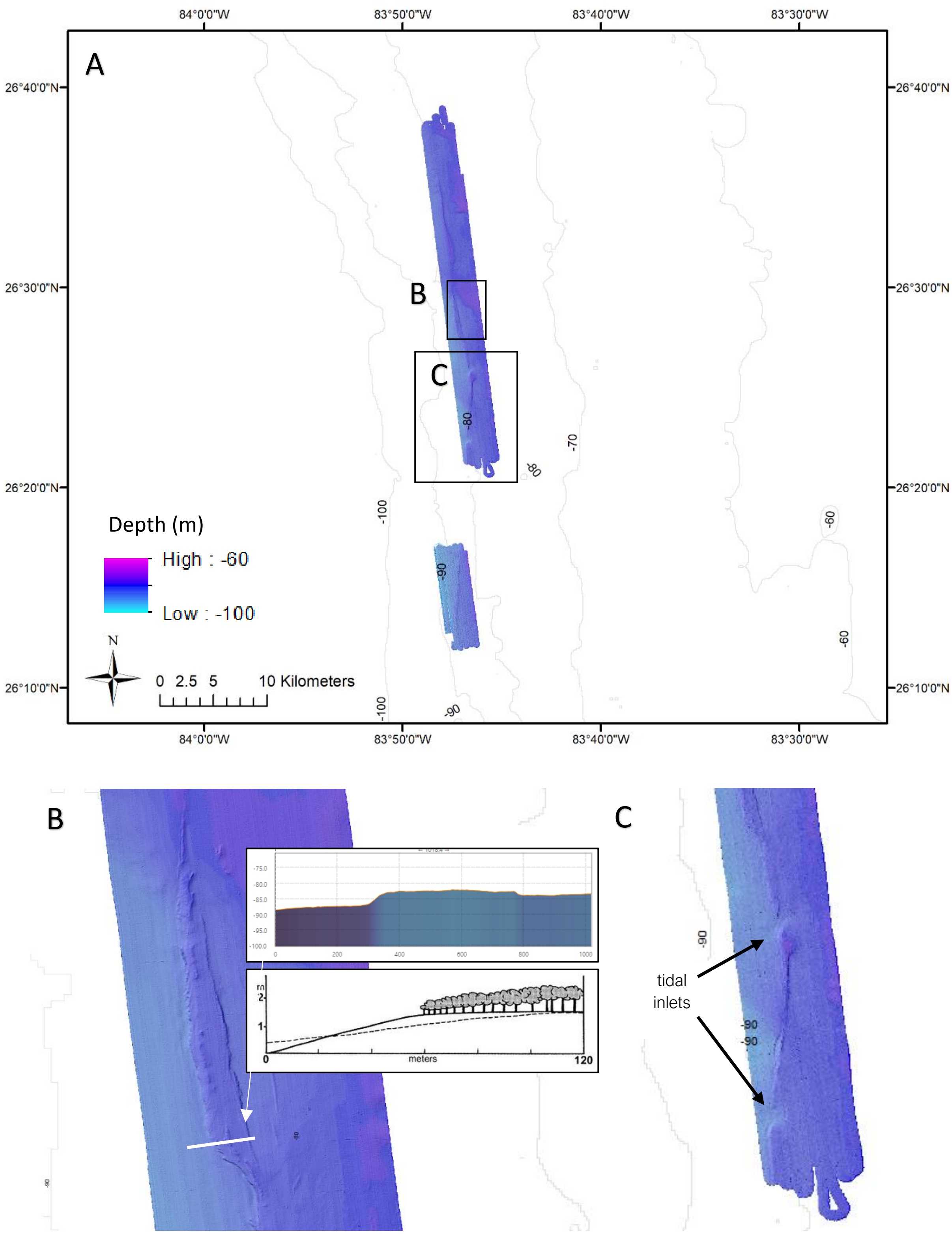

Figure 18: (A) Shoreline 18 – Northern Pulley Ridge. (B) Built up segments of shoreline which may correspond to a mangrove platform (10x exaggeration profile, *top*); comparison with schematic of a mangrove platform from Bird (2005), *bottom*. (C) Breaks in the shoreline that may correspond to ancient tidal inlets that had cut through the shoreline.

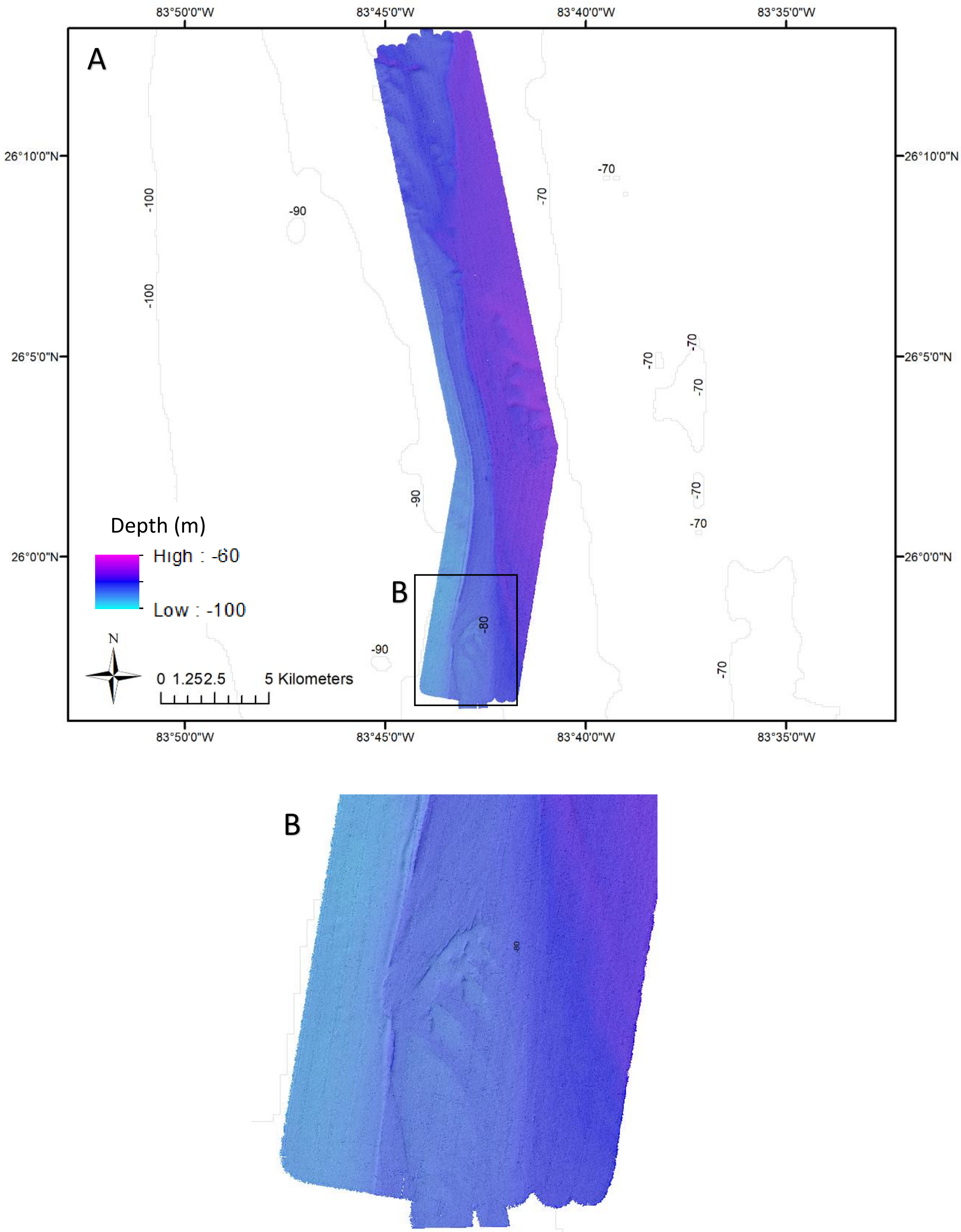

Figure 19: (A) From east to west: Shorelines 19, 20 – Northern Pulley Ridge. (B) Depressions occurring behind shoreline 20 and coinciding with a break in the shoreline ridge suggesting a potential overwash fan or lagoonal deposit.

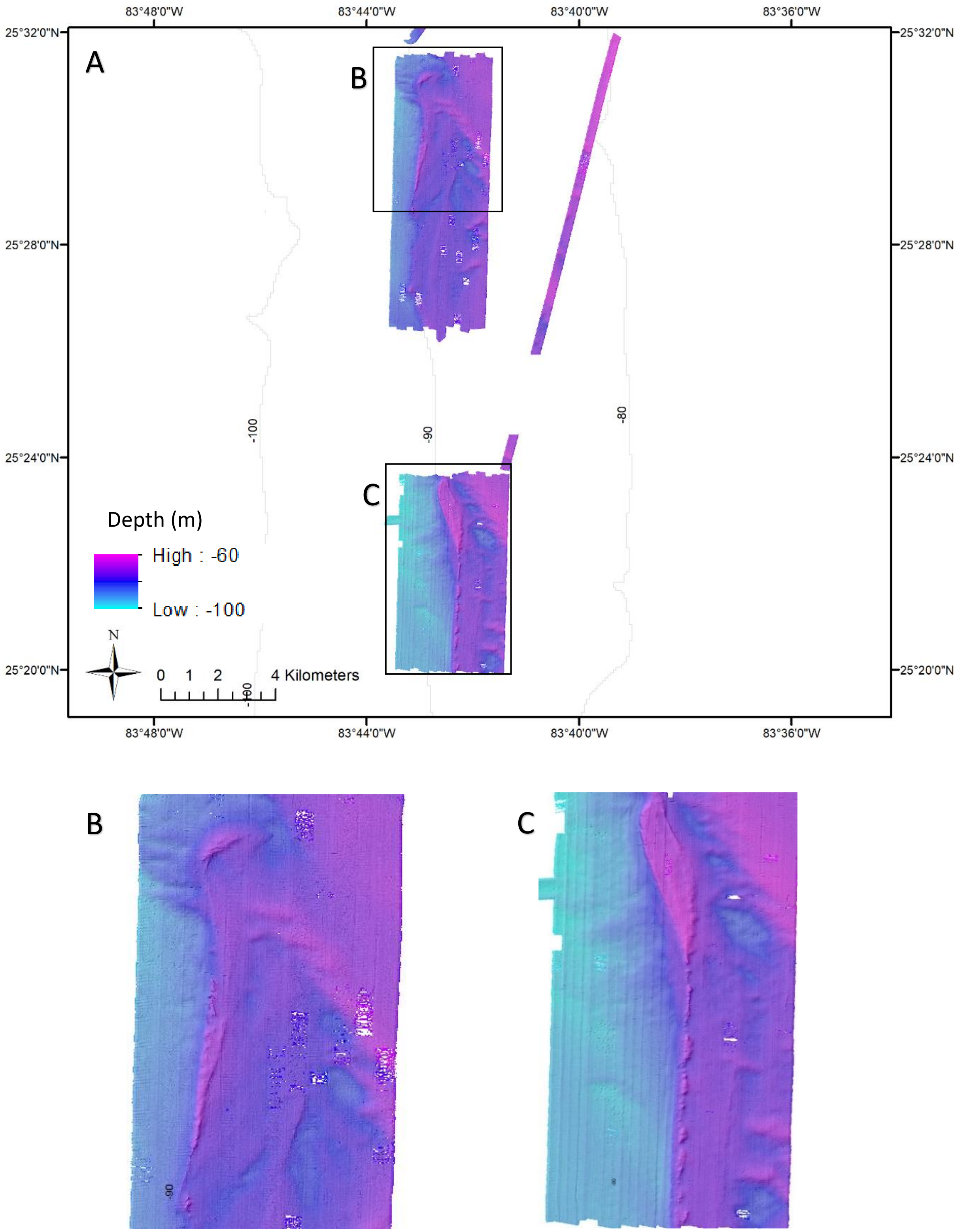

Figure 20: (A) Shoreline 21 – Northern Pulley Ridge. (B) Hairpin bend and (C) recurved spit structures.

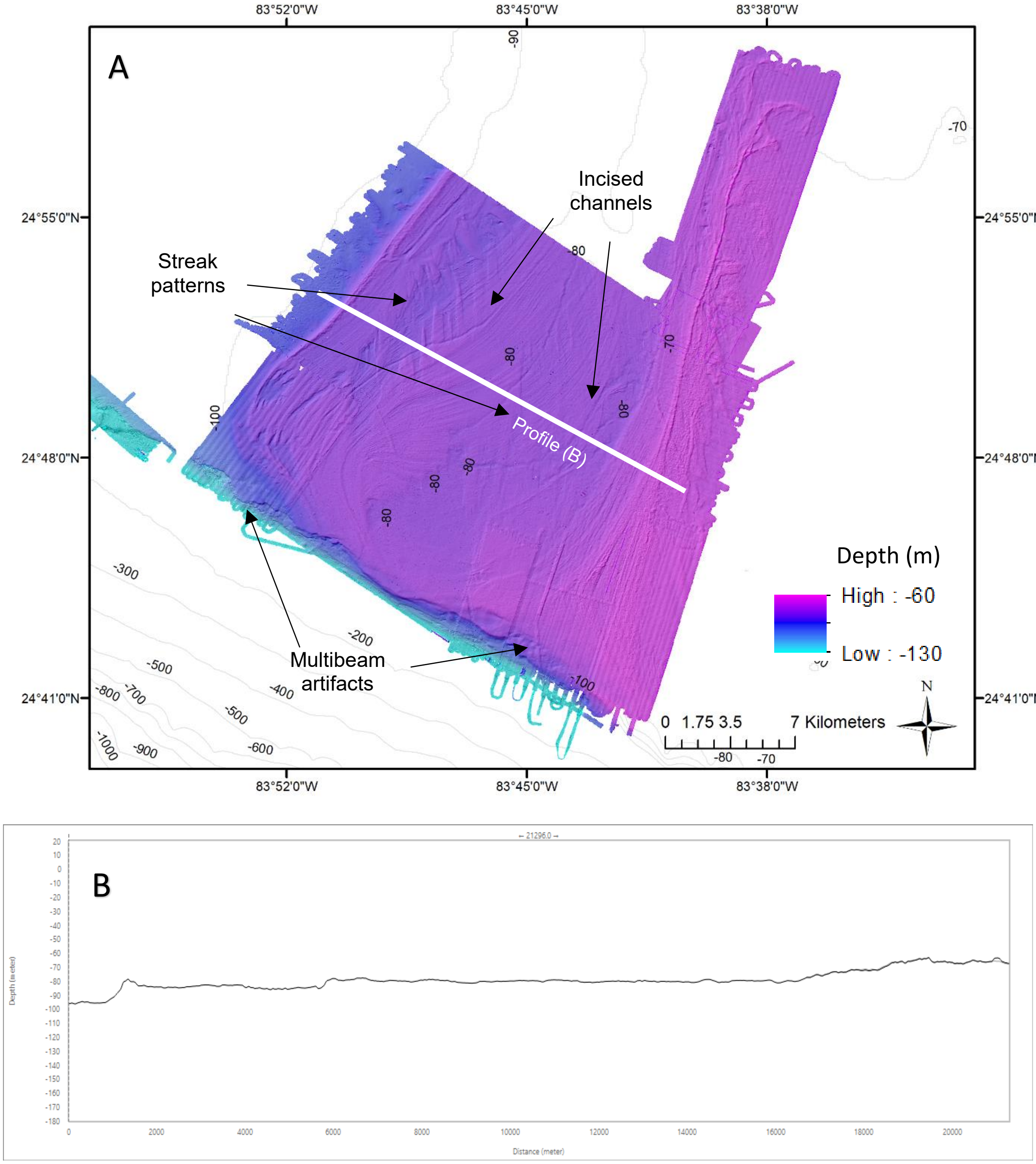

Figure 21: (A) Shorelines 22, 23 and 24 at Southern Pulley Ridge. Parallel lines on the southwestern and southeastern corners are artifacts in the multibeam data from ship tracks. (B) Profile across shorelines 22-24 at 20x vertical exaggeration.

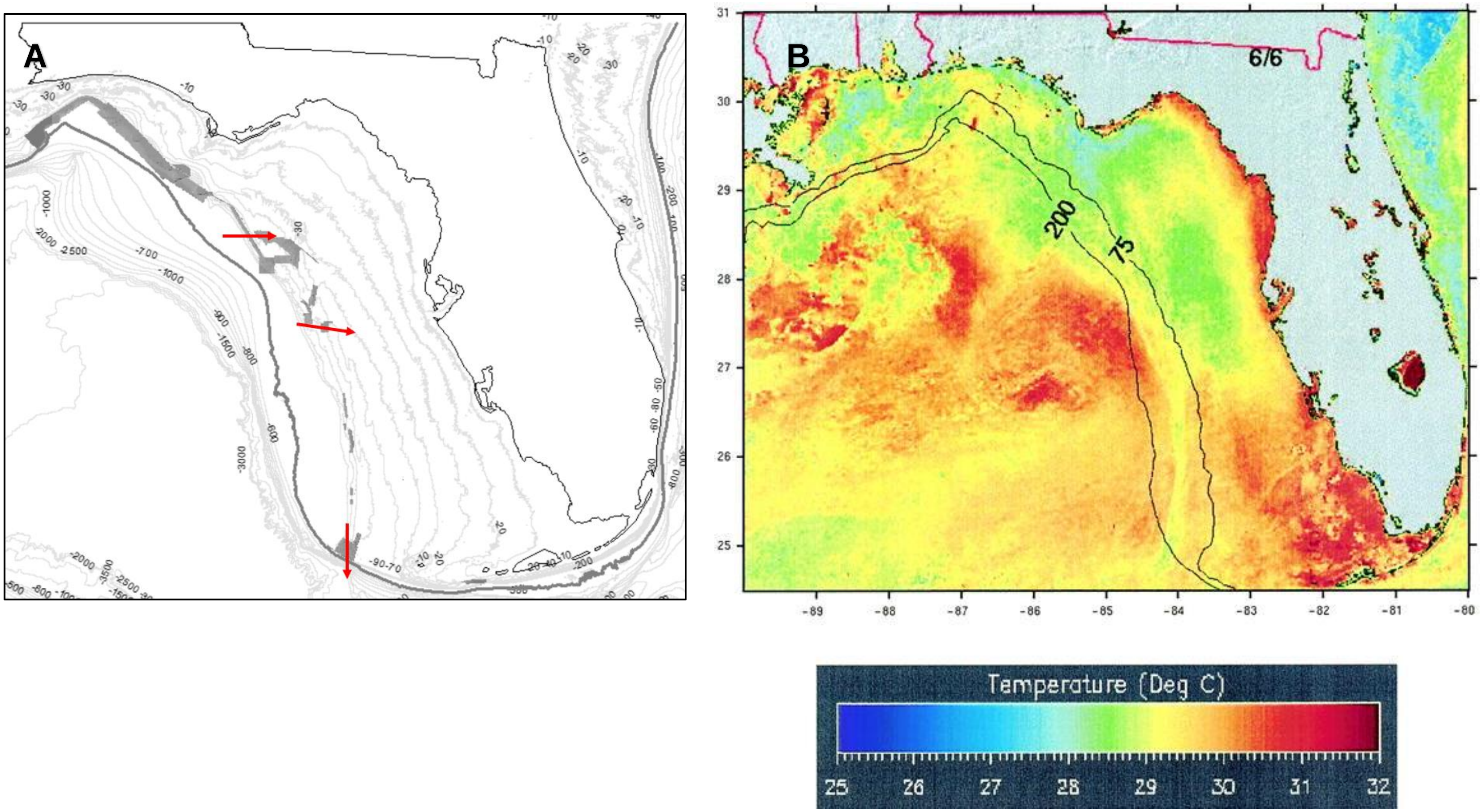

Figure 22: (A) Vectors showing orientation of sedimentary bedforms and seabed striations seen in the bathymetry that are suggested to be connected to the flow direction of the Loop Current. (B) Sea surface temperature (SST) on June 6, 2000 obtained (with permission) from the Applied Physics Laboratory at the Johns Hopkins University. High temperatures (in red) indicate the penetration of the Loop Current front onto the WFS (Weisberg and He, 2003).

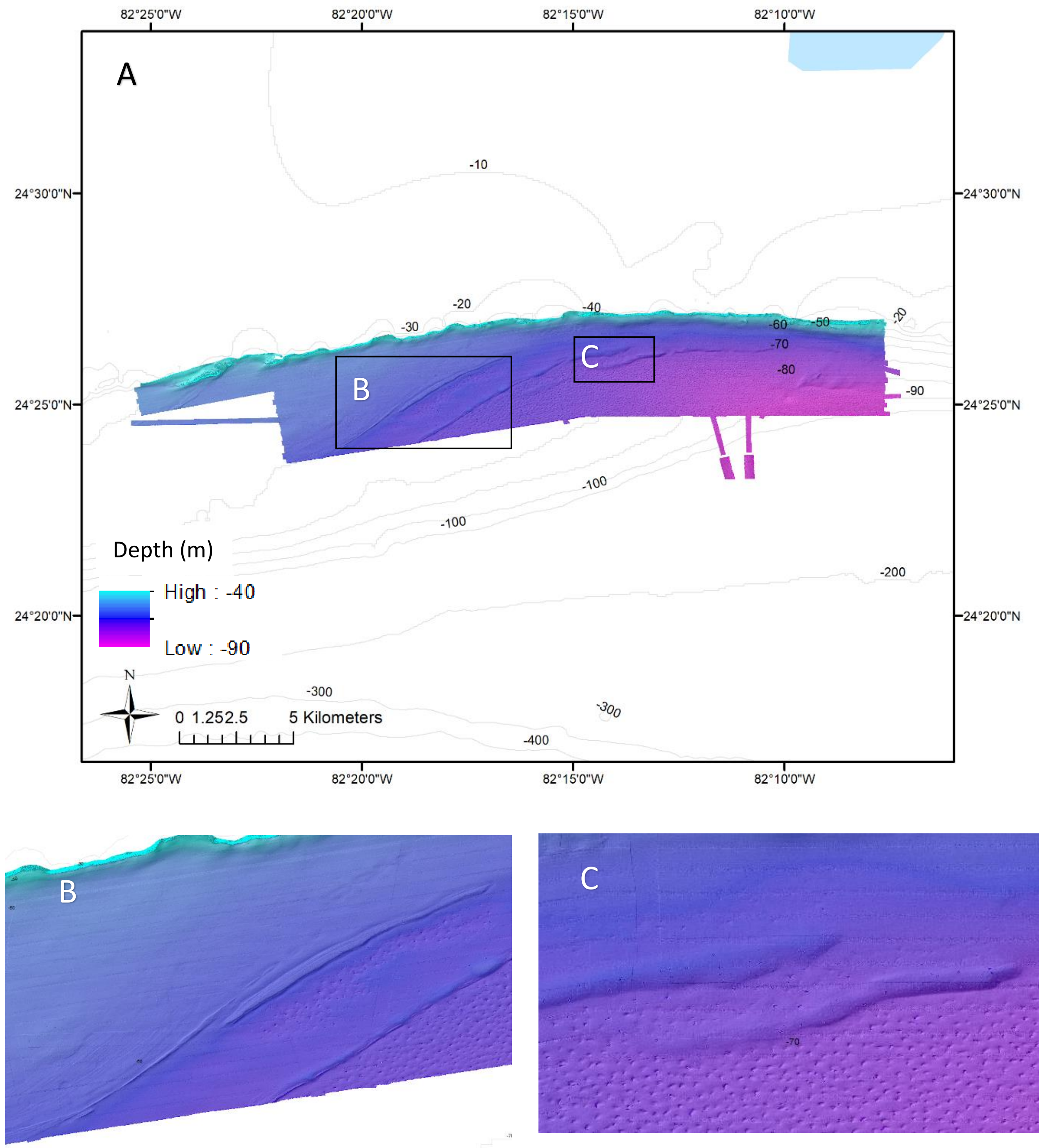

Figure 23: (A) From north to south: Shorelines 25, 26, 27 – Marquesas Key. (B) Shoreline 25 close up showing well-defined ridge, and a portion of shoreline 26 showing the partially covered ridge. (C) Shorelines 26 and 27 close up showing lower relief of ridges.

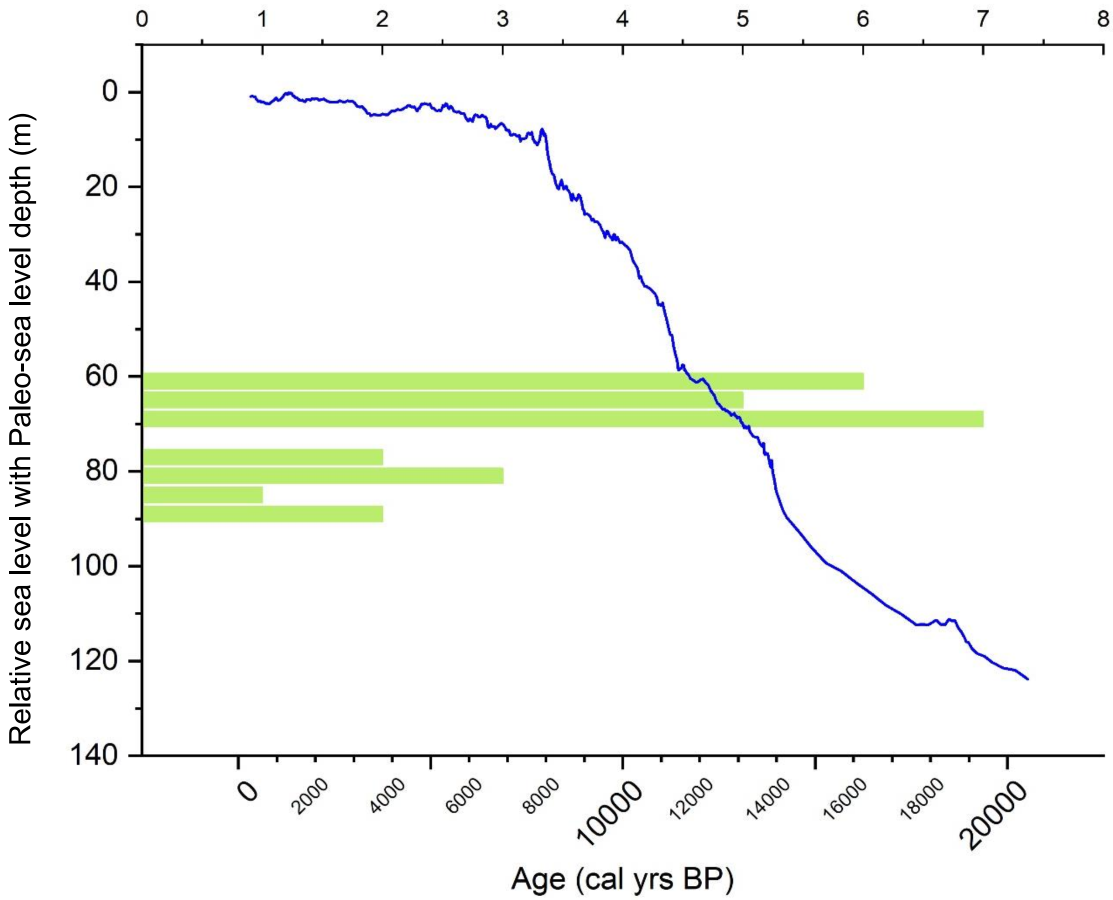

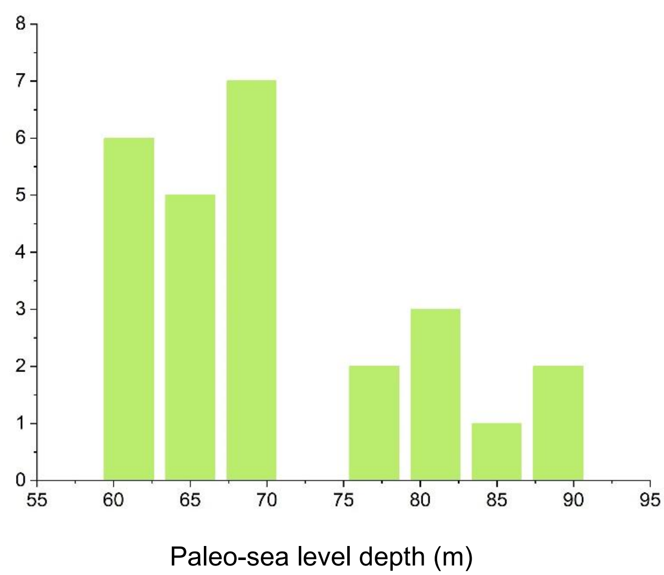

Figure 24: (A) 9-point moving average for post-LGM Gulf of Mexico sea level curve (*in blue*, data derived from Joy, 2019) with a histogram of paleo-sea levels - as derived from paleoshoreline depths - on the west Florida shelf overlain (*green*). (B) Call out of same histogram (flipped) of paleo-sea level depths.

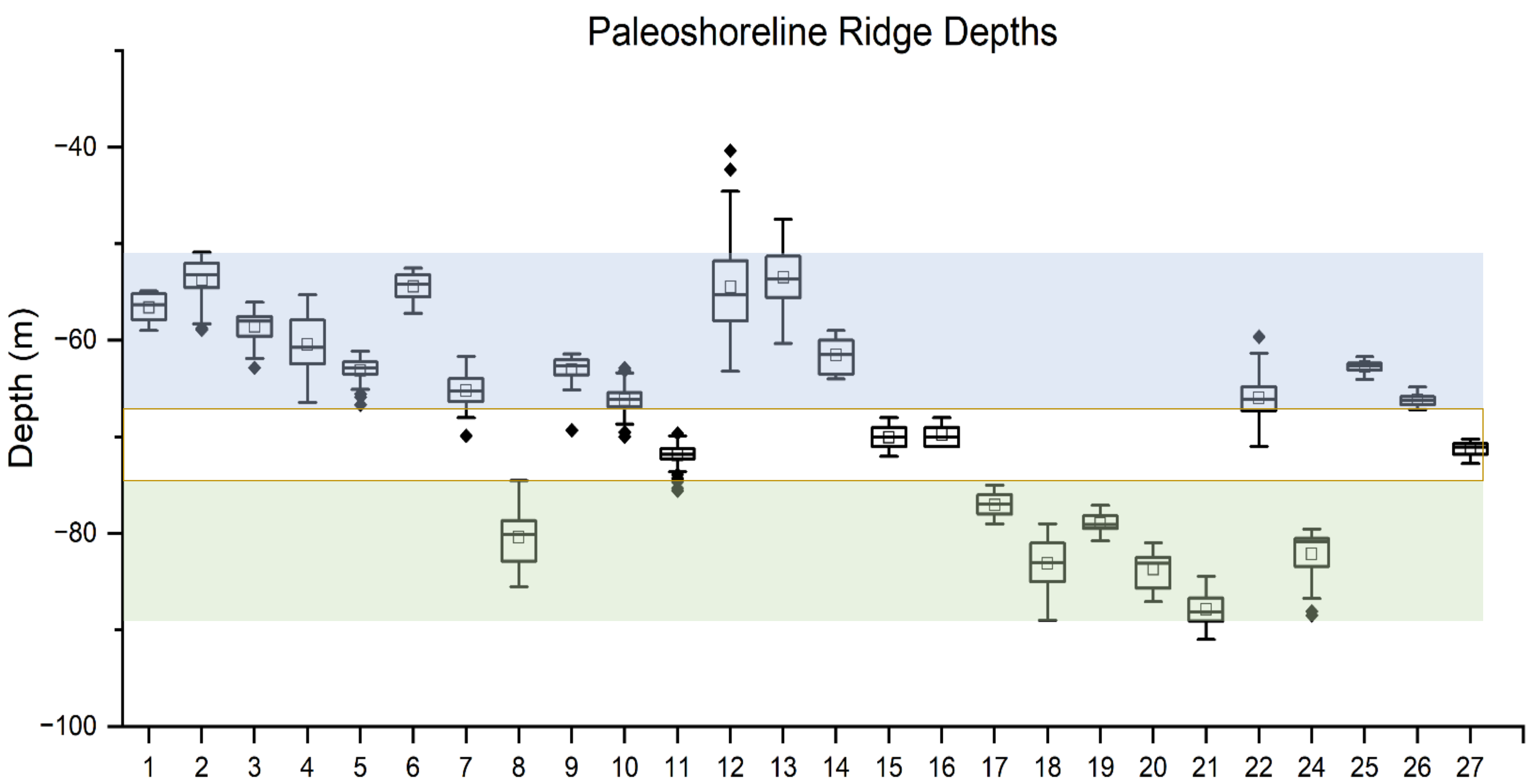

Figure 25: Box plot showing depth ranges of individual paleoshorelines derived from along-ridge profiles across the West Florida Shelf from NW to SE. Box: 25 – 75% depth range; horizontal line represents median depth; box represents mean; and whiskers represent range within 1.5 interquartile range. Blue band indicates period of extensive shoreline formation centered around a modal value of ~-60 m. Green box indicates secondary period of shoreline formation centered around a modal value of ~-85 m. White box with the gold outline indicates an intermediary period of shoreline formation centered at ~-70 m.

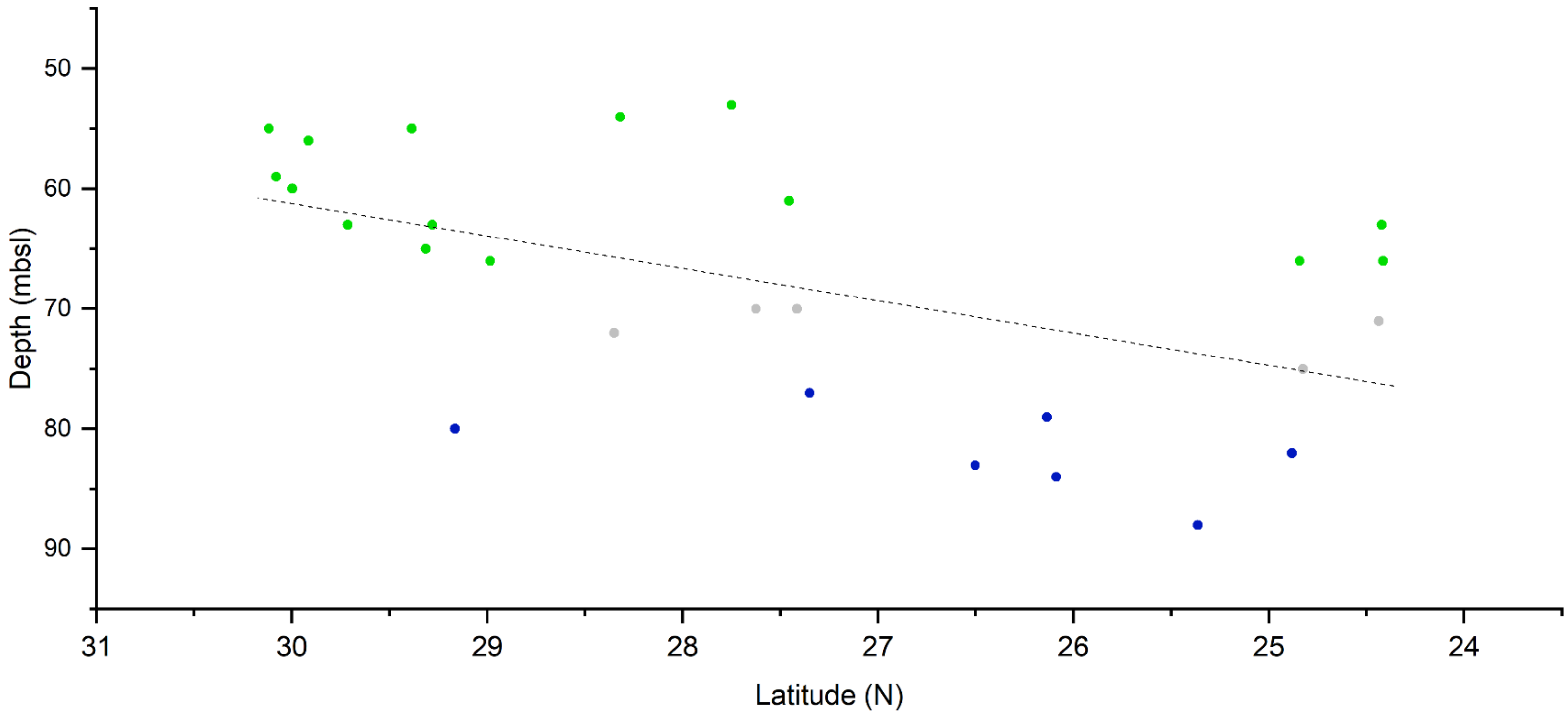

Figure 26: Relationship between paleoshoreline depth versus latitude. The relationship shows a general trend of increasing depth the further south on the shelf you go with the exception of the shallower shorelines at Pulley Ridge and Marquesas Key and the deep shoreline at Madison-Swanson. Figure plots shorelines in a north to south progression with shoreline 1 as first on the left and shoreline 27 as last to the right. Color legend: Green: Group 3 shorelines (~11.0 - 12.7 ka); Grey: Group 2 shorelines (~12.9 - 13.6 ka); Blue: Group 1 shorelines (~13.6 - 14.2 ka).

CHAPTER 4:

DISCUSSION

4.1 Geomorphology and Formational Processes

Our analysis of WFS paleoshorelines has produced several key findings, which we can summarize as follows: (i) the majority of shorelines exhibit a barrier island or beach shoreline type morphology, but a few exhibit morphology consistent with other coastal settings – predominantly mangrove platforms; (ii) there is a general deepening trend from one shoreline to the next as you move south along the shelf with the exception of the shallower shorelines at the SW Florida Middle Grounds, the Elbow, the Eastern Pulley Ridge and the Marquesas Key (Fig. 26), and (iii) superimposed on the overall trend of increasing shoreline depth with latitude, there is a secondary trend along individual shorelines, in which, beginning at the Madison-Swanson delta and continuing southwards, the shorelines dip to the south as if the features were either created asynchronously (e.g., with a component of sea level migration northwards, as well as an expected landwards component) or else tilted after their synchronous formation. Whether the inter-shoreline deepening trend towards the south is the result of the underlying geologic framework or rather a reflection of the areas that have or haven't been mapped is a question that will only be answered when more of the WFS has been mapped and most paleoshorelines are accounted for. The intra-shoreline trend of southerly dipping shoreline axes however, may be explained by some form of isostatic adjustment of the crust or mantle, which will be discussed later in this section.

4.1.1 – Paleoshoreline Geomorphology

Shorelines 1-4 on the NW corner of the WFS, along with shoreline 9 on the Madison-Swanson delta, all exhibit a simple straight to arcuate barrier island/beach shoreline morphology (Appendix 3). Modern day analogs for all of them can be found along the Gulf Coast from Dauphin Island, AL to St. Pete Beach, FL. Shorelines 5, 6, and 7 switch to a more intricate morphology consisting of complexes of discontinuous ridges with parallel ridges backing them similar to the coastlines near Cape San Blas, St. George Island, and Fort DeSoto, FL. When examined from a larger-scale perspective, Shoreline 8 appears to be a continuation of shoreline 7 just to its west. A gap in bathymetric data coverage obscures the location where the two segments connect (Fig. 9B), but considering a distance of only ~3 km between the ends of each segment across the gap in coverage, it is reasonable to assume they are segments of the same paleo coastal system.

Shoreline 9 is somewhat of an outlier. The closest analog for it on the modern coast would be the Florida Keys archipelago. Despite their physical similarity, it is difficult to explain how shoreline 9 could have formed by the same carbonate depositional processes that formed the Keys. What is more aligned with the processes known in this region is a siliciclastic depositional one similar to what formed Dog Island and St. George Island at the head of the Apalachicola River delta especially considering shoreline 9's location at the edge of the Madison-Swanson delta. The difference between shoreline 9 and those in the Apalachicola region is that shoreline 9 lacks a smooth wave-worked seaward facing front that you would expect on a wave-dominated coast. Instead, it exhibits overall a much rougher topography that resembles the limestone islands of the Keys. A possible explanation for this discrepancy could be that shoreline 9 was initially a barrier island with a smooth coastline, but was subsequently colonized by carbonate reef-forming organisms giving it the modern rough topography. While no ground-truthing has been performed, the USGS does classify this feature as a reef (USGS, 2018).

Shoreline 10, which consists of a complex of discontinuous ridges resembles the ridge complexes at shorelines 5, 6, and 7 although the interconnectedness of the ridges in 10 is not as readily apparent due to the narrowness of the bathymetric data set cutting off a complete view of the area. One subfeature of shoreline 10 that stands apart is a small pocket beach-like feature at the southern end. In the bathymetry, a short ridge is flanked on either side by small seaward projections resembling a pocket beach with headlands. However, upon closer inspection, the headlands should be expected to be at the same elevation, if not higher than the shoreline, but they are not. Instead, a more appropriate analog for this feature would be a small cape with redirected sandbars emerging from the ends of the cape like the one found in Ochlockonee Bay, FL (Appendix 3).

Shoreline 11 shifts from shorter discontinuous ridges to long, continuous ones similar to what you might see along the modern SW Everglades coastline with embayments punctuating the winding coast. Another shoreline with a similar appearance is shoreline 17 at the western, deeper edge of the Radius-Ulna. Interestingly, the two features occur at a similar depth range between -71 and -76 m.

At shoreline 12, a new morphology appears – the coastal spit and strand plain. Evidence of longshore sediment transport reworking sands into curved spits and prograding ridges is apparent in shorelines 12, 13, 14, and 21-24. These features also fall in a similar depth range between -50 m and -65 m (with the exception of the deeper portion of Pulley Ridge). It appears that at this time, sediment accumulation and transport was an active process most likely due to a slowdown in sea level rise which allowed for sediment accumulation to dominate in a constructive manner.

In the Radius-Ulna region, another shift occurs and it is the first time that evidence of a structure other than a beach or reef appears. Shorelines 15, 16, 17, and (potentially) 18 and 19 contain evidence that flat-topped mangrove platforms formed in this region which is consistent with the modern coastline of Florida. Indication of a mangrove environment includes cross-sectional profiles which differ from previous profiles through barrier islands and beaches. Instead of a dune or shoreline ridge from which the neighboring seafloor slopes away, these shorelines have a broad flat-topped platform that drops off in a seaward direction presumably where sea level stood at the time (Bird, 2005). Presumably some of these mangrove shorelines were backed by lagoonal environments – comparable to Caladesi and Sanibel Islands today. Others, like shoreline 17 may be more like the Ten Thousand Islands region where expansive mangroves are not separated by a back bay, but directly abut the coast (Appendix 3).

Shorelines 19 and 20 were briefly discussed by Hine et al. (2008) who interpreted seismic data of the feature to represent paleoshoreline facies as well as a deeper, potential relic reef at ~-85 m. Hine et al. (2008) connect these features with the paleoshorelines described by Locker et al. (1996) off the Florida Keys and illustrate that they line up at almost exactly the same depths indicating they were likely contemporaneously formed. Additionally, Hine et al. (2008) point out that the existence of reef build ups in the SW corner of the shelf indicates a dominance of carbonate production which distinguishes it from other previously described regions of the shelf. Shorelines 25-27 off the Florida Keys are likely the same paleoshorelines, if not neighboring ones, that Locker et al. (1996) described as being carbonate shorelines and shoals.

Taking what is known about the paleoshorelines examined in this study along with observations of shorelines on the modern coast of Florida, a zonation scheme can be ascribed based on broad-reaching patterns in shoreline and shelf geomorphology. Beginning in the northwest corner off the panhandle, both ancient and modern shorelines have long, streamlined barrier island morphologies and they formed on large deltaic lobes, reflective of the siliciclastic, wave-dominated coastal regime on that part of the shelf. Moving southeast through the Big Bend area and it's equivalent on the mid to outer shelf, shorelines become thinner and discontinuous reflecting a shift from a siliciclastic sediment-dominated regime to an increasingly mixed one with sandy coasts, marshes, and mangrove environments. This mixed regime seems to persist throughout most of the west central part of the shelf until it transitions to the carbonate-rich region of the SW Florida Shelf.

4.1.2 – Trends in Paleoshoreline Ridge Axes and Shelf Depth

After comparing paleoshoreline depths for use in age-depth correlations, a previously undescribed pattern among the individual submerged shorelines was discovered. Beginning at shoreline 5 (-86.245° N, 29.733° W) on-southward, shorelines with any north-south component show a southward dipping trend along their axes; that is to say, the shorelines are consistently deeper in the southern end than their north. The shorelines for which these observations hold true include shorelines 5, 6, 9, 10, 12, 13, 14, 15, 18, 19, 20, 23, and 24 (see Appendix 4 for details of each). The differences in individual shoreline depths from north to south endpoints vary anywhere between 2 m and ~ 11 m. Furthermore, the assemblage of paleoshorelines when viewed as a whole, also exhibit a deepening progression from north-south suggesting a potential gradual tilt that may be found on the WFS. Additional evidence pointing to this deformation can be found in tidal records along the Gulf of Mexico coastline. Stations have recorded subsidence along most of the Gulf Coast with the notable exception of the NE Gulf of Mexico at Cedar Key and Apalachicola where tide gauges record uplift (Letetrel et al., 2015). Could this uplift be a related compensation for subsidence occurring in the south of the platform?

A similar trend has previously been reported along several subaerially exposed Pleistocene paleoshorelines in north-central Florida including the ~ 80 m Trail Ridge shoreline (Opdyke et al., 1984; Willett, 2006; Adams et al., 2010; Woo et al., 2017). This phenomenon has been attributed to one or a combination of factors including: glacial isostatic adjustment, mantle dynamics aka 'dynamic topography', and karst driven flexural isostasy. For the latter in particular, the N-S trend in shoreline tilt would be expected since most of the karst geology in the state of Florida is concentrated to the north of the state. Thus, elevated rates of dissolution and subsequent rebound would be expected and has been modelled with a north to south trend. The difficulty in understanding which one, or combination of processes, is driving uplift is that modelling the various scenarios requires better constraints on rates of change driven by each one of these processes (Creveling et al., 2019).

If we consider the most likely proposed rates of karst-induced uplift of 0.022 – 0.019 mm/yr (Woo et al. 2017), the rates are too low to account for the amount of uplift that is seen in our shoreline inventory. If we assume that karst dissolution is a dominant process on the tilting of the shorelines, then in order to achieve along-ridge variations of 2-11 m, the shorelines must be between 90 – 580 ka; substantially older than the proposed post-LGM ages inferred by other studies, by our analysis in this study, and dated directly in some locations (Locker et al., 1996). The implication would be that the majority, if not all, shorelines on the WFS are ancient features that have been modified by geological processes over multiple glacial-interglacial cycles, and probably not related to sea level change during the last deglaciation.

Given the fresh geomorphic appearance of many of the landforms, their lack of substantial burial (most have only some Holocene veneer in the subsurface information published to-date), and the existence of absolute radiocarbon ages from the Keys showing deglacial timing for some of our deepest shoreline observations, we do not view the karst dissolution hypothesis as being a major control on shoreline position and shape. What cannot be ruled out and requires further investigation is that a component of GIA related to ice unloading over North America is present in the shoreline tilting that has not been captured up to now. Geodynamic processes associated with ice loading and unloading are shown to have had major effects on the geomorphology of southern United States, even in areas that are often considered stable (e.g. Wickert et al. 2019). Regardless, it is clear that some force(s) is causing uplift and tilt in the north-central Florida region, and its reach likely extends offshore to the shelf. To fully understand the combination of forces at play in the deformation of the WFS, more data are needed to fully quantify the effects of GIA, karst dissolution, and mantle dynamics.

4.2 Paleoshoreline Age Estimation and Sea Level History

Fluctuations in local relative sea level reflect important geodynamic processes that include global eustatic sea-level changes, as well as isostatic adjustment from sources such as ice-sheet loading and topographic mass change. Well-resolved geomorphological records of past sea level positions such as those presented in this thesis provide insights into how these various elements of the Earth system have evolved over time. Crucially, as we have already described, the physiographic and geologic setting of the WFS allows for direct ties between the modern depths of remnant coastal landforms and the likely equivalent eustatic sea level position during their formation, without major convolution from other geodynamic influences.

The occurrence of preserved sea level indicators, such as paleoshorelines and drowned reefs, from -45 to -90 m is well-documented already across the Gulf of Mexico and Caribbean region (Fairbanks, 1989; Locker et al., 1996; Gardner et al., 2005, 2007; Jarrett et al., 2005; Sherman et al., 2010; Allee et al., 2012; Khanna et al., 2017). These features have been previously associated with slowdowns or still-stands in the rate of sea level change, which enabled the formation and development of shorelines, followed by a subsequent sea level rise that was rapid enough to leave them preserved in place. By joining newly described data sets with existing ones across the WFS, it is possible to incorporate these features into an emerging comprehensive and broader picture of regional sea level history for the eastern Gulf of Mexico. We describe two major groupings of shoreline occurrences, bracketing -51 to -67 m (mode at -60 m), and -75 to -90 m (mode at -77 m). In between these two main age-depth groupings, there is an intermediary period centered around -70 m when shorelines are suggested to have formed at a lower rate because of their scarcity at this depth (Fig. 25).

The oldest grouping of paleoshorelines occur around -80 m, bracketing ~ -75 m to -90 m. Shorelines 8, 17, 18, 19, 20, 21, and 24 fall into this group being the deepest shorelines within our inventory. The inferred sea level at the time of formation of these shorelines is estimated to be between -77 and -87 m which based on the Bchron 95% chronology gives these shorelines an estimated age of 13.6 - 14.2 ka. Using estimated age ranges from the 95% chronology for these depths it is concluded that this time period was characterized by a minimum rate of sea level rise of approximately 21.7 mm yr^{-1} and a maximum rate of rise of 34.2 mm yr^{-1}. Shorter time frames within this range could yield lower rates, for example the slowdown that appears to begin ~13.7

ka and end ~13.2 ka. During this slowdown, rates of rise were as low as 0.4 mm yr^{-1}. An age range of 13.6 - 14.2 ka puts the formation of these shorelines at a time following MWP-1A which is believed to have occurred ~14.5 ka and preceding the Younger Dryas global cooler period ~11.6 - 12.9 ka. While rates of SLR are believed to be high, even exceeding the predicted rate of overstepping of 16 mm yr^{-1} that Donoghue (2011) proposed, evidence seems to contradict the idea that rates even as high as 34.2 mm yr^{-1} can inhibit shoreline formation. To the contrary, at this time, expansive coastal systems, like Southern Pulley Ridge, appear to have been able to build out features such as massive strand plains at this time. On a sediment-starved carbonate ramp, this poses an intriguing quandary as to how such a prolific sedimentary system could have formed, especially at a time when rates of sea level rise should have overtopped them.

Following the oldest group of shorelines, an intermediary group centered around -70 m contains a smaller number of shorelines, but still contains evidence of active coastal depositional processes occurring at that time. Shorelines 11, 15, 16, and 27 formed at estimated sea levels between -70 and -74 m. Based on the 95% chronology, it gives these shorelines an estimated age of 12.9 - 13.6 ka. As previously mentioned, the Bchron chronology indicates a period of slowdown between 13.2 - 13.7 ka which encompasses much of the estimated period of formation for these intermediary shorelines. With lower rates of sea level rise, it is easy to reconcile the evidence of shoreline formation at this time with the sea level record, differing from the deeper group of shorelines that formed when rates of sea level rise were much higher. Perhaps when rates of SLR are lower, the coastal environment shifts from a sandy shoreline, to a swamped mangrove setting that has adapted to the steady encroachment of sea water. Alternatively, it could be that shoreline ridges were present but were simply not preserved due to the slower reworking of sediments and erosion that occurs as sea level rises more steadily. When this occurs, we posit that very little or much more subtle geomorphological evidence for former sea level is left behind.

Corroborating the hypothesis of shoreline formation at this depth, Khanna et al. (2017) described a series of terraces off the coast of Texas descending from a shallower reef crest at ~ -60 m. One of these terraces occurs at -70.5 ± 1.5 m. While systematic dates for the terraces were not produced, a radiocarbon date of 10,580 ± 155 years BP from the reef crest at -68 m, and 18,900 ± 370 years BP from the base of the bank place the terrace within a window that would be similar to the estimated 12.9 - 13.6 ka age range of the ~ -70 m shorelines.

The morphology of these shorelines varies – some of them having typical beach shoreline morphologies, but others appearing to exhibit morphology similar to mangrove platforms which are built up into table top-like platforms by the entrapment of sediment in the root systems of mangrove trees. None of the shorelines exhibit evidence of exceptionally high rates of sedimentation like seen at Pulley Ridge, but instead are on par with what would be expected of shorelines on the modern Florida coast.

The youngest group of paleoshorelines occurs around -60 m bracketing -51 to -67 m. This is the largest grouping which includes shorelines 1-7, 9, 10, 12, 13, 14, 22, 25 and 26. The inferred sea level at the time of formation of these shorelines ranges from -48 m to -67 m which, based on the 95% chronology, places the age of formation for this group between 11.0 - 12.7 ka. Shorelines 1-7 were previously described by Gardner et al. (2005; 2007). They concluded that age estimates were uncertain due to the fact that there were multiple time periods over the past 150,000 years in which sea level was suitable for the formation of shelf-edge deltas and their overlying barrier islands. Of the proposed suitable time periods, the deglaciation following the Last Glacial Maximum (specifically around 11-12 ka) is one possible age of formation; however, the authors instead propose that the more likely timeframe for formation was during MIS-3, at ~30-60 ka. In contrast, Khanna et al. (2017) described ten drowned reefs, on the shelf-edge of Texas, whose crests now lie at the same depth of ~ -60 m. Contrary to the regression interpretation of Gardner et al. (2005), based on radiocarbon dating of these reef crests, they concluded that their demise occurred ~11.5 - 12.3 ka coinciding with the end of the Younger Dryas cool period and the onset of a major meltwater pulse - MWP-1B – released from the Laurentide ice sheet. Additionally, based on seismic stratigraphic investigations of the ridges running through the SW Florida Middle Grounds and the Elbow, shorelines 12 and 13, are interpreted to have been shallow shoals and/or non-marine beach deposits that formed when the pace of sea-level rise slowed at around -60 m during the Younger Dryas cool period (Stanley Locker, *pers. comm.*, *2019*).

Taken together, when considering the number of well-preserved landforms corresponding to similar depths at approximately -60 m alongside newer radiocarbon-based age constraints for some of them, it is reasonable to conclude that the shorelines correspond to formation during the more recent deglaciation and sea level inundation rather than during a sea level lowstand or event corresponding to MIS-3. In addition, for the latter interpretation to hold true, would require shorelines to have formed during an MIS-3 maximum flooding event or sea-level plateau preceding the fall leading up to the Last Glacial Maximum, and subsequently having survived intact and unmodified through the following transgression from a sea-level low of >-120 m to modern. In the northwest Gulf of Mexico, sea levels that formed deltas at the Colorado and Brazos paleo-river fronts during marine isotope stage 3 are argued to have been at or above -42.8 m +/- 6.7 m, and may even have been shallower (-29 to -31 m). Indeed, in most Earth models for the Gulf of Mexico, sea level heights from MIS5e (120 ka) onwards are shown to remain well above -60 m until the major sea-level regression into the last glacial at approximately 32 ka (Simms et al. 2009). Consequently, it is more likely that the Texas reefs along with shorelines in this youngest group formed contemporaneously and were subsequently drowned by rapid sea level rise that was felt across the Gulf of Mexico sometime ~11.2 kyrs ago. This age is supported by absolute age data as well as depth-age correlations to a known Gulf of Mexico sea-level curve for the last deglaciation (Joy, 2019).

There are very limited examples of features deeper than the ones described in this work. Those that are reported in literature include a series of discontinuous ridges – parallel to and deeper downslope of Pulley Ridge (shorelines 22-24) – referred to as Howell Hook, as well as a belt of 'seismic patch reefs' west of The Elbow (shoreline 13) colloquially known as the "Sticky Grounds" (Hine et al., 2008). These features lie at a similar depth of ~120 m and are postulated to be LGM lowstand features. Aside from these, no other lowstand markers are reported beyond the lower limit of our proposed paleoshoreline chronology on the WFS. It may be that more exist, but owing to the irregular profile of the shelf beyond the -120 m isobath (Fig. 3), glacial lowstand shorelines simply may not have been formed or easily preserved.

The only reported sea level indicators in waters shallower than those described in our study is the ancient carbonate banks that form the foundation beneath the living reefs at the Florida Middle Grounds (Mallinson et al., 2014). Based on seismic stratigraphic investigation of the features, it is believed that the original reef growth was bracketed by meltwater pulses at 11.5 (MWP-1B) and 8.5 ka (MWP-1C) (Mallinson et al., 2014; Donoghue, 2011; Lambeck et al., 2014; Joy, 2019). The ancient reefs are believed to have formed on top of the older preserved paleoshorelines that formed contemporaneously with the nearby SW Florida Middle Grounds and Elbow shorelines. That said, if any more preserved shorelines were to be found, it could be expected they might lie at similar depths to the paleoshorelines found in this inventory or perhaps at the shallower depth of the drowned vermetid reefs at the Florida Middle Grounds (-23 m) (Mallinson et al., 2014). Since must of the WFS remains unmapped, particularly in the shallower depth range (~ -23 m) that would coincide with a possible (though lesser constrained) MWP-1C, it is possible we may still uncover more preserved shoreline features as mapping efforts increase the footprint of multibeam bathymetry data.

Using estimated age ranges from the 95% chronology it is estimated that the time period proposed for the shorelines in this inventory was characterized by a minimum rate of sea level rise of approximately 10.5 mm yr^{-1} and a maximum rate of rise of 13.6 mm yr^{-1}. This time period aligns almost exactly with the proposed timeframe for the Younger Dryas global cooling period. Therefore, it is consistent that so many shorelines would have formed when rates of sea level rise were significantly slower than the previous, higher rates. The appropriate conditions for formation, however, are only one half of the puzzle. The ability of those shorelines to have been preserved on the seafloor is another clue to sea level history at that time. As suggested by Khanna et al. (2017), the same pulse of rapid sea level rise that drowned the reefs on the Texas coast was likely responsible for drowning this group of shorelines on the Florida coast. The timing of MWP-1B is well-supported by the fact that so many shorelines were preserved in place across the WFS because it requires that some mechanism – in this case, rapid sea level rise – was necessary to leave them preserved in place without major reworking.

Looking at the inventory of paleoshorelines on the WFS, what becomes clear is that these shorelines formed in close succession – in geological terms – to one another. Rather than a series of starts and stops in sea level rise that allowed for the formation of shorelines in punctuated steps, this assemblage of features seems to point to a more dynamic process of shoreline formation that occurred both through periodic still stands as well as through gradual sea level rise over time. Such apparently close successions of paleoshorelines on the WFS support the proposed mechanism of barrier island response to transgression, termed *overstepping*, which occurs when barrier sedimentation cannot keep up with the rate of sea level rise and remnant barrier islands are left imprinted on the seafloor (Rampino and Sanders, 1980). An alternative model for this type of shoreline formation and retreat has been suggested by Ciarletta et al. (2019) wherein shorelines retreat in response to both sea level rise (allogenic forcing) as well as internal dynamics (autogenic forcing) to create kilometer-scale spacing between succeeding shorelines.

In addition to the connections made between paleoshorelines across the shelf and the Texas Gulf Coast, we can continue correlating these features to similar ones across other parts of the Gulf of Mexico and Caribbean region. The WFS paleoshorelines also align closely with a series of shelf-edge reefs and paleoshorelines on the continental slopes of Mississippi-Alabama (-74 to -82 m and -66 m) Puerto Rico (-60 to -80 m), Jamaica (-55 to -65 m), and Belize (-40 to -60 m) (Sager et al., 1991; Goreau and Land 1974; James and Ginsburg 1979; Sherman et al., 2010) therefore demonstrating the potential to tie local sea level history to a broader-reaching regional sea level history for the Gulf of Mexico and Caribbean Sea.

4.3 Mesophotic Coral Ecosystems

With global ocean temperatures and seawater acidification on the rise, coral reef habitats worldwide are suffering massive losses due to the degradation of carbonate reef-builders. With this in mind, scientists believe it is important to prioritize the study of mesophotic coral ecosystems (MCEs) – which are found in the same depth zone as the paleoshorelines identified in this study – as many of the same coral species that are found in shallow water reefs can be found here and can therefore serve as sources for reseeding or restoring their shallower counterparts (NOAA, 2023).

The topographic highs associated with submerged paleoshorelines offer an ideal substrate for MCEs (Koenig et al., 2000; Jarrett et al., 2005; Sherman et al., 2010; Locker et al., 2010; Khanna et al., 2017; Murawski, 2020). It has been pointed out that the gentle slope of the WFS along with its potential for preserving carbonate sedimentary features should make the area prime for MCE habitability. Studies have already shown that flourishing reef communities exist on abandoned paleoshoreline ridges at different locations across the shelf. Habitat Areas of Particular Concern (HAPCs) have been established at both the Florida Middle Grounds and Pulley Ridge where large reefs cover over 1,500 km^2 (Reed et al., 2019; Mallinson et al., 2014), and Marine Protected Areas (MPAs) have been created at Madison-Swanson and Steamboat Lumps covering 405 km^2 (Fig. 27). This has been done not only for the protection of the corals, but to regulate fishing pressure on spots that have been identified as spawning grounds for commercially important species like gag grouper (*Mycteroperca microlepis*) and scamp (*M. phenax*) (Coleman et al., 2004). Additionally, practices such as trawling and anchoring are widely regarded as having damaging effects on delicate corals, but in order to address the issue, the first step must be to characterize the habitats in question which requires high-resolution mapping (Koenig et al., 2000).

Habitat classification work completed at the SW Florida Middle Grounds (aka 'the Mustache') and 'the Elbow,' which lie just south of the Florida Middle Grounds HAPC, showed that the features contain the topographic classifiers – i.e., high-relief hardgrounds – which qualify them as 'essential fish habitat' (Ilich et al., 2021). Considering that both the SW Florida

Middle Grounds and The Elbow are intensely fished features, this work suggests that other well-known fishing grounds across the shelf (e.g., ‘the 40-fathom break’) may require future evaluation for regulation and protective measures as they may prove to be important habitat sites. Based on isobath contours alone, we can make predictions of where we might find others similar features on the WFS. Both the SW Florida Middle Grounds and The Elbow (shorelines 12 and 13) occur on isobath excursions which emerge from the otherwise shoreline-parallel contours like peninsulas (Fig. 28). Similar excursions can be seen in at least three other locations where the shelf has yet to be mapped.

This study provides a base map which identifies a shelf-wide belt through the -45 to -90 m depth zone containing suitable candidates for important reef habitats based on an understanding of the geology of the features. Some sites have previously been identified as suitable candidates based on reports from fishermen but lacked the necessary bathymetry to confirm their presence (e.g. shorelines 10 and 11). In other cases, sites were studied using indirect methods (e.g., subbottom profiling) and determinations of whether or not reef cover was present were inconclusive at best (shorelines 19 and 20 in Hine et al., 2008). Additionally, we present previously undescribed sites with features that contain characteristics for being prime MCE habitat candidates (shorelines 14-17). Considering the topographical indicators previously defined, together with data recording the presence of corals throughout the depth zone of interest (NOAA Deep-Sea Coral & Sponge Map Portal), the weight of evidence should fuel further examination with more focused studies across the region.

In a 2007 report by a NOAA affiliate on the state of deep-sea (>50 m) coral ecosystems in the Gulf of Mexico, it was stated that there is ‘tremendous potential’ for important coral and fish habitat to be identified on the southwest Florida shelf (Brooke and Schroeder, 2007). It was further noted that the area is a high priority region for future research, and it has since led to new exploratory projects along the edge of the WFS as well as the creation of new HAPCs (Amendment 9 - Coral Habitat Areas Considered for Management in the Gulf of Mexico, 2019). Despite these efforts, much of the area identified by this research remains poorly explored, and none of the most recent HAPCs include sites mentioned in this study. Therefore, the need remains for both deeper examination and better data coverage across the WFS.

As stated by Locker et al. (2010) – "the single most important issue from a mapping perspective is the lack of knowledge on the potential extent of MCEs." They emphasized the need for identifying suitable sites based on geological characteristics as well as subsequent ground truthing to confirm whether or not an MCE is present. Based on the extent of MCEs that have already been identified on the surrounding shelf of Florida, combined with topographic characteristics that align with known prerequisites for MCE formation, it is clear that the need for further exploration of submerged paleoshoreline features is needed. With the newly consolidated bathymetric data sets presented here, we hope to enable scientists to more precisely target areas of interest for focused studies on MCEs.

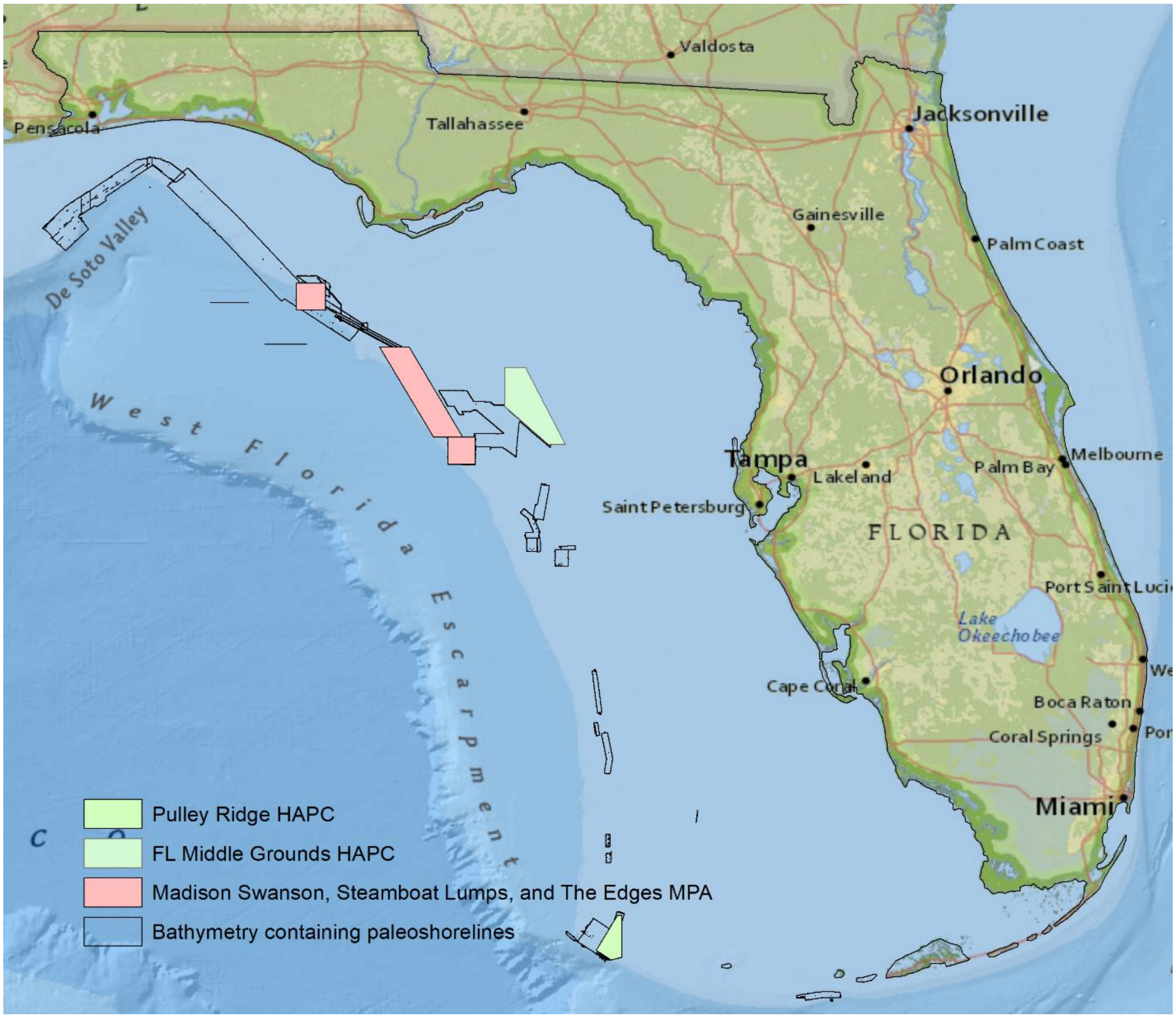

Figure 27: Footprints of bathymetric data containing paleoshoreline features analyzed in this project (hollow outlines). Areas denoting Habitat Areas of Particular Concern (HAPC's) at Pulley Ridge and the Florida Middle Grounds, as well as Marine Protected Areas (MPA's at Madison Swanson, Steamboat Lumps, and The Edges) are marked by colored polygons.

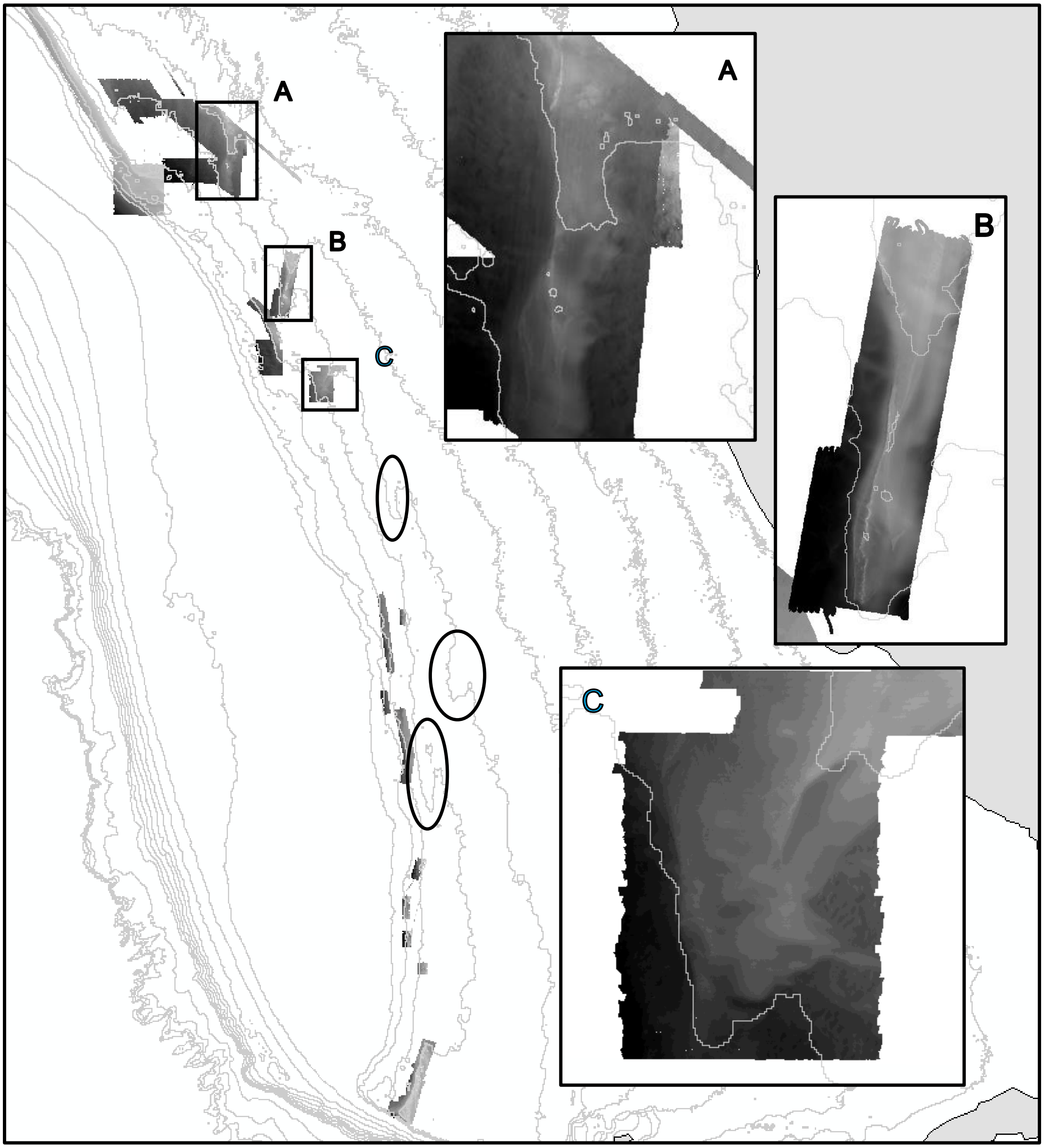

Figure 28: (A) The SW Florida Middle Grounds (shoreline 12), (B) The Elbow (shoreline 13), and (C) the Radius-Ulna (shoreline 15) as examples of shorelines that occur along excursions in local isobaths along with examples (circled) of other locations where the isobaths present similar southward excursions. Multibeam bathymetry does not exist in these locations, but it is highly likely that lithified paleoshoreline features could be found there.

CHAPTER 5:

CONCLUSIONS

The work presented here has investigated sea level history in the eastern Gulf of Mexico using the largest compilation of submerged paleoshoreline sea level indicators to present. Combining interpretations from previous studies with new bathymetric data, a hypothetical sea level scenario for the period between ~11.0 - 14.3 ka is put forth. Based on sea level indicators recorded by proxy in preserved paleoshoreline features, it appears that following MWP-1A ~14.5 ka, one or several periods of sea level rise were slow enough for shorelines to form between -90 and -75 m (~14.2 – 13.6 ka). From ~12.9 - 13.6 ka it is presumed that the rate of sea level rise increased leading to the creation of less shorelines than in the previous several thousand years. Those that did form are preserved between -74 and -70 m. Coinciding closely with the onset of the Younger Dryas global cool period ~12.7 ka, the most recent group of paleoshorelines examined (from -51 to -67 m) were able to form readily, as rates of sea level rise significantly decreased. Sometime between 11.0 - 11.2 ka these shorelines were abruptly abandoned and submerged, most likely during MWP-1B, which released a pulse of meltwater from the Laurentide ice sheet.

What our findings suggest is that the majority of shoreline preservation occurred when rates of SLR were sufficiently high enough to rapidly inundate the sea floor topography. The discovery of what resemble swamped mangroves in the west-central shelf (Radius-Ulna + Northern Pulley Ridge regions) records the kind of coastal environmental record that slow sea level rise leads to (e.g., wetlands).

The timeline put forth here (Fig. 29) is, as expected with any dating work that lacks absolute dates, subject to caveats. For one, it stands in contrast to the timeline previously put forth by Locker et al. (1996) who dated paleoshorelines off the Florida Keys. Their radiocarbon dates place features between -65 and -80 m at an age of 14.5 - 13.78 ka, dates which depart significantly from those put forth here. Additionally, it is suggested that there are neotectonic forces at play that very likely have played some role in distorting the original positions of shorelines on the shelf. Therefore, the historic sea levels ascribed to the shorelines here are subject to interpretation depending on where the shorelines are believed to have formed relative to their current orientations.

Finally, this work continues pushing forward the effort to bring attention to important coral and fish habitats on the WFS. Despite the emphasis that has been put on exploring high-relief carbonate features that are present here, relatively little change has come from the work so far completed, and much remains to be explored. Therefore, we present a new, updated roadmap for scientists who wish to explore the potential ecological riches of mesophotic coral ecosystems that are both confirmed or expected to be present on the WFS. While the potential for discovery is still greatly untapped, anthropogenic pressures have eased little which means that the urgency to study these habitats only becomes greater by the day.

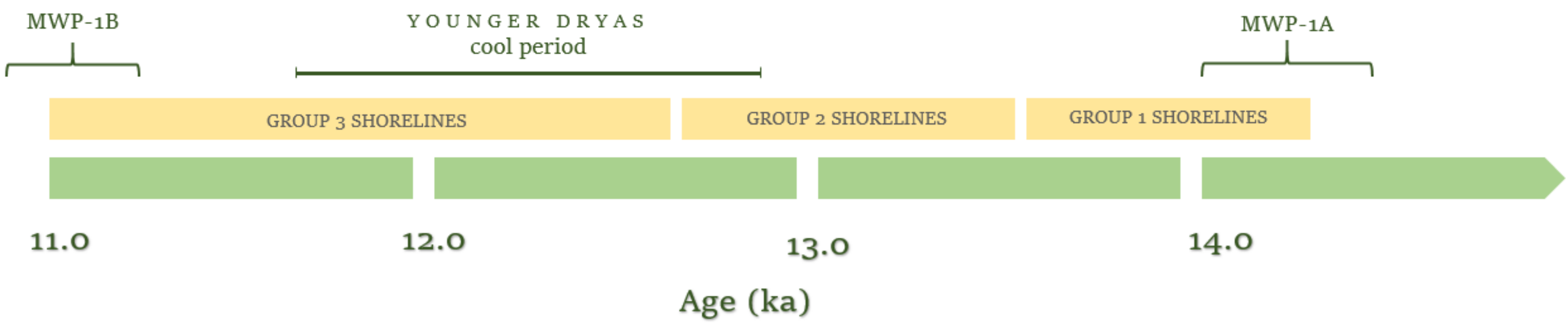

Figure 29: Proposed timeline for eastern Gulf of Mexico sea level history between 11.0 – 14.3 ka based on age-depth correlation of submerged paleoshorelines on the west Florida shelf. Group 1 shorelines correspond to those found between -90 and -75 m.. Group 2: -74 to -70 m. Group 3: -67 to -51 m. MWP-1A is believed to have begun at ~14.5 ka, the Younger Dryas global cool period lasted from ~12.9 – 11.6 ka, and MWP-1B is believed to have begun at ~11.2 ka.

CHAPTER 6:

FUTURE WORK

Future work will likely involve researchers from various disciplines. From the perspective of climate scientists who want to understand how sea level change altered shorelines in the past, mapping of (ideally) the entire WFS will uncover a potentially rich record of sea level history thanks to the broad, low-relief canvas upon which past sea levels have been able to leave their imprint on. The timing of the Seabed 2023 mapping initiative will spur on the work of mapping this large area. It has already led to the creation of regional activities like FCMaP, who paved the way with data inventories and gap analyses, and the Florida Seafloor Mapping Initiative, which will introduce $100 million to collect topobathy lidar data across the state and surrounding coastal waters. This effort, however, will require additional resources to map the entire shelf. It is hoped that through the combined efforts of government funded initiatives, local industry work (e.g., Saildrone, Woolpert), academia, and even the emerging field of crowd-sourced bathymetry, the entirety of the Florida continental shelf will one day be mapped.

For geologists who are interested in the formational history of paleoshorelines and the timing/influence of past climate events (like meltwater pulses) concentrated efforts to collect subbottom profiles, sediment cores, and absolute age dates (e.g., U-Th, radiocarbon) are needed. Potential sources of support for this work not only include individual grant-funded projects, but could even potentially fall under the prevue of entities like the Florida Flood Hub at USF's College of Marine Science that will focus on coastal resiliency issues centered around sea level change.

Finally, ecologists and fisheries management bodies should consider the great potential that the WFS offers for discovering rich reef habitats. While much of the exploration in the Gulf of Mexico has been driven by the needs of extractive industries (e.g., oil and gas), it would be wise to continue the push for exploration for the sake of science and conservation. NOAA Ocean Exploration has already set a precedent for this type of work with their expeditions to the edge of the shelf and Pulley Ridge whose goals were to explore deep coral habitats (NOAA, 2014, 2022). At a period in human history when we are realizing our potential for causing massive ecological disruption, the time is now to turn the tide and use our power of discovery for restorative purposes.

REFERENCES

Adams, P. N., Opdyke, N. D., & Jaeger, J. M. (2010). Isostatic uplift driven by karstification and sea-level oscillation: Modeling landscape evolution in north Florida. Geology, 38, 531-534.

Allee, R. J., David, A. W., & Naar, D. F. (2012). 30 - Two Shelf-Edge Marine Protected Areas in the Eastern Gulf of Mexico. (Eds.) Harris, P. T. & Baker, E. K., Seafloor Geomorphology as Benthic Habitat (pp. 435-448). Elsevier.

Amendment 9 - Coral Habitat Areas Considered for Management in the Gulf of Mexico, 85 Fed. Reg. 65740 (October 16, 2020) (codified at 50 CFR Parts 622 and 635).

Benson, D. J., Schroeder, W.W., & Shultz, A.W. (1997). Sandstone hardbottoms along the western rim of DeSoto Canyon, Northeast Gulf of Mexico. Gulf Coast Association of Geological Societies Transactions, 47, 43–48.

Bird, E. (2005) Mangroves, Geomorphology. (Ed.) Schwartz, M. L., Encyclopedia of Coastal Science (pp.611-613). Springer Netherlands.

Blanchon, P., & Shaw, J. (1995) Reef drowning during the last deglaciation: Evidence for catastrophic sea-level rise and ice-sheet collapse. Geology, 23, 4-8.

Brizzolara, J. L., Grasty, S. E., Ilich, A. R., Gray, J. W., Naar, D. F., & Murawski, S. A. (2020). Characterizing benthic habitats in two Marine Protected Areas on the West Florida shelf. In Seafloor Geomorphology as Benthic Habitat.

Brooke, S., & Schroeder, W. (2007). State of deep coral ecosystems in the Gulf of Mexico region: Texas to the Florida Straits. *The State of Deep Coral Ecosystems of the United States*.

Brooks, G. R., Doyle, L. J., Davis, R. A., Dewitt, N. T., & Suthard, B.C. (2003). Patterns and controls of surface sediment distribution: west-central Florida inner shelf. Marine Geology, 200. 307-342.

Clark, P. U., Mitrovica, J. X., Milne, G. A., & Tamisiea, M. E. (2002). Sea-Level Fingerprinting as a Direct Test for the Source of Meltwater Pulse 1A. Science, 295, 2438-2441.

Chappell, J., Omura, A., Esat, T., McCulloch, M., Pandolfi, J., Ota, Y., & Pillans, B. (1996). Reconciliation of late Quaternary sea levels derived from coral terraces at Huon Peninsula with deep sea oxygen isotope records. Earth and Planetary Science Letters, 141, 227-236.

Coleman, F. C., Baker, P. B., & Koenig, C. C. (2004). A Review of Gulf of Mexico Marine Protected Areas: Successes, Failures, and Lessons Learned. Fisheries, 29, 1-33.

Creveling, J. R., Austermann, J., & Dutton, A. (2019). Uplift of Trial Ridge, Florida, by Karst Dissolution, Glacial Isostatic Adjustment, and Dynamic Topography. Journal of Geophysical Research: Solid Earth, 124, 12349-13562.

Davis, Jr., R. A. & Clifton, H. E. (1987). Sea-level change and the preservation potential of wave-dominated and tide-dominated sequences. (Eds.) Nummendal, D., Pilkey, O.H., Howard, J.D., Sea-level Fluctuation and Coastal Evolution, Society of Economic Paleontologists and Mineralogists Special Publication vol. 41., pp.167-178.

Donoghue, J. H. (2011). Sea level history of the northern Gulf of Mexico coast and sea level rise scenarios for the near future. Climate Change, 107, 17-33.

Donahue, S. (2014). Multibeam Report for NF-14-07. NOAA NCEI Bathymetric Data Viewer. Retrieved 02/25/2022. https://www.ngdc.noaa.gov/ships/nancy_foster/NF-14-07_mb.html

Dowdeswell, J. A., Canals, M., Jakobsson, M., Todd, B. J., Dowdeswell, E. K., & Hogan, K. A. (2016). Atlas of Submarine Glacial Landforms: Modern, Quaternary and Ancient. Geological Society, London, 46, 3014.

Fairbanks, R. G. (1989) A 17,000-year glacio-eustatic sea level record: influence of glacial melting rates on the Younger Dryas event and deep-ocean circulation. Nature, 342. 637-642.

Falco, G. D., Antonioli, F., Fontolan, G., Presti, V. L., Simeone, S., & Ronielli, R. (2015). Early cementation and accommodation space dictate the evolution of an overstepping barrier system during the Holocene. Marine Geology, 369, 52-66.

Ferrini, V. L., & Flood, R. D. (2006). The effects of fine-scale surface roughness and grain size on 300 kHz multibeam backscatter intensity in sandy marine sedimentary environments. Marine Geology, 228, 153-172.

Florida Department of Environmental Protection. (2022). Florida Seafloor Mapping Initiative Overview. Florida Geographic Information Office’s website. https://www.floridagio.gov/pages/fsmi.

Gardner, J. V., Dartnell, P., Sulak, K. S., Calder, B. R., & Hellequin, L. (2001). Physiography and Late Quaternary-Holocene Processes of Northeast Gulf of Mexico Outer Continental Shelf off Mississippi and Alabama. Gulf of Mexico Science, 1118.

Gardner, J. V., Dartnell, P., Mayer, L. A., Clarke, J. E. H., Calder, B. R., & Duffy, G. (2005). Shelf-edge deltas and drowned barrier-island complexes on the northwest Florida outer continental shelf. Geomorphology, 64, 133-166.

Gardner, J. V., Calder, B. R., Clarke, J. E. H., Mayer, L. A., Elston, G., & Rzhanov, Y. (2007). Drowned shelf-edge deltas, barrier islands and related features along the outer continental shelf north of the head of De Soto Canyon, NE Gulf of Mexico. Geomorphology, 89, 370-390.

Gonidec, Y. L., Lamarche, G., & Wright, I. C. (2003). Inhomogenous substrate analysis using EM300 backscatter imagery. Marine Geophysical Researches, 24, 311-327.

Goreau, T. F., & Land, L. S. (1974) Fore-reef morphology and depositional processes, North Jamaica. (ed) Laporte LF. Reefs in time and space, Society of Economic Paleontologists and Mineralogists. Special Publication 18, Tulsa, OK, pp 77–89.

Gowan, E. J., Zhang, X., Khosravi, S., Rovere, A., Stocchi, P., Hughes, A. L. C., Gyllencreutz, R., Mangerud, J., Svendsen, J.-I., & Lohmann, G. (2021). A new global ice sheet reconstruction for the past 80 000 years. Nature Communications, 12(1), 1199.

Hapke, C. J., Baumstark, R., Druyor, R., Fredericks, X., Kramer, P., Jackson, K., McEachon, L. (2022). Establishing seafloor mapping priorities for coastal states. Ocean & Coastal Management, 216, 105942.

He, R., & Weisberg, R. H. (2003). A Loop Current Intrusion Case Study on the West Florida Shelf, Journal of Physical Oceanography, 33(2), 465-477

Hine, A. C. (2013). *Geologic History of Florida: Major Events that Formed the Sunshine State*. Gainesville: University Press of Florida.

Hinkel, J., Aerts, J. C. J. H., Brown, S., Jiménez, J. A., Lincke, D., Nicholls, R. J., Scussolini, P., Sanchez-Arcilla, A., Vafeidis, A., & Addo, K. A. (2018). The ability of societies to adapt to twenty-first-century sea-level rise. Nature Climate Change, 8(7), 570-578.

Ilich, A. R., Brizzolara, J. L., Grasty, S. E., Gray, J. W., Hommeyer, M., Lembke, C., Locker, S. D., Silverman, A., Switzer, T. S., Vivlamore, A., & Murawski, S. A. (2021). Integrating Towed Underwater Video and Multibeam Acoustics for Marine Benthic Habitat Mapping and Fish Population Estimation. Geosciences, 11(176).

IPCC, 2021: Summary for Policymakers. In: Climate Change 2021: The Physical Science Basis. Contribution of Working Group I to the Sixth Assessment Report of the Intergovernmental Panel on Climate Change [Masson-Delmotte, V., P. Zhai, A. Pirani, S.L. Connors, C. Péan, S. Berger, N. Caud, Y. Chen, L. Goldfarb, M.I. Gomis, M. Huang, K. Leitzell, E. Lonnoy, J.B.R. Matthews, T.K. Maycock, T. Waterfield, O. Yelekçi, R. Yu, and B. Zhou (eds.)]. In Press

Jarrett, B. D., Hine, A. C., Halley, R. B., Naar, D. F., Locker, S. D., Neumann, A. C., Twichell, D., Hu, C., Donahue, B. T., Jaap, W. C., Palandro, D. & Ciembronowicz, K. (2005). Strange bedfellows - a deep-water hermatypic coral reef superimposed on a drowned barrier island; southern Pulley Ridge, SW Florida platform margin. Marine Geology, 214(4), 295-307.

James, N. P., & Ginsburg, R. N. (1979) The seaward margin of the Belize barrier and atoll reefs. Blackwell Scientific Publications.

Joy, S. (2019) The trouble with the curve: Reevaluating the Gulf of Mexico sea-level curve. Quaternary International, 525. 103-113.

Kazimierski, W., & Jaremba, M. (2023). On Quality Analysis of Filtration Methods for Bathymetric Data in Harbour Areas through QPS Qimera Software. Sensors, 23(11), 5076.

Khanna, P., Droxler, A. W., Nittrouer, J. A., Tunnell Jr, J. W., & Shirley, T. C. (2017). Coralgal reef morphology records punctuated sea-level rise during the last deglaciation. Nature Communications, 8(1), 1046.

Koenig, C. C., Coleman, F. C., Grimes, C. B., Fitzhugh, G. R., Scanlon, K. M., Gledhill, C. T., & Grace, M. (2000). Protection of Fish Spawning Habitat for the Conservation of Warm-temperate Reef-fish Fisheries of Shelf-edge reefs of Florida. Bulletin of Marine Science, 66(3), 593-616.

Lambeck, K., Hélène, R., Purcell, A., Sun, Y., & Sambridge, M. (2014). Sea level and global ice volumes from the Last Glacial Maximum to the Holocene. Proceedings of the National Academy of Sciences, 111, 15296-15303.

Larter, R. D., Anderson, J. B., Graham, A. G. C., Gohl, K., Hillenbrand, C.-D., Jakobsson, M., Johnson, J. S., Kuhn, G., Nitsche, F. O., Smith, J. A., Witus, A. E., Bentley, M. J., Dowdeswell, J. A., Ehrmann, W., Klages, J. P., Lindow, J., Cofaigh, C. Ó., & Spiegel, C. (2014). Reconstruction of changes in the Amundsen Sea and Bellingshausen Sea sector of the West Antarctic Ice Sheet since the Last Glacial Maximum. Quaternary Science Reviews, 100, 55-86.

Leventer, A., Williams, D. F., & Kennett, J. P. (1982). Dynamics of the Laurentide ice sheet during the last deglaciation: evidence from the Gulf of Mexico. Earth and Planetary Science Letters, 59, 11-17.

Lidz, B. H., & Shinn, E. A. (1991). Paleoshorelines, Reefs, and a Rising Sea: South Florida, USA. Journal of Coastal Research, 7, 203-229.

Locker, S.D., Hine, A.C., Tedesco, L.P., & Shinn, E.A. (1996) Magnitude and timing of episodic sea-level rise during the last deglaciation. Geology, 24(9), 827-830.

Locker, S. D., Armstrong, R. A., Battista, T. A., Rooney, J. J., Sherman, C., & Zawada, D. G. (2010). Geomorphology of mesophotic coral ecosystems: current perspectives on morphology, distribution, and mapping strategies. Coral Reefs, 29, 329-345.

Mallinson, D., Hine, A., Naar, D., Locker, S., & Donahue, B. (2014) New perspectives on the geology and origin of the Florida Middle Ground carbonate banks, West Florida shelf, USA. Marine Geology, 355, 54-70.

Mellet, C. L., & Plater, A. J. (2018) Drowned Barriers as Archives of Coastal-Response to Sea-level Rise. In L. J. Moore and A. B. Murray (Eds.), *Barrier Dynamics and Response to Changing Climate* (pp. 57-89). Springer International Publishing.

Miller, K. G., Browning, J. V., Schmelz, W. J., Kopp, R. E., Mountain, G. S., & Wright, J. D. (2020). Cenozoic sea-level and cryospheric evolution from deep-sea geochemical and continental margin records. Science Advances, 6(20).

Mitrovica, J. X., Gomez, N., Clark, P. U. (2009). The Sea-Level Fingerprint of West Antarctic Collapse. Science, 323, 753.

Murawski, S., Lembke, C., Locker, S., Grasty, S., Hommeyer, M., and Ilich, A. (2020). Continental shelf seafloor mapping, benthic habitat surveys, and reef fish assessments in the eastern Gulf of Mexico. Zenodo. https://doi.org/10.5281/zenodo.8381010

Murawski, S., Lembke C., Gray, J., Brizzolara, J., & Hommeyer, M. The Elbow [map]. Data collected December 2015. 4×4-m grid. "The Elbow Data Products." Last updated May 2016. Retrieved from: http://www.marine.usf.edu/scamp/data-products/theelbowdata. Funding provided by the National Fish and Wildlife Foundation (NFWF): GEBF Grant #45892.

National Oceanic and Atmospheric Administration. NOAA Deep-Sea Coral & Sponge Map Portal. National Centers for Environmental Information at https://www.ncei.noaa.gov/maps/deep-sea-corals/mapSites.htm.

National Oceanic and Atmospheric Administration. Southeast Deep Coral Initiative: Exploring Deep-Sea Coral Ecosystems off the Southeast U.S. https://oceanexplorer.noaa.gov/explorations/17sedci/welcome.html.

National Oceanic and Atmospheric Administration. (2014). Coral Ecosystem Connectivity 2014: From Pulley Ridge to the Florida Keys. https://oceanexplorer.noaa.gov/explorations/14pulleyridge/background/missionplan/missionplan.html

National Oceanic and Atmospheric Administration. (2022). Combining Habitat Suitability and Physical Oceanography for Targeted Discovery of New Benthic Communities on the West Florida Slope. https://oceanexplorer.noaa.gov/explorations/22hydrosmac/welcome.html

National Oceanic and Atmospheric Administration (2023). What are Mesophotic Coral Ecosystems? https://oceanservice.noaa.gov/facts/mesophotic.html.

Nienhaus, J. H. (2019). Effect of tidal inlet stabilization on barrier island morphodynamics. Coastal Sediments, 85-90.

Opdyke, N. D., Spangler, D. P., Smith, D. L., Jones, D. S., & Lindquist, R. C. (1984). Origin of the epeirogenic uplift Pliocene-Pleistocene beach ridges in Florida and development of the Florida karst. Geology, 12, 226-228.

Oppenheimer, M., Glavovic, B. C., Hinkel, J., van de Wal, J., Magnan, A. K., Abd-Elgawad, A., Cai, R., Cifuentes-Jara, M., DeConto, R. M., Ghosh, T., Hay, J., Isla, F., Marzeion, B., Meyssignac, B., Sebesvari, Z., 2019: Sea Level Rise and Implications for Low-Lying Islands, Coasts and Communities. In: IPCC Special Report on the Ocean and Cryosphere in a Changing Climate (eds.) Pörtner, H.-O., Roberts, D. C., Masson-Delmotte, V., Zhai, P., Tignor, M., Poloczanska, E., Mintenbeck, K., Alegría, A., Nicolai, M., Okem, A., Petzold, J., Rama, B., Weyer, N. M.. Cambridge University Press, Cambridge, UK and New York, NY, USA, pp. 321-445.

Pan, L., Line, G. A., Latychev, K., Goldberg, S. L., Austermann, J., Hoggard, M. J., & Mitrovica, J. X. (2022). Quaternary Science Reviews, 290, 107644.

Passos, T. U., Webster, J. M., Braga, J. C., Voelker, D., Renema, W., Beaman, R. J., Nothdurft, L. D., Hinestrosa, G., Clarke, S., Yokoyama, Y., Barcellos, R. L., Kinsela, M. A., Nothdurft, L. N. & Hubble, T. (2019). Paleoshorelines and lowstand sedimentation on subtropical shelves: a case study from the Fraser Shelf, Australia. Australian Journal of Earth Sciences, 66(4), 547-565.

Pillans, B., Chappell, J., & Naish, T. R. (1998). A review of the Milankovitch climate beat: template for Plio-Pleistocene sea-level changes and sequence stratigraphy. Sedimentary Geology, 122, 5-21.

Puglise, K. A., Hinderstein, L. M., Marr, J. C. A., Dowgiallo, M. J., & Martinez, F. A. (2009). Mesophotic Coral Ecosystems Research Strategy: International Workshop to Prioritize Research and Management Needs for Mesophotic Coral Ecosystems. Silver Spring, MD: NOAA National Centers for Coastal Ocean Science, Center for Sponsored Coastal Ocean Research, and Office of Ocean Exploration and Research, NOAA Undersea Research Program.

Rampino, M. R., & Sanders, J.E. (1980). Holocene transgression in South-central Long Island, New York. Journal of Sedimentary Research, 50, 1063-1079.

Railsback, R. B., Gibbard, P. L., Head, M. J., Voarintsoa, N. R. G., & Toucanne, S. (2015). An optimized scheme of lettered marine isotope substages for the last 1.0 million years, and the climostratigraphic nature of isotope stages and substages. Quaternary Science Reviews, 111, 94-106.

Reed, J. K., Farrington, S., David, A., Harter, S., Pomponi, S. A., Diaz, M. C., Voss, J. D., Spring, K. D., Hine, A. C., Kourafalou, V. H., Smith, R. H., Vaz, A. C., Paris, C. B. & Hanisak, M. D. (2019). Pulley Ridge, Gulf of Mexico, USA. In *Coral Reefs of the World*: Springer Nature.

Riggs, S. R., Snyder, S. W., Hine, A. C., & Mearns, D. L. (1996). Hardbottom morphology and relationship to the geologic framework: mid-Atlantic continental shelf. Journal of Sedimentary Research, 66, 830–846.

Roe, G. H., Christian, J. E., & Marzeion, B. (2021). On the attribution of industrial-era glacier mass loss to anthropogenic climate change. The Cryosphere, 15(4), 1889-1905.

Rolland, T., Monna, F., Buoncristiani, J. F., Magail, J., Esin, Y., Bohard, B., & Chateau-Smith, C. (2022). Volumetric Obscurance as a New Tool to Better Visualize Relief from Digital Elevation Models. Remote Sensing, 14(4), 941.

Salzmann, L., Green, A., & Cooper, J. A. G. (2013). Submerged barrier shoreline sequences on a high energy, steep and narrow shelf. Marine Geology, 346.

Schroeder, W.W., Shultz, A.W., & Dindo, J.J. (1988). Inner-shelf hardbottom areas, northeastern Gulf of Mexico. Transactions of the Gulf Coast Association of Geology Society, 38, 535–541.

Shackleton, N. J. (1987). Oxygen Isotopes, Ice Volume, and Sea Level. Quaternary Science Reviews, 6, 183-190.

Sherman, C., Nemeth, M., Ruiz, H., Bejarano, I., Appeldoorn, R., Pagan, F., Scharer, M., & Weil, E. (2010). Geomorphology and benthic cover of mesophotic coral ecosystems of the upper insular slope of southwest Puerto Rico. Coral Reefs, 29, 347-360.

Smillie, Z., Stow, D., & Esentia, I. (2019). Deep-Sea Contourites Drifts, Erosional Features and Bedforms. In J. K. Cochran, H. J. Bokuniewicz, & P. L. Yager (Eds.), Encyclopedia of Ocean Sciences (Third Edition) (pp. 97-110). Academic Press.

Swift, D.J.P., Niederoda, A. W., Vincent, C.E., & Hopkins, T.S. (1985). Barrier island evolution, middle Atlantic shelf, USA, Part I: Shoreface dynamics. Marine Geology 63, 331-361.

Twichell, D. C., Parson, L. M., & Paull, C. K. (1990). Variations in the styles of erosion along the Florida Escarpment, eastern Gulf of Mexico. Marine and Petroleum Geology, 7(3), 253-266.

United States Geological Survey (2018). Seafloor Mapping – West Florida shelf, Gulf of Mexico. Accessed May, 05, 2023 at https://cmgds.marine.usgs.gov/data/pacmaps/fl-pers4.html.

Wickert, A. D., Anderson, R. S., Mitrovica, J. X., Naylor, S., & Carson, E. C. (2019). The Mississippi River records glacial-isostatic deformation of North America. Science Advances, 5(1), eaav2366.

Willett, M. A. (2006). Effect of Dissolution of the Florida Carbonate Platform on Isostatic Uplift and Relative Sea-Level Change. Florida State University. https://diginole.lib.fsu.edu/islandora/object/fsu:169215/datastream/PDF/view

Woo, H. B., Panning, M. P., Adams, P. N., & Dutton, A. (2017). Karst-driven flexural isostasy in North-Central Florida. Geochemistry, Geophysics, Geosystems, 18.

APPENDICES

Appendix 1 - Paleoshoreline descriptions from literature

Shoreline	Descriptions in Literature
1	*Gardner et al (2007):* • DeSoto Canyon ➔ divide between terrigenous Mississippi River muddy sediment to east and allochthonous carbonates to the west • Between 54-58 m isobaths • Continuous 8.4 km long, 40 m wide slightly curved feature that trends NE and faithfully parallels the isobaths • Landward flank rises as much as 2.5 m above seafloor on NW flank whereas seaward flank has up to 8 m of relief • Ridge appears almost completely buried on SW end but progressively less buried towards the NE • A "moat" as much as 2m deep runs in front of the ridge • Ridges are interpretted to be drowned barrier islands almost identical in morphology to modern barriers and similar paleo-barriers (Pulley Ridge). Enough time had to remain after delta formation to allow for the development and cementation of the barriers
2	*Gardner et al (2007):* • Between 51-53 m isobaths • Continuous, gently curved 20.6 km long, 40 m wide feature with 0.5-1.0 m relief on landward side and 4-6 m relief on seaward side • NE section appears partially buried compared to SE portion • 1 m deep "moat" • Pronounced series of large depressions found immediately landward of ridge – as much as 300 m long, 200 m wide, and 1 m deep; steep E,W side and gently N,S sides; have *lower* backscatter compared to adjacent seafloor
3	*Gardner et al (2007):* • Complex feature with 2 subparallel ridges trending WNW found between 56-59 m isobaths • More continuous southern ridge is 6.2 km long, 40 m wide, with 2 m relief on N side and 6.5 m relief on S side • Northern ridge has two segments separated by what appears to be a middle buried segment • Profiles across complex show that sediment may be dammed behind northern ridge and partially protected southern ridge from burial
4 (EW Destin Ridges)	*Gardner et al (2005):* • Two en echelon ridges arising from the 65 m isobath • EDR is 1.8 km long and trends 081° WDR is 2.75 km long trending 087° • Both ridges have more relief in the W section that their E section • Acoustic backscatter is considerably higher on ridges (-21 to -22 dB) than surrounding delta surface (-28 to -30 dB) *Doyle and Sparks (1980)*: • described a carbonate-rich facies (although they did not mention coral debris) restricted to the area of the Destin delta. Coral debris was described in the surficial sediments from similar water depths on the Alabama–Mississippi outer continental shelf (Ludwick and Walton, 1957), hence it would not be surprising to find coral reefs at this latitude on the NW Florida shelf.
5	*Gardner et al (2005):* • 2.4 km long, <40 m wide and <2 m high • A 0.5 m deep, <60 m wide "moat" parallels the west side of the ridge and ends where the ridge terminates • Does *not* have an appreciable backscatter signature
	• 1.31 km long ridge with 0.5 m of relief and <50 m wide

	• *No acoustic backscatter signature* • Similar moat to one on D parallels western side of E (50 m wide and <1 m deep) • Well-developed shelf-edge ridge complex (linear to curvilinear ridges) in water depths ranging from 60-68 m • Encompasses over 50 km^2 along SW margin of the delta • Steeper faces of ridge segments face seaward • Area just north of the main ridge contains a complex region of 2 curved orthogonal sets of ridges 0.25 m high, 10-20 m wide, and as much as 2000 m long • *Higher* acoustic backscatter than surrounding seafloor
6 & 7	*Gardner et al (2005):* • A series of ridge complexes built upon older, some partially buried, complexes • Deeper segment (along 65 m isobath) is 17.95 km long and varies from 20 to 150 m in width; 2-4 m of relief along ridge front and a 1 m deep, 20 m wide moat immediately seaward of SW facing sections • A 440 m wide pass is located along the SW facing portion of the ridge • Shallower segment (along 55 m isobath) – Gardner labels them as *older* (implying a progradational system); shallower ridges have *higher* backscatter than deeper ones • (*Koenig et al, 2000* and USGS site: https://cmgds.marine.usgs.gov/data/pacmaps/fl-persp.html → **reef**)
8 (Outer Madison Swanson)	*Gardner et al (2005):* • Main curvilinear ridge front is a near-continuous 13.5 km long rim along the S edge of the platform between depths of 75-85 m • Ridge front rises 4 to 8 m high – highest in the E section; as much as 80 m wide – bifurcates in the eastern section with a shorter ridge breaking off behind the main ridge • Backscatter of ridges are typically higher than the surrounding surfaces *Allee et al. (2012):* • Madison-Swanson is a 394 km^2 area located ~60 km southwest of Cape San Blas, Florida, at the margin of the continental shelf and slope in 60–140m of water and is a site of spawning aggregations of gag (Mycteroperca microlepis) and other reef fish species • This prominent feature within Madison-Swanson is a continuous, ~13 km long curved ridge ~6 m (up to 10 m) tall and ~80 m wide in ~80 m of water depth • High-resolution seismic stratigraphy and 300-kHz multibeam data show that the Madison-Swanson MPA is a drowned river delta that is estimated to have formed between 58,000 and 28,000 years ago
10 (Twin Ridges)	*Briere et al. (1999):* • Identified as two parallel ridges ("rocky ledges") *Koenig et al. (2000):* • Two 6 km long pronounced rocky ridges extending up to 15 m off the seabed • Trend NW roughly parallel to present W FL coastline • Identified as a shelf-edge reef - define the ridge areas as rocky outcrops in 60-75 m of water (*Hine et al. 2008* define the 75m isobath as the shelf/slope boundary)
11 (The Edges + Steamboat Lumps)	*Koenig et al. (2000):* • low-relief shelf-edge reefs *Brizzolara et al. (2020):* • low slope, low rugosity throughout

(*not part of this inventory but used as a reference)* Florida Middle Grounds	*Hine et al. (2008):* • a complex cluster of small carbonate banks in the mid to outer-shelf setting • The entire WFS lies in the global "chlorozoan zone" where skeletal sediments are dominated by hermatypic corals and calcareous green algae • Represents a relict or "give-up" reef – reef growth is likely limited by excess nutrients and the associated increase in bioerosion rates; seasonal plumes are believed to originate from the Loop Current interacting with the platform margin which produces upwelling and entrains high-nutrient water masses from fluvial discharge (e.g. MS River) • A diverse and complex geomorphology which is a product of the interplay of carbonate production, climate and sea-level change, and physical oceanographic processes • Bedforms, sediment patterns, and scour patterns indicate an influence of southward-flowing and off-shelf directed currents • One theory (based on subbottom) is that they are lithified paleoshorelines upon which the FMG corals were recruited • Possible enhanced MS River discharge ~4.2 ka may have terminated reef development ➔ ALTERNATE age theory is that it dates to MIS 5 or 3 (~80 or 40 ka) and provided recruitment sites for Holocene coral reef development • An enclave of tropical species (local and brought up by Loop Current) co-existing with temperate species • No massive reef-building Scleractinia like those in Caribbean → a dissimilar community to that found at Flower Garden Banks
13 (The Elbow)	*Ilich et al. (2021):* • Hypothesized to be an ancient sea level stand shaped by wave action approximately 12,000 years ago • Contains both hard bottom (rock) and soft bottom (sand) habitats • Supports benthic invertebrate assemblages including sponges, gorgonians, and sea urchins along with a diverse community of reef fishes • Surveyed area ranged in depth from 45 to 65 m • Contains a 16-km long linear ridge running north to south • Site chosen as a test bed due to the expected ubiquity of such hard-bottom ridges (formed by paleoshorelines) across the west Florida shelf • Vessel monitoring systems (i.e. satellite tracking) data have identified the site as a "hot spot" for reef fishing going hand-in-hand with an interest in the area by fisheries management
18 (Northern Pulley Ridge)	*Hine et al. (2008):* • Part of what is considered the full length of Pulley Ridge (~300 km long) → Pulley Ridge is a multiple-ridge complex that lies between the 60-90 m isobaths and extends N to S along the outer WFS' • "The northern ridge supports a heterotrophic octocoral-dominated community that does not contribute to a reefal accumulation like that in the south"
19 & 20 (Northern Pulley Ridge)	*Hine et al. (2008):* • Less pronounced ridges and paleoshorelines and in some places a distinct 2-3 m high scarp at ~85 m depth → suggests that the modern relief of some ridges may have been produced by erosional processes during sea level rise • *OR* as in the case of the deeper ridge at 80 m (in QR) ridges may reflect late relic Pleistocene reef buildups – yet to be identified (widely-spaced dredge hauls did not yield any coral-reef material) • Carbonate sediment production, probably oolitic in nature, was much greater along the extreme SW corner of the WFS than anywhere else • "Strikingly similar to the structures identified by Locker et al. (1996) on the S. FL margin"

22, 23, & 24 (Southern Pulley Ridge)	*Jarrett et al. (2005):* • Displaying maximum local relief up to 10 m, this reef-capped ridge (Southern Pulley Ridge) forms the southeastern component of a more extensive, ~200-km-long rocky ridge system called Pulley Ridge • Horizontal layered bedding patterns are apparent both in outcrop and in seismic reflection profiles. Further, these tabular rocks often display rectilinear jointing, consistent with beachrock formation • Most likely, both sets of ridges – Pulley Ridge and those described by Locker et al. (1996) at Marquesas Key – are contemporaneous even though not physically contiguous • The Pulley Ridge complex is lithified which indicates that carbonate sediments constituting these paleoshorelines were subject to rapid sub-aerial and submarine cementation, allowing them to resist erosion during ensuing sea level rise • direct observations of the 80–90-m-deep ridge seaward of SPR show no indications of reefal accretion (other than capping) • From seismic reflection profiles across SPR and its seaward component, the dominant internal acoustic facies consist of layered, continuous, clearly traceable parallel to subparallel stratal surfaces consistent with a barrier island depositional setting • Two episodes of paleoshoreline development are mapped from the subsurface of Pulley Ridge • A drumstick morphology, multiple prograding beah ridges, recurved spits, relict inlets and tidal channels, and a well-developed cuspate promontory (cape), all classic barrier island features, are evident in the multibeam imagery • Carbonate sediments may be rapidly cemented due to their propensity toward early diagenesis; thus, rapid cementation allows for significantly higher preservation potential of lowstand carbonate coastal deposits *Allee et al. (2012):* • Pulley Ridge is a 100+ km-long series of N–S trending, drowned barrier islands on the southwest Florida shelf ~250km west of Cape Sable, Florida • Appears to be formed on top of an ancient coastal barrier island or strand line dating back approximately 14,000 years before present when sea level was ~65–80m lower • Presently, Pulley Ridge periodically underlies the Loop Current, which feeds into the Gulf Stream western boundary current • The most recent rise in sea level occurred after the last deglaciation (~14Ka), and evidence of this rapid sea level transgression has been observed in the preservation of several paleoshorelines at the approximate depths of 65, 70, and 80m in the Pulley Ridge area which correlate well with similar depths near the Marquesas Keys along the southern edge of the Florida platform • The extensive cross-cutting N–S and E–W preserved bedform structures in Pulley Ridge were most likely formed and then modified by the rapid fluctuations in sea level described earlier *Reed et al. (2019):* • The southern terminus of Pulley Ridge supports a mesophotic coral ecosystem (MCE) at depths of 59–105 m and is the deepest known photosynthetic coral reef off the continental United States • Based on its geomorphology, Pulley Ridge was divided into three regions: Main Ridge, Central Basin, and West Ridge • The Main Ridge is the shallowest area ranging from 59 m on top of the ridge to 75 m at the base, the Central Basin is from 72 to 83 m in depth, and the West Ridge is the deepest at 76–105 m

	• All three regions of southern Pulley Ridge (Main Ridge, Central Basin, and West Ridge) are MCE habitat and generally consist of low rugosity, low relief (< 0.5 m), rock/coral pavement, and rubble substrate *Hine et al. (2008):* • preserved because it was constructed from carbonate and sand-sized sediments that cement rapidly in shallow marine and freshwater/SW groundwater transition • Drowned shoreline becomes a rocky substrate surrounded by finer-grained, uncemented sediments • Believed to be a contemporary western extension of these shorelines found off Key West • Coral cover is a ***biostrome*** (laterally extensive) and not a ***bioherm*** (vertical framework constructed) – a coralline-algae-coral dominated reef • "It seems likely that the coral community at Pulley Ridge is widespread throughout the Caribbean, Bahamas and Gulf of Mexico and awaits further exploration in a depth range that is not easily accessible by SCUBA, but considered shallow for many submersibles"
25, 26 & 27	*** ***Possibly same, nearby or partial shorelines of the ones described by Locker et al. 1996*** *Locker et al. (1996):* • S1 – shoal; S2 – "near or at the beach;" S3 – "transition from shallow marine and/or foreshore beachrock to meteoric vadose (above water table) environments of cementation in the updip direction;" S4 – "phreatic environment below a *freshwater* water table" • S4 shoreline (58-65 mbsl) may be beach or back-beach deposits but were exposed to a higher water table – indicates a wetter climate; (Grimm et al. [1993] documented a wet climate phase in Florida at this time (13,720 yr B.P.) *Hine et al. (2008):* • the area is a classic rimmed platform margin; the southern portion [of the shelf] supports reefs along the margin which defines the shelf-slope break • Healthy coral reef development occurs when ideal conditions for substrate availability, water quality and stable or slowly rising SL simultaneously converge. The diversity of reefs dispersed on the FL platform indicate that such convergence is neither simultaneous or ubiquitous. • *S*-SW portion of the FL platform remains to this day a carbonate-dominated province

Appendix 2 - Bathymetric Datasets: Systems and Processing Specifications

Dataset	Data Format	Source	Sonar Type	Patch Test	Positioning + Navigation	Post-Processing	SVP collection
DeSoto Canyon	ESRI Grid – 8m resolution	USGS – 2002 on RV *Moana Wave*	300-kHz Kongsberg Dual-head EM3000 MBES	Yes	DGPS-aided inertial navigation system w Applanix POS/MV IMU + dual Trimble model 4000 receivers; accuracies of ±0.5 m	n/a	SeaBird model 19-02 CTD several times a day + sensor @ transducer depth
NW Florida Shelf	ESRI Grid – 8m resolution	USGS – 2001 on RV *Moana Wave*	95-kHz Kongsberg EM1002 MBES	Yes	DGPS-aided inertial navigation system w Applanix POS/MV IMU + dual Trimble model 4000 receivers; accuracies of ±0.5 m	n/a	SeaBird model 19-02 CTD several times a day + sensor @ transducer depth
NE Madison Swanson	ASCII XYZ – 10m resolution	USF – 2002	300-kHz Kongsberg EM3000 MBES	yes	Applanix POS/MV	Caris HIPS/SIPS	AML sound velocity probe + CTD
Madison Swanson Gap	BAG – 2m resolution	USF C-SCAMP Project – RV *Weatherbird II*	400-kHz Reson SeaBat 7125	Yes	DGNSS Applanix POS MV Oceanmaster 320	Caris	AML Minos X SVP and SeaBird CTD
Twin Ridges	ASCII XYZ	USF - 2006 RV *Suncoaster*	Kongsberg Simrad EM3000 MBES	n/a	Applanix POS/MV	Caris HIPS/SIPS	AML sound velocity probe
The Edges	ASCII Grid	USF - multiyear	n/a	yes	Applanix POS/MV	Caris HIPS/SIPS	AML sound velocity probe + CTD
Steamboat Lumps	ESRI Grid – 4m resolution	USGS – 2001 on RV *Moana Wave* + USF - 2010	95-kHz Kongsberg EM1002 MBES 300-kHz Kongsberg Simrad EM3000 MBES	Yes	DGPS-aided inertial navigation system w Applanix POS/MV IMU + dual Trimble model 4000 receivers; accuracies of ±0.5 m	n/a	SeaBird model 19-02 CTD several times a day + sensor @ transducer depth
SW Florida Middle Grounds	BAG - 4m	USF C-SCAMP 2016	400-kHz Reson Seabat 7125 MBES	Yes	Applanix POS/MV	Caris, Qimera	AML Minos X SVP and SeaBird CTD
The Elbow	BAG - 4m resolution	USF – 2015 RV *Bellows*	400 kHz Reson SeaBat 7125 MBES	Yes	Applanix POS/MV	Caris HIPS/SIPS 10.2	AML Oceanographic MicroX @ sonar

Dataset	Data Format	Source	Sonar Type	Patch Test	Positioning + Navigation	Post-Processing	SVP collection
							head + AML Oceanographic MinosX w an SVX change sound velocity sensor
Radius-Ulna	BAG – 3m resolution	USF C-SCAMP, RV *W.T. Hogarth*	400 kHz Reson T50-R Dual Head MBES	Yes	Applanix POS/MV	Qimera	AML Oceanographic MicroX @ sonar head + AML MinosX w SV X-change sound velocity sensor
Northern Pulley Ridge	ASCII Grid – 5m resolution	NOAA Fisheries + USF	300-kHz Kongsberg Simrad EM3000 MBES	n/a	n/a	n/a	n/a
Pulley Ridge	ASCII XYZ	USGS – 2005 – RV's *Bellows* & *Suncoaster*	300-kHz Kongsberg Simrad EM3000 MBES	yes	POS/MV 320-V2	Caris HIPS/SIPS	Sea Bird CTD
Florida Keys	BAG	NOAA National Marine Sanctuaries – NOAA Ship *Nancy Foster* 2014	Reson SeaBat 7125 MBES	No	n/a	n/a	CTD

Appendix 3 – Paleoshoreline Geomorphology and Modern Analogs

Shoreline	Cross-sectional Profile	Modern Analog

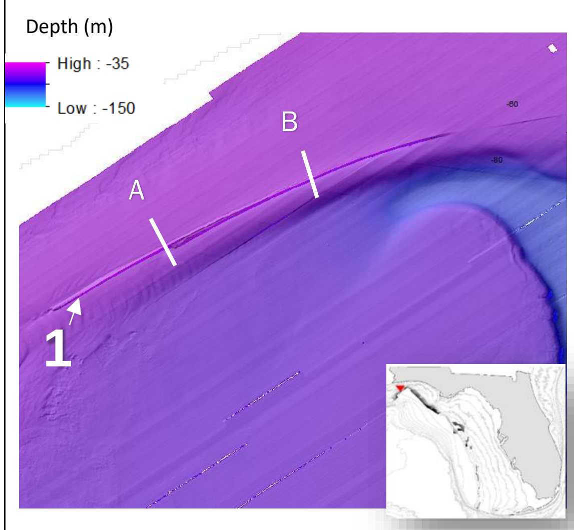

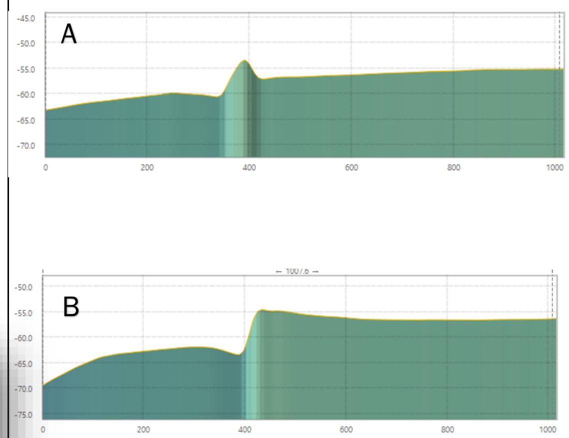

Pensacola Beach, FL

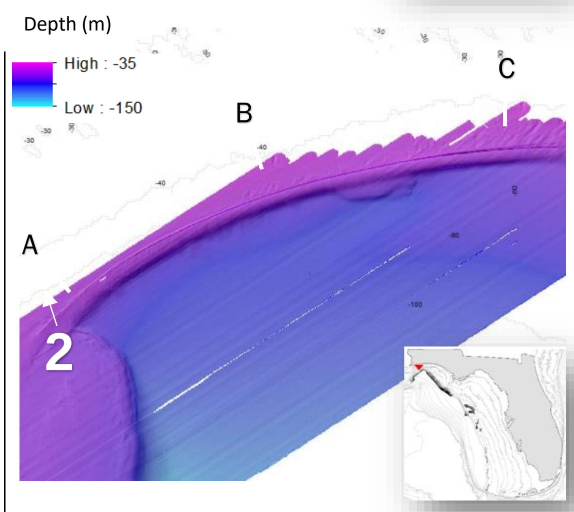

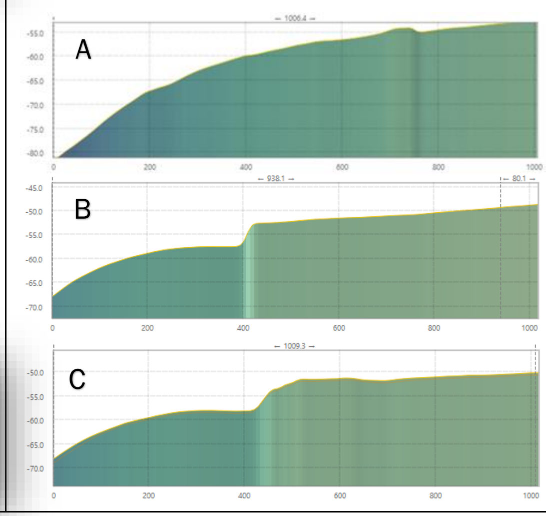

Destin to Panama City, FL

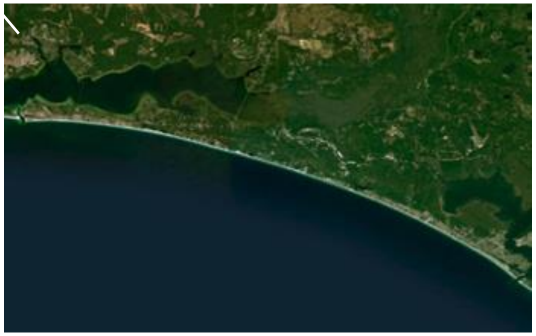

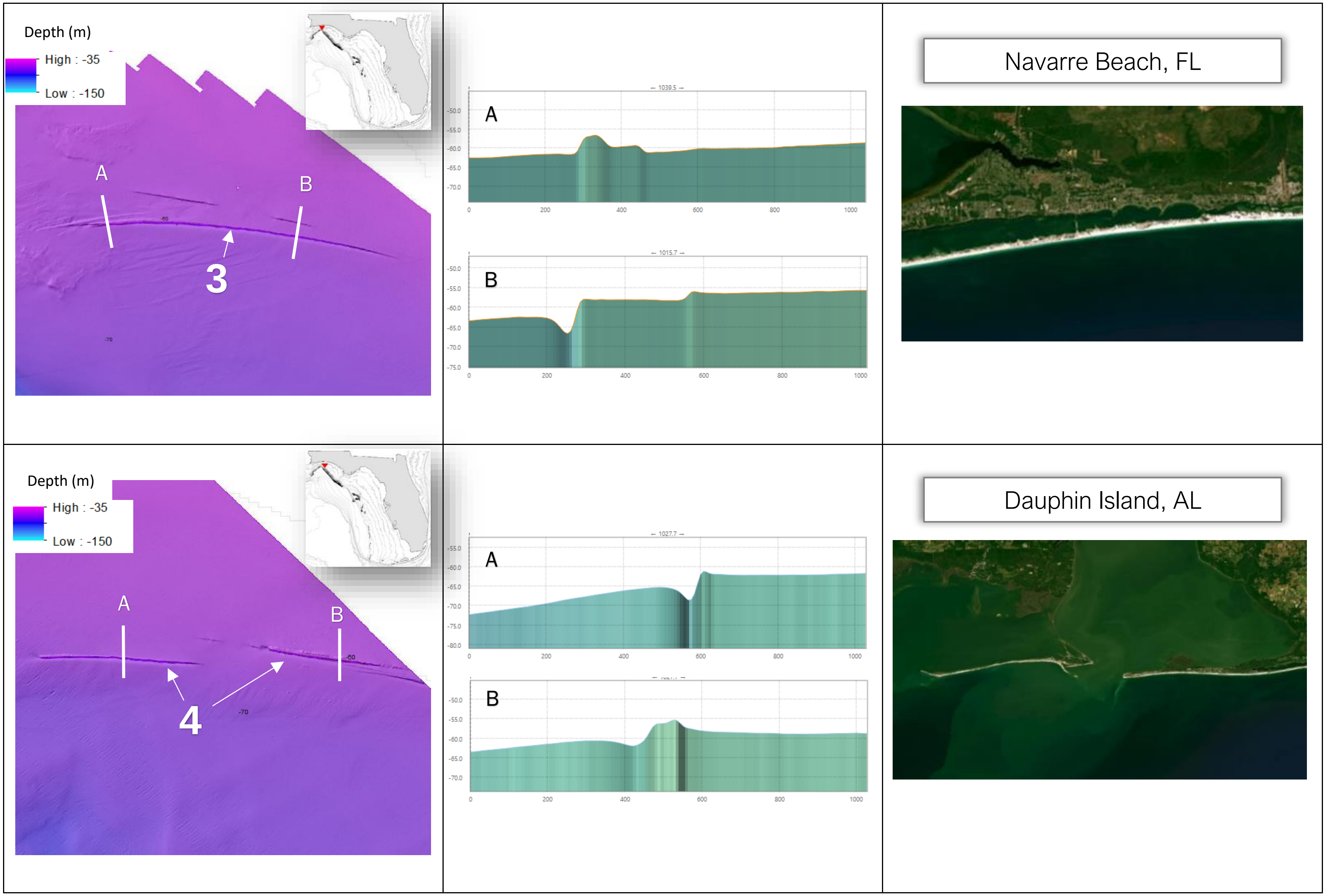
Depth (m)
High : -35
Low : -150
A
B
3
A
B
Navarre Beach, FL
Depth (m)
High : -35
Low : -150
A
B
4
A
B
Dauphin Island, AL

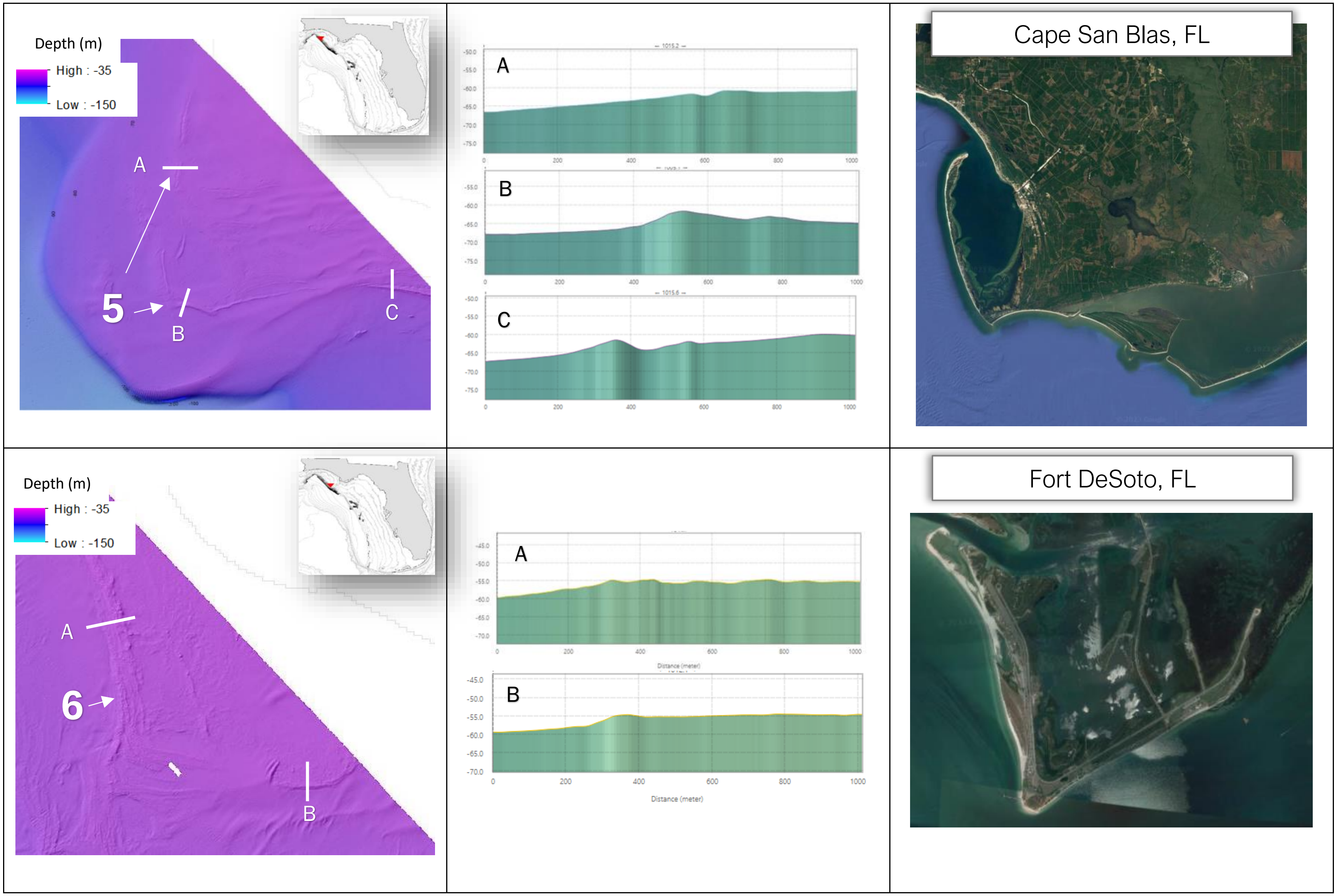
Depth (m)
High : -35
Low : -150
A
5
B
C
Cape San Blas, FL
Depth (m)
High : -35
Low : -150
A
6
B
Distance (meter)
Fort DeSoto, FL

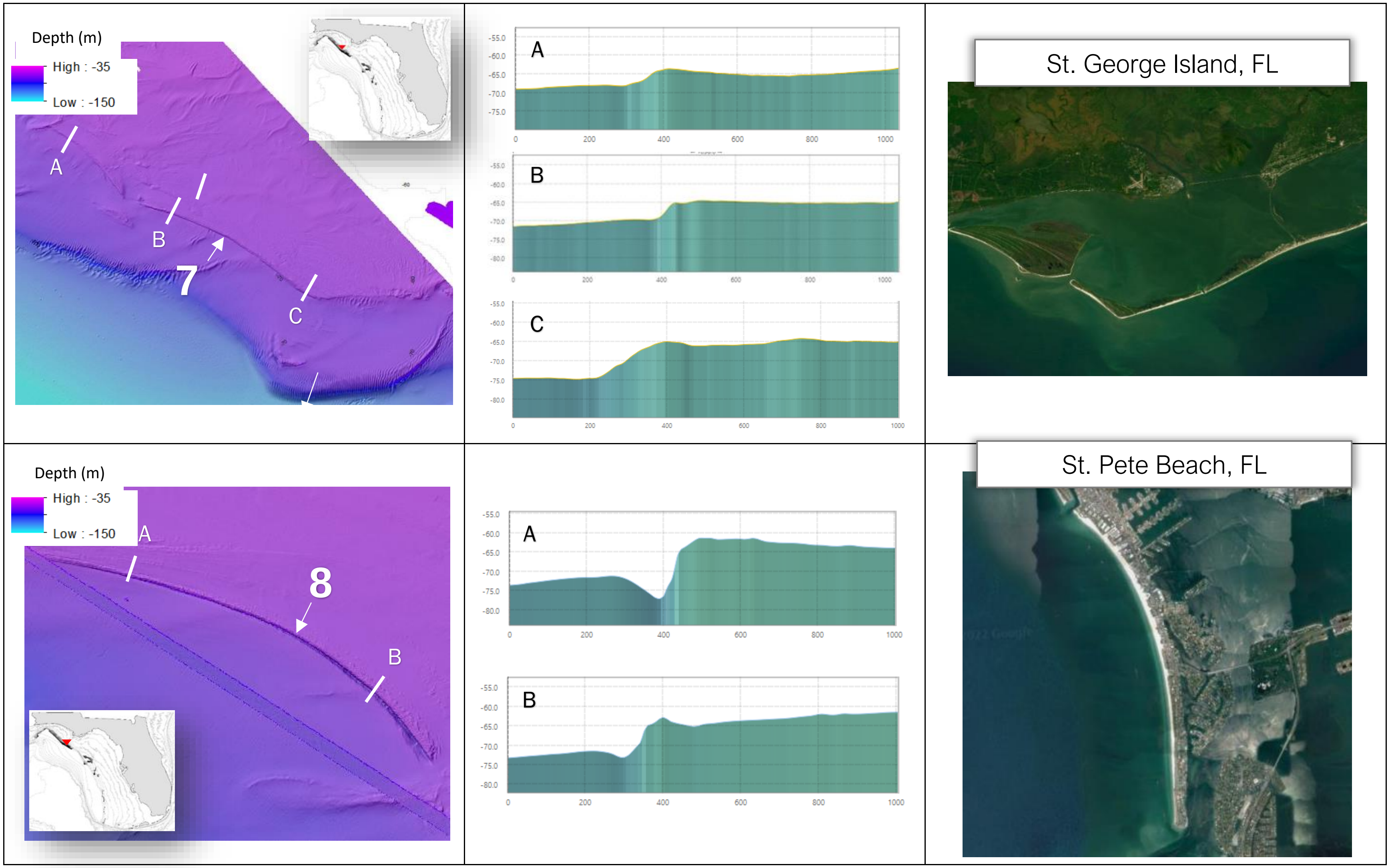
Depth (m)
High : -35
Low : -150
A
B
7
C
A
B
C
St. George Island, FL
Depth (m)
High : -35
Low : -150
A
8
B
A
B
St. Pete Beach, FL

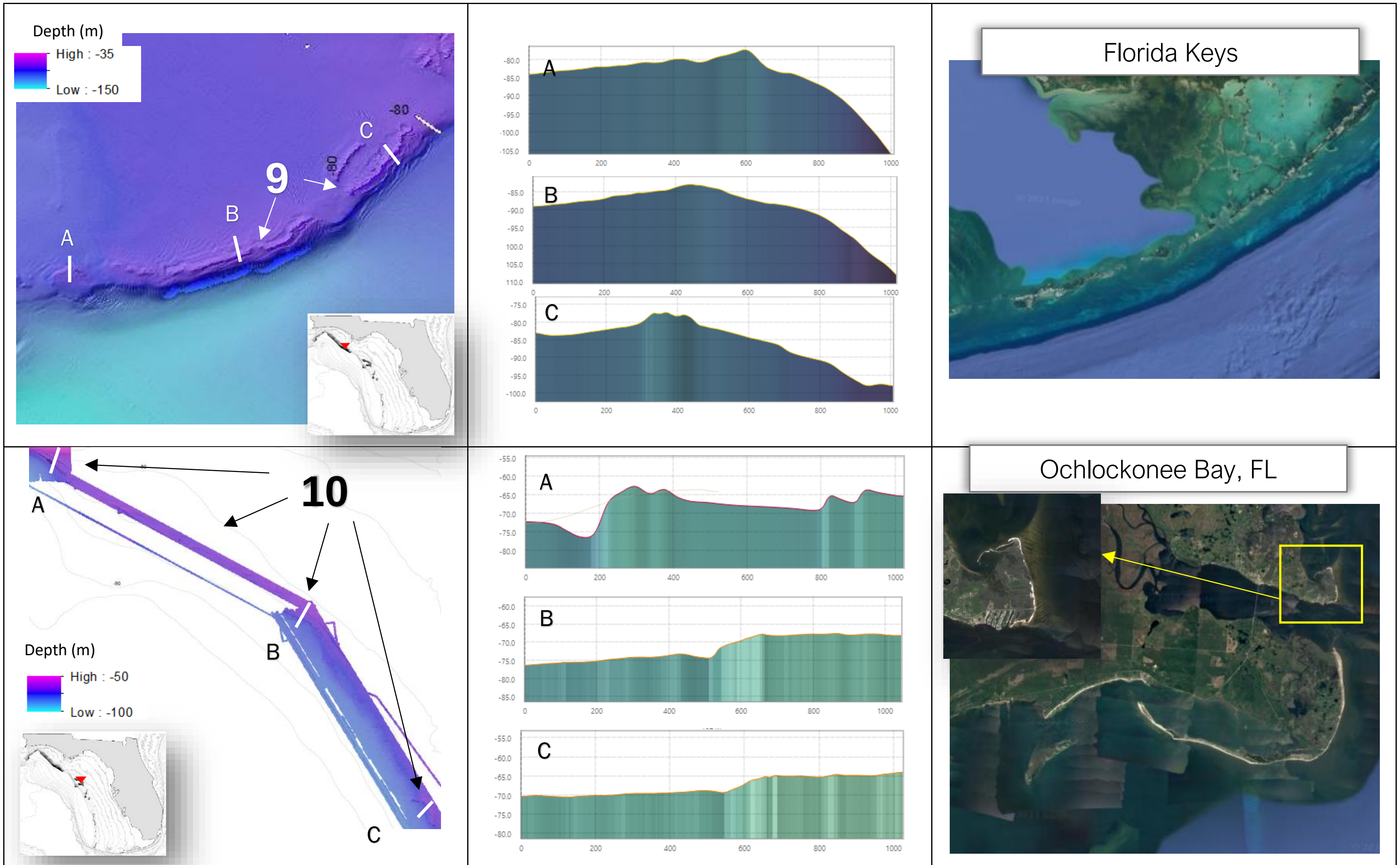
Depth (m)
High : -35
Low : -150
9
A
B
C
-80
Florida Keys
10
Depth (m)
High : -50
Low : -100
A
B
C
Ochlockonee Bay, FL

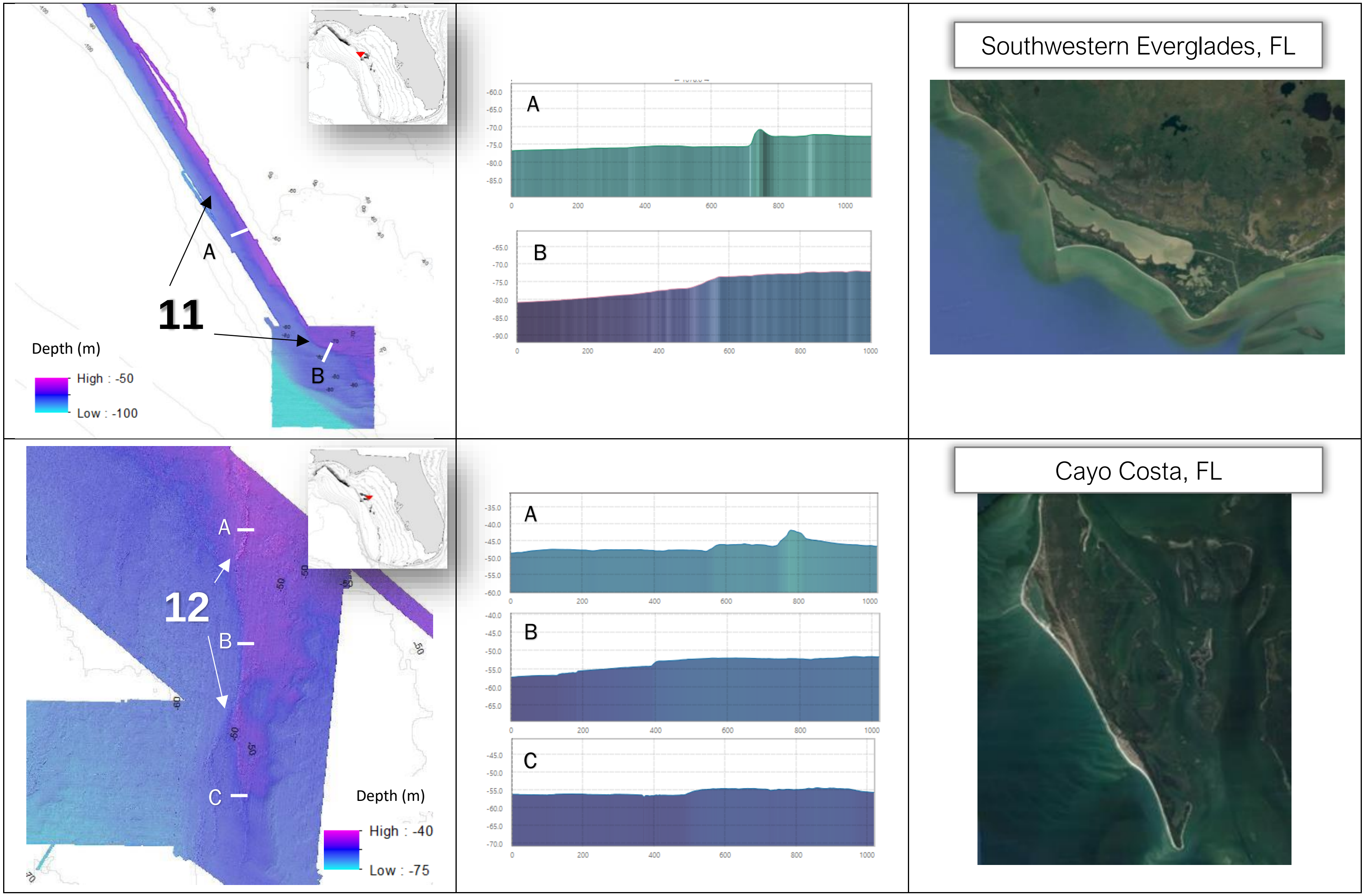
11
A
B
Depth (m)
High : -50
Low : -100
Southwestern Everglades, FL
12
A
B
C
Depth (m)
High : -40
Low : -75
Cayo Costa, FL

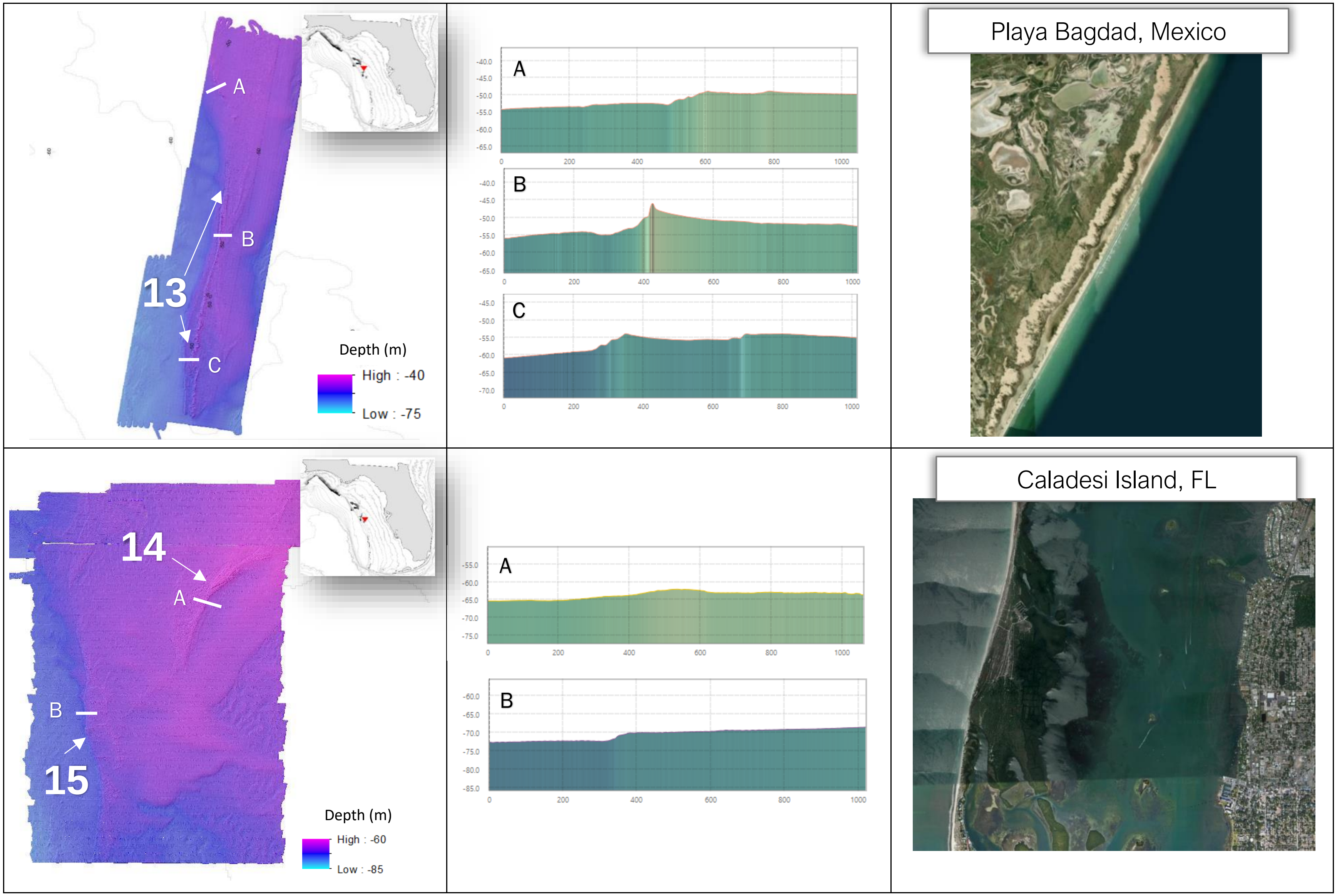
A
B
C
13
Depth (m)
High : -40
Low : -75
Playa Bagdad, Mexico
14
A
B
15
Depth (m)
High : -60
Low : -85
Caladesi Island, FL

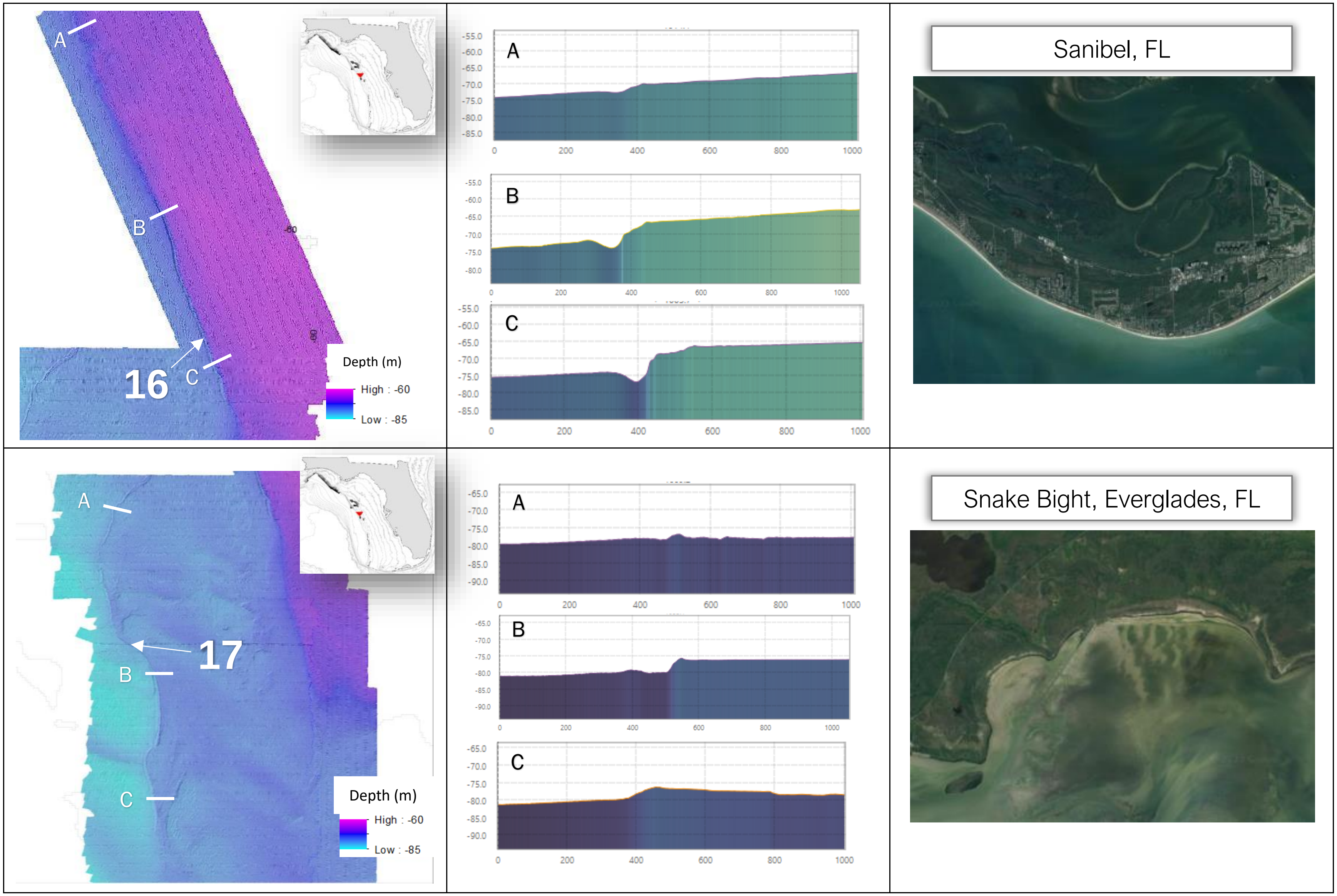
A
B
16
C
Depth (m)
High : -60
Low : -85
Sanibel, FL
A
17
B
C
Depth (m)
High : -60
Low : -85
Snake Bight, Everglades, FL

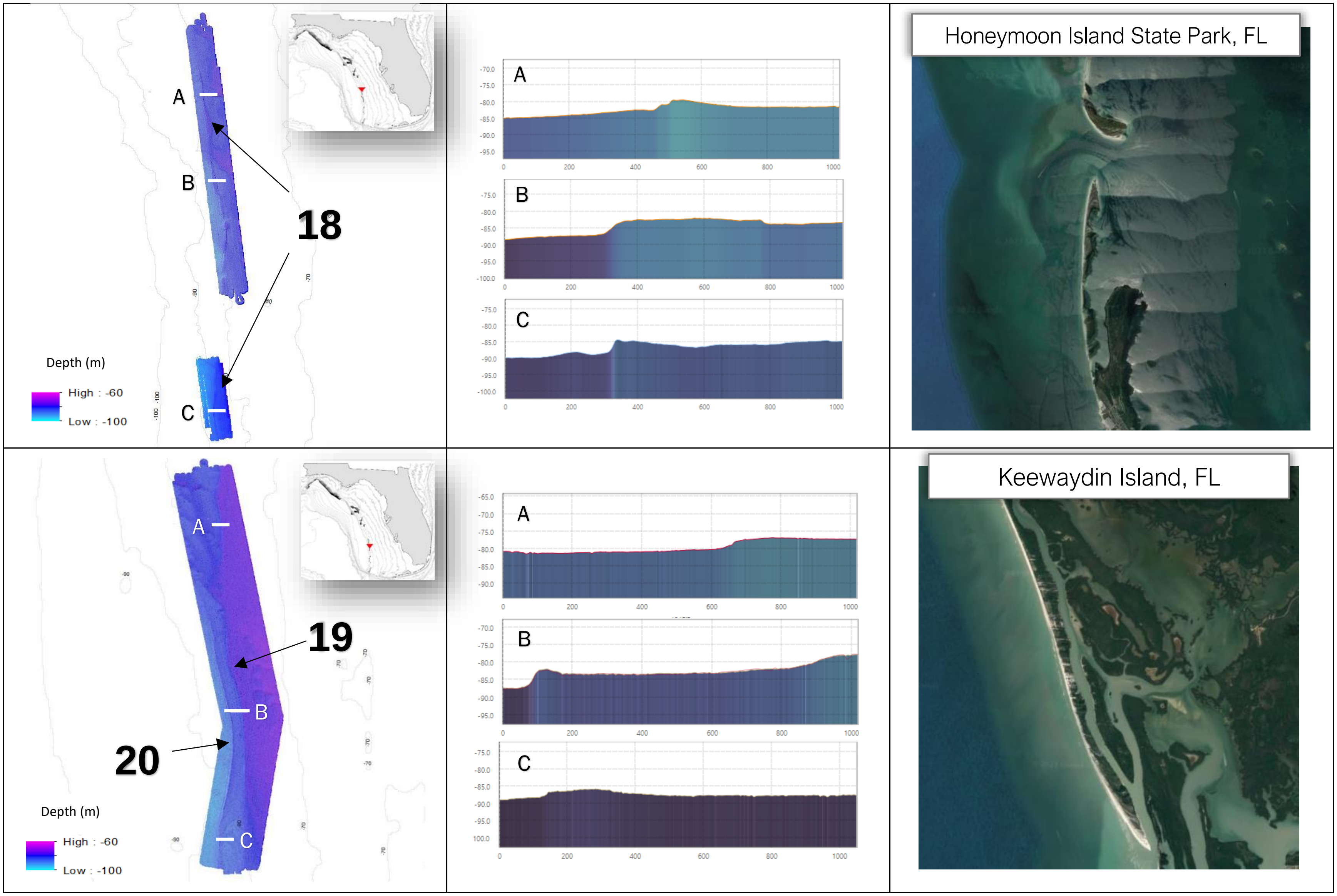
A
B
18
Depth (m)
High : -60
Low : -100
C
Honeymoon Island State Park, FL
A
19
B
20
Depth (m)
High : -60
Low : -100
C
Keewaydin Island, FL

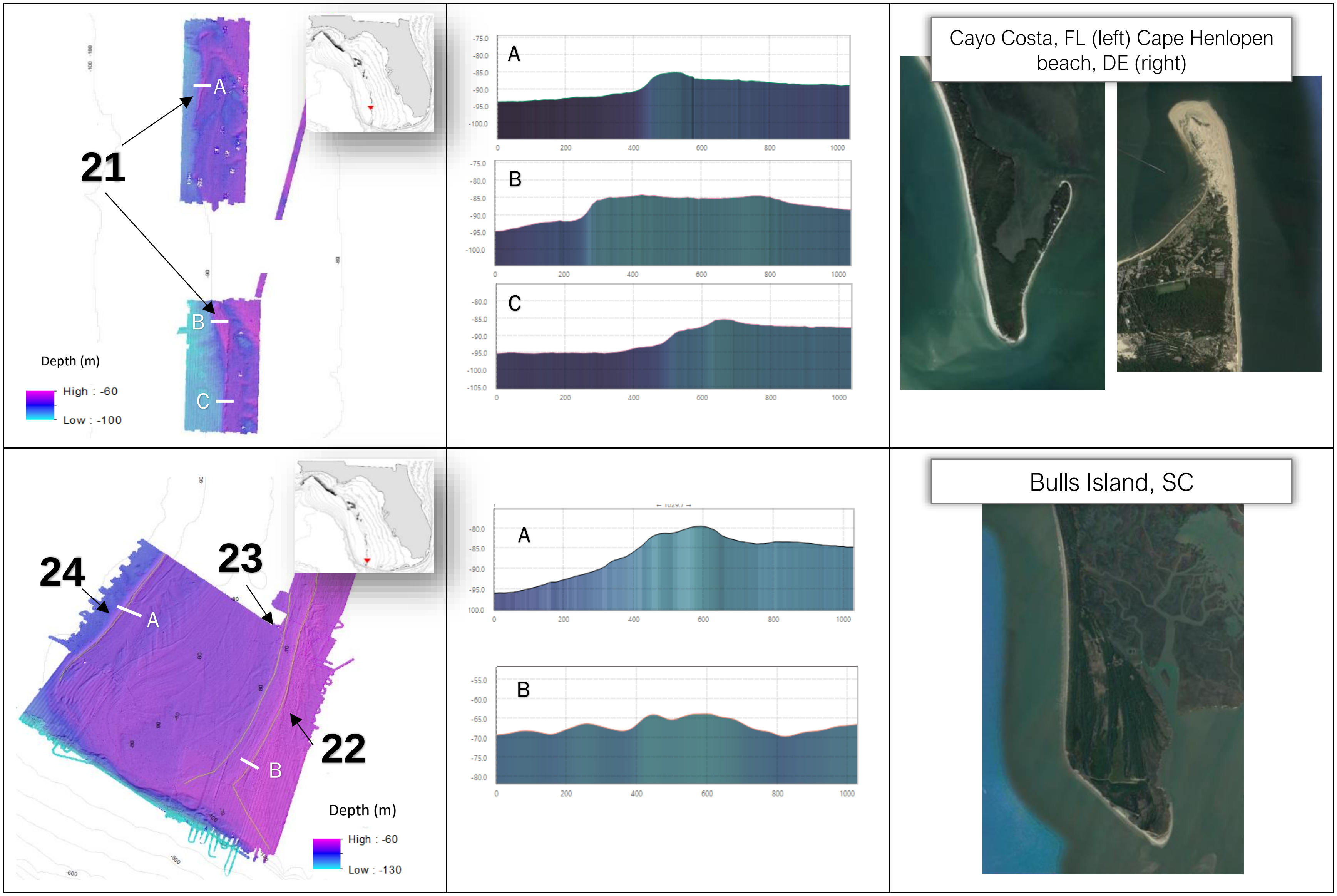
21
A
B
C
Depth (m)
High : -60
Low : -100
Cayo Costa, FL (left) Cape Henlopen beach, DE (right)
24
23
22
A
B
Depth (m)
High : -60
Low : -130
Bulls Island, SC

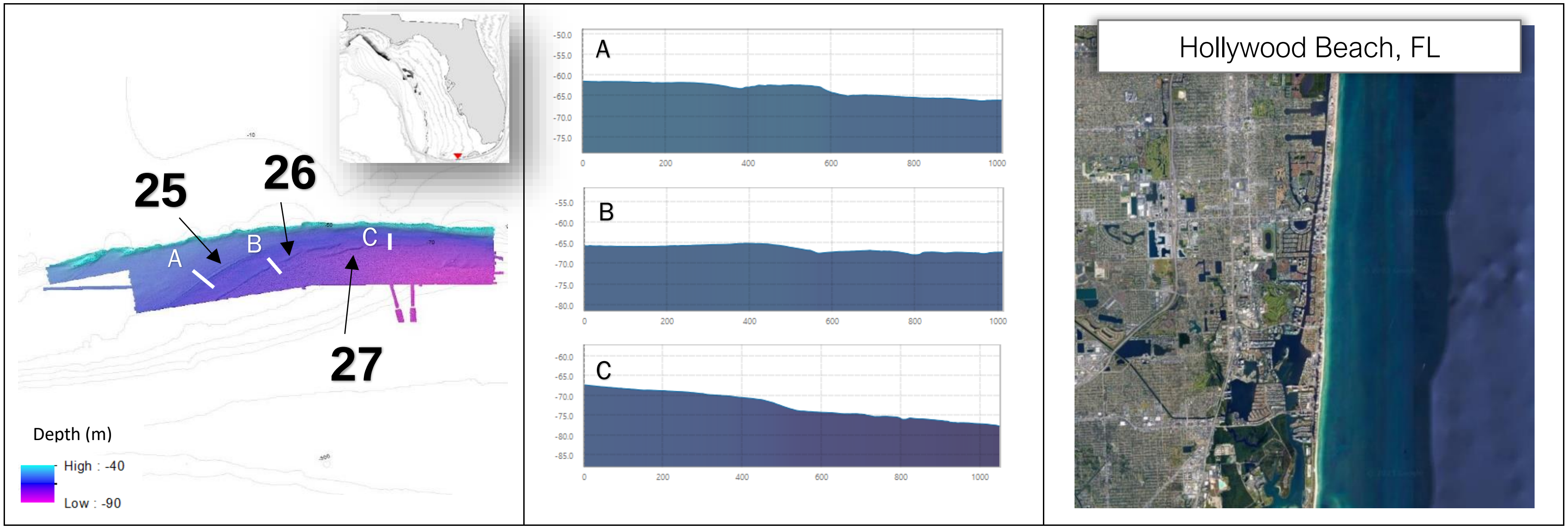
25
26
27
A
B
C
Depth (m)
High : -40
Low : -90
A
B
C
Hollywood Beach, FL

Appendix 4 – Shoreline Axial Profiles

Shorelines 1 - 3

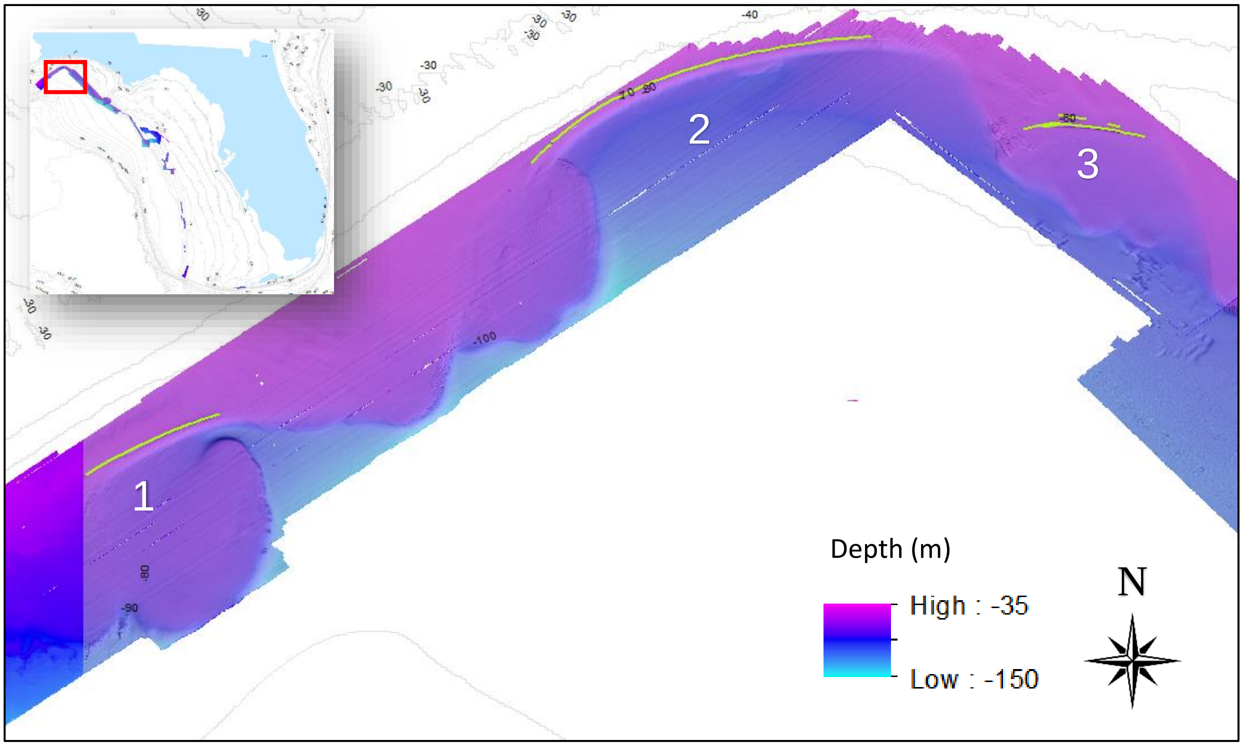

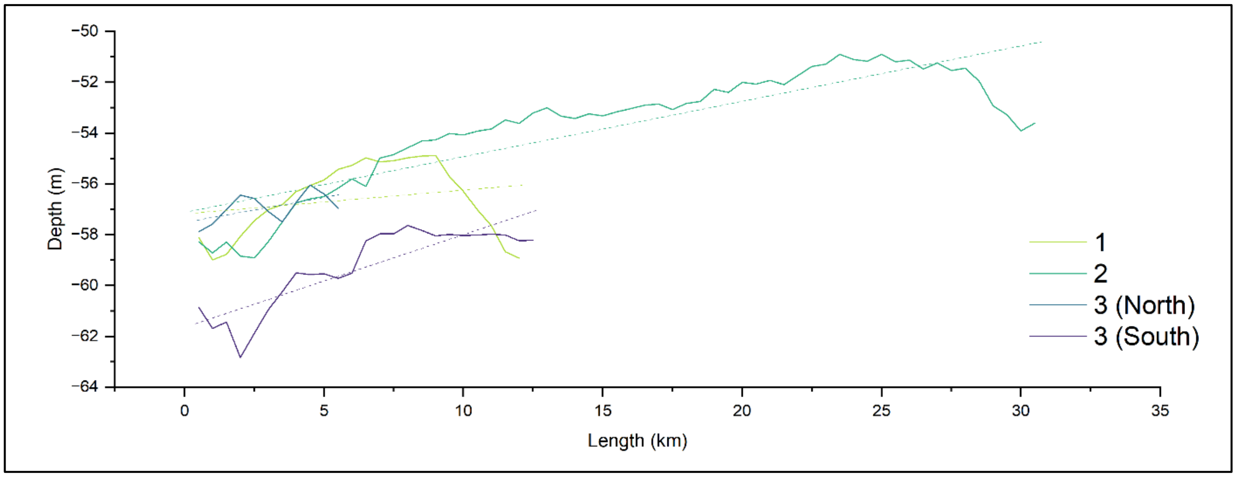

Note: Lime green lines on map view indicate locations of shorelines. Profile colors represent individual shorelines and have no scientific significance.

Shoreline 4, 6, 7

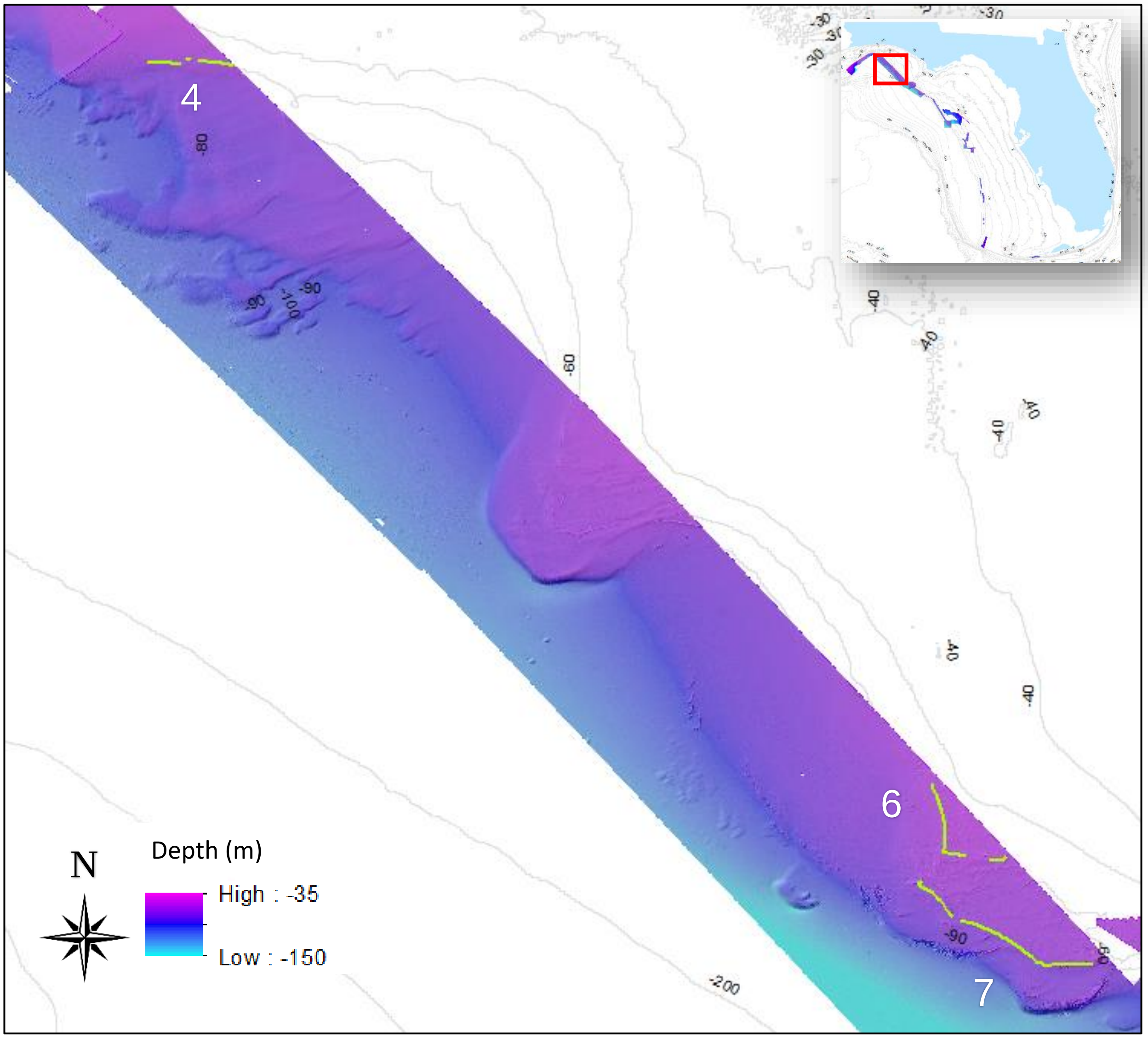

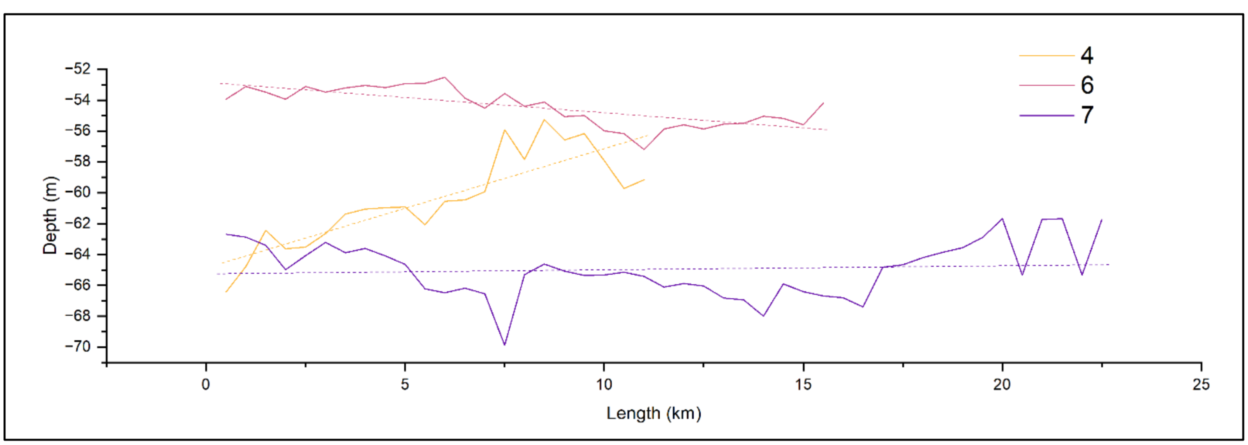

Shoreline 5

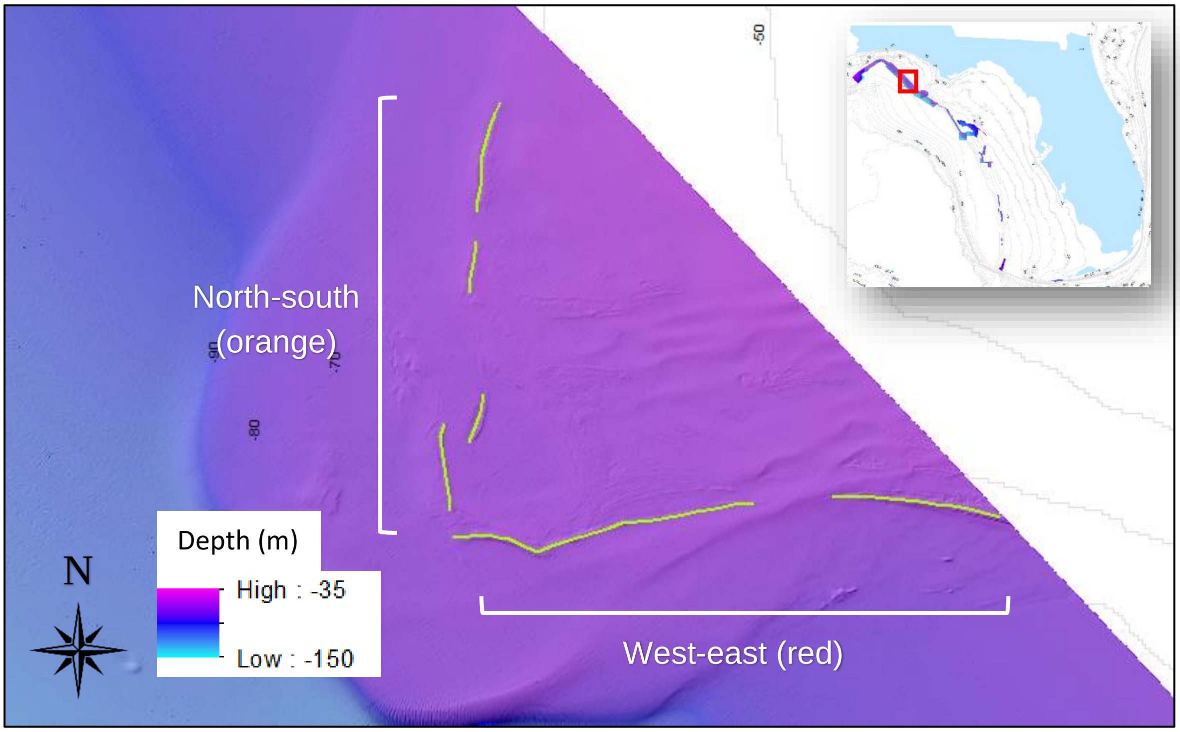

North-south (orange)
West-east (red)
Depth (m)
High : -35
Low : -150
N
-50
-70
-80

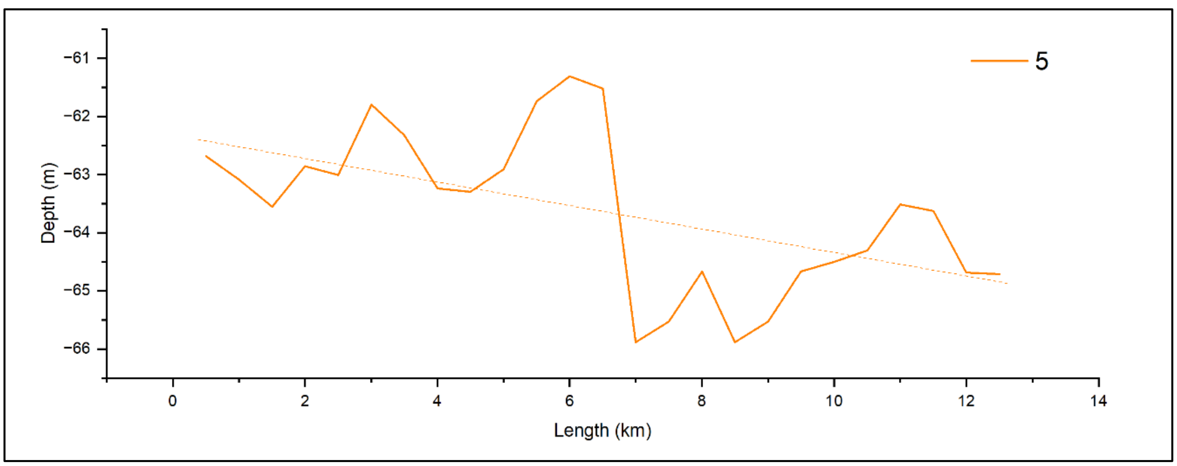

5
Depth (m)
Length (km)
-61
-62
-63
-64
-65
-66
0
2
4
6
8
10
12
14

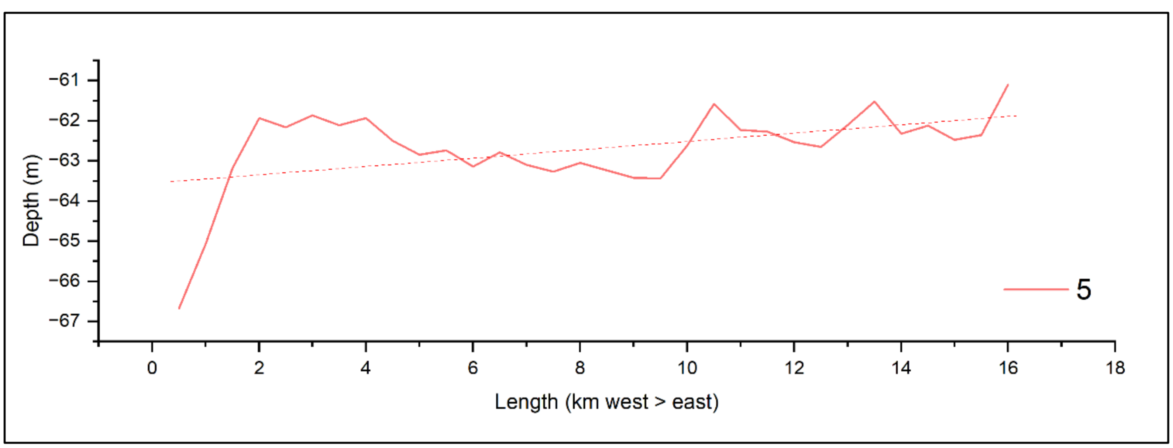

5
Depth (m)
Length (km west > east)
-61
-62
-63
-64
-65
-66
-67
0
2
4
6
8
10
12
14
16
18

Shorelines 8 and 9

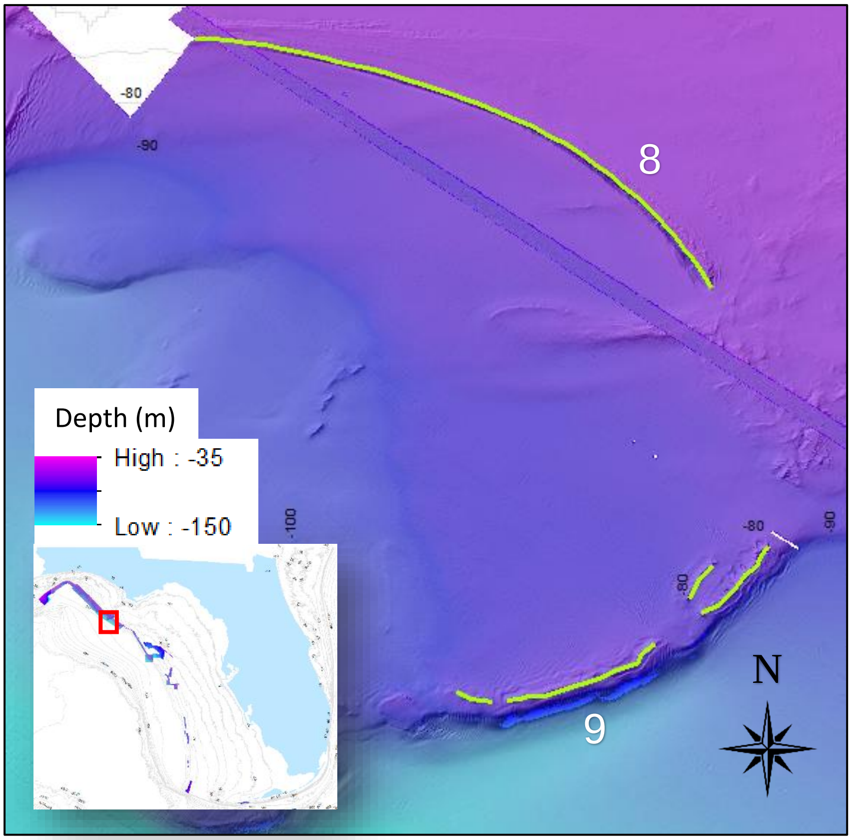

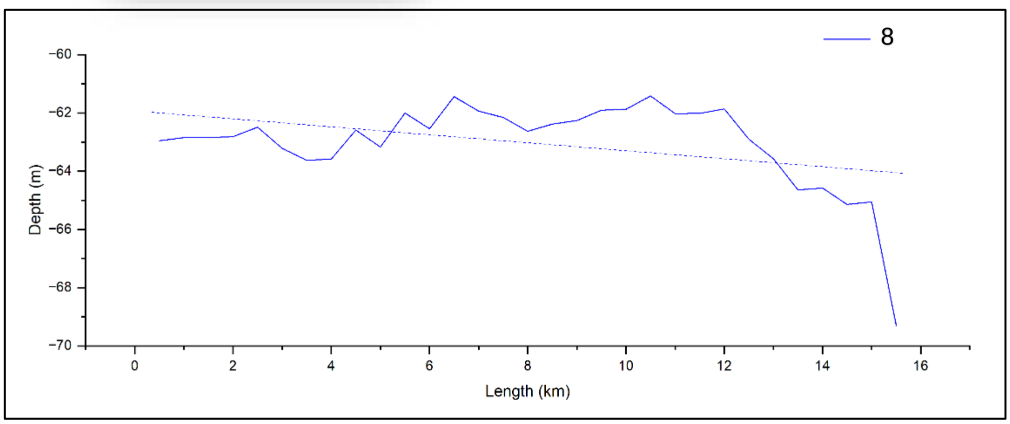

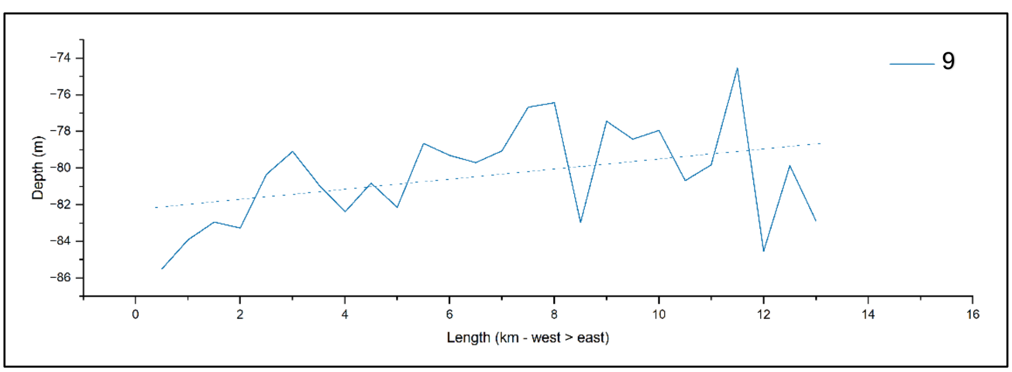

Shorelines 10 and 11

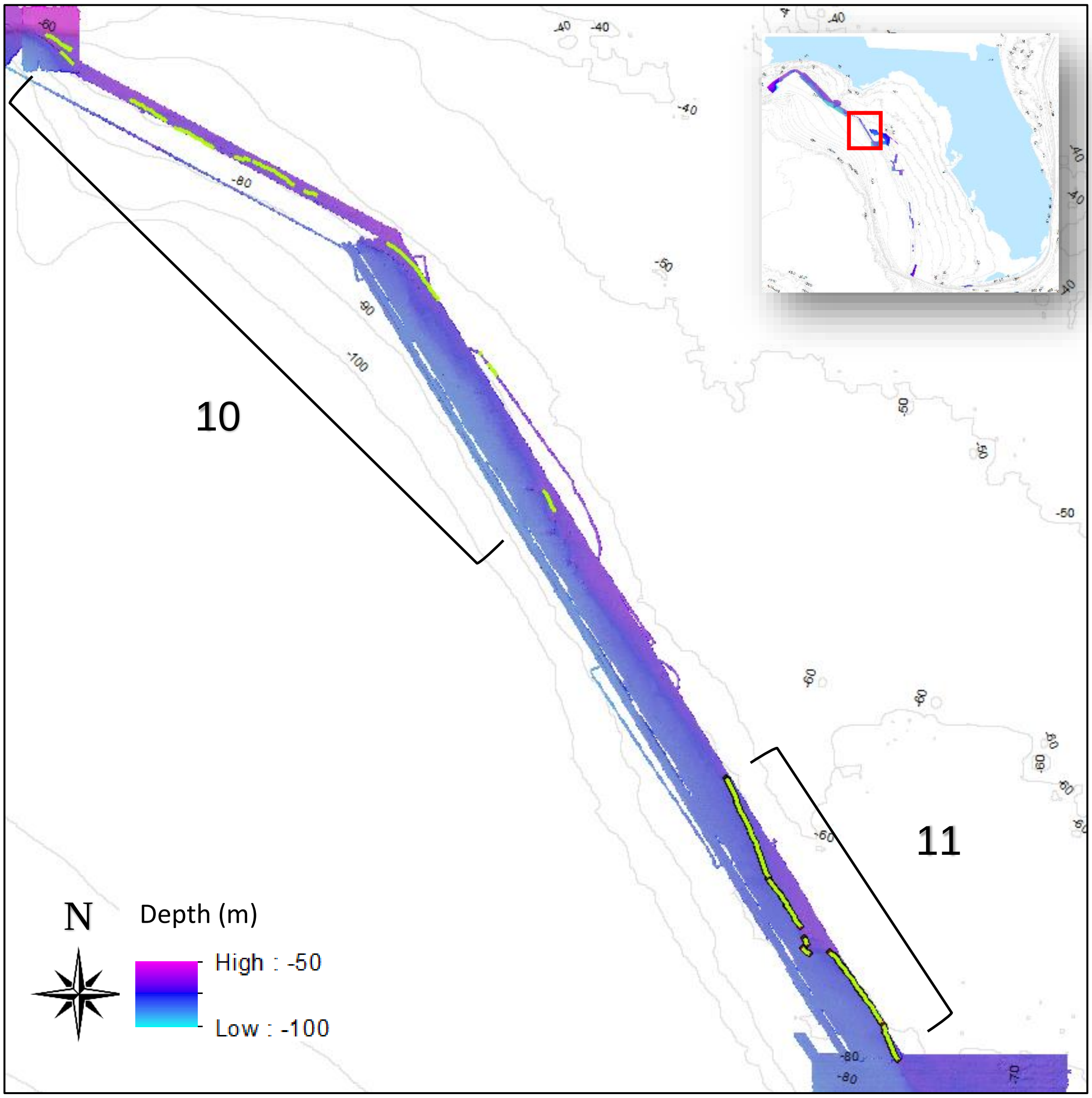

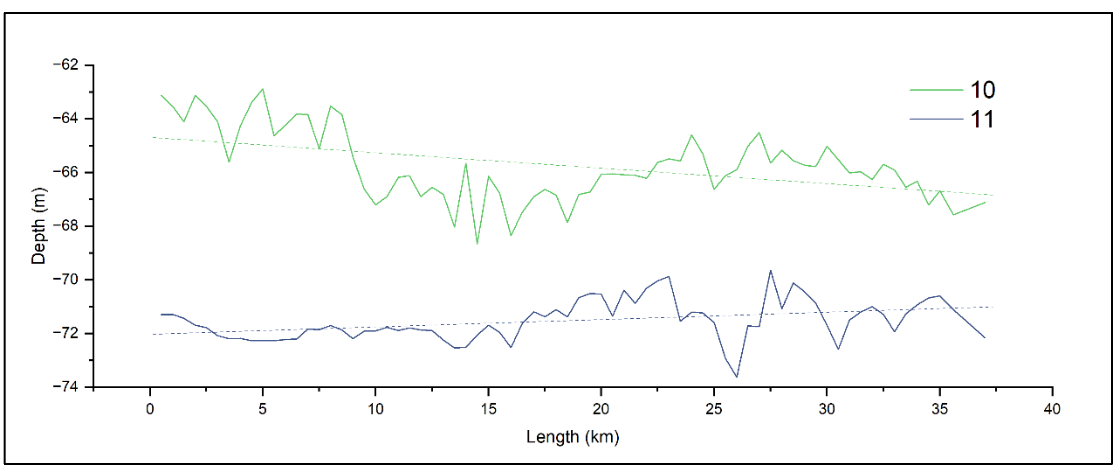

Shorelines 12 and 13

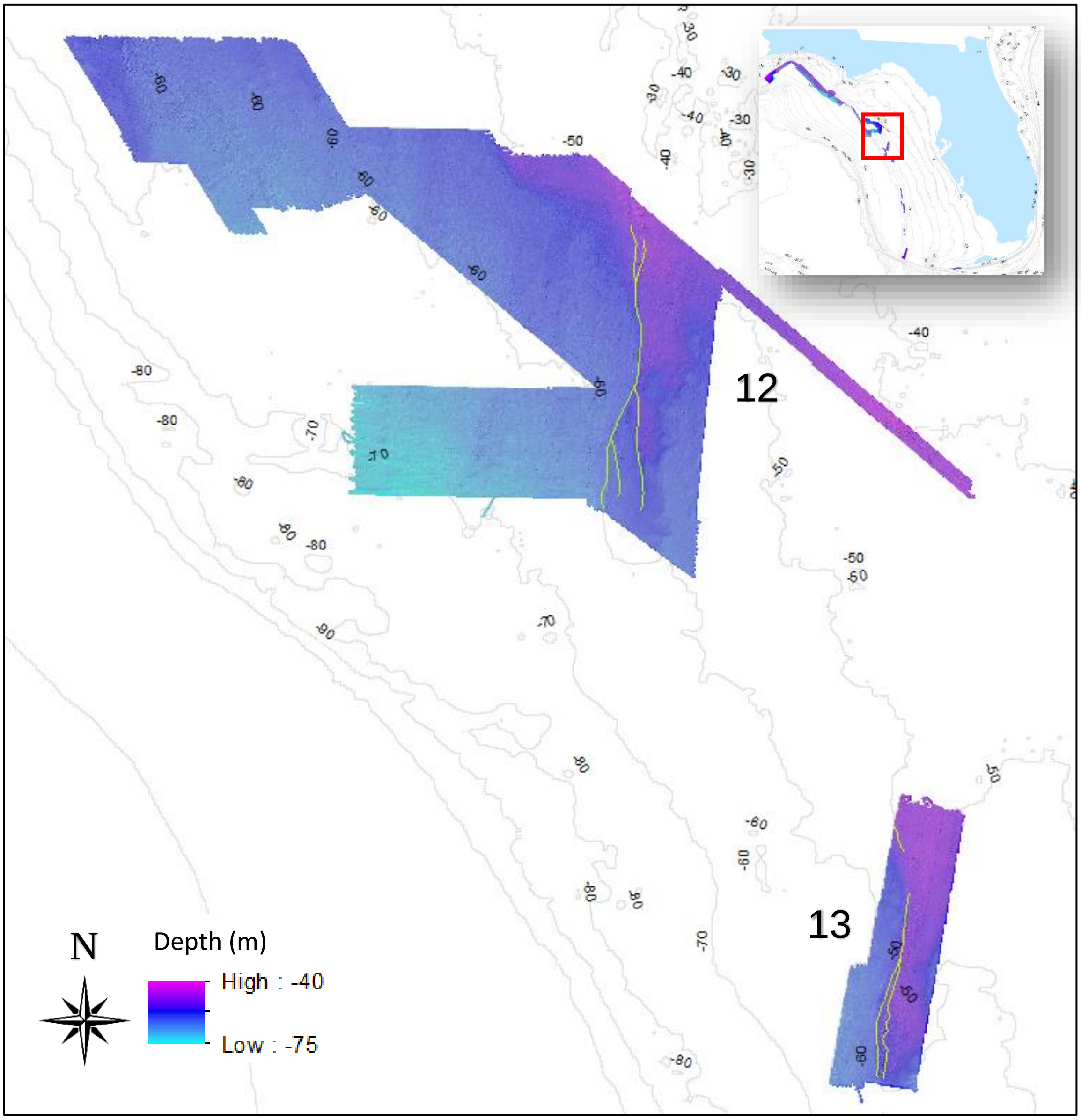

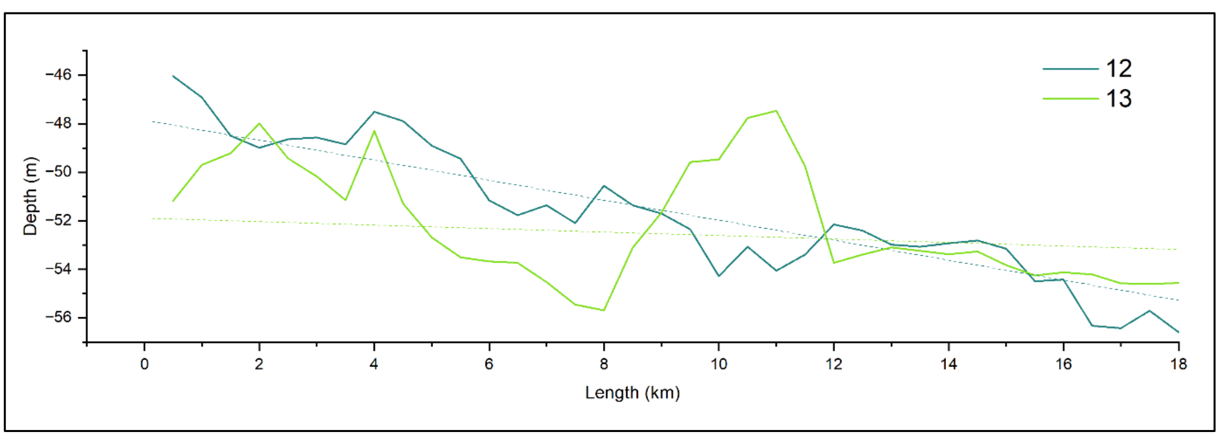

Shorelines 14 - 17

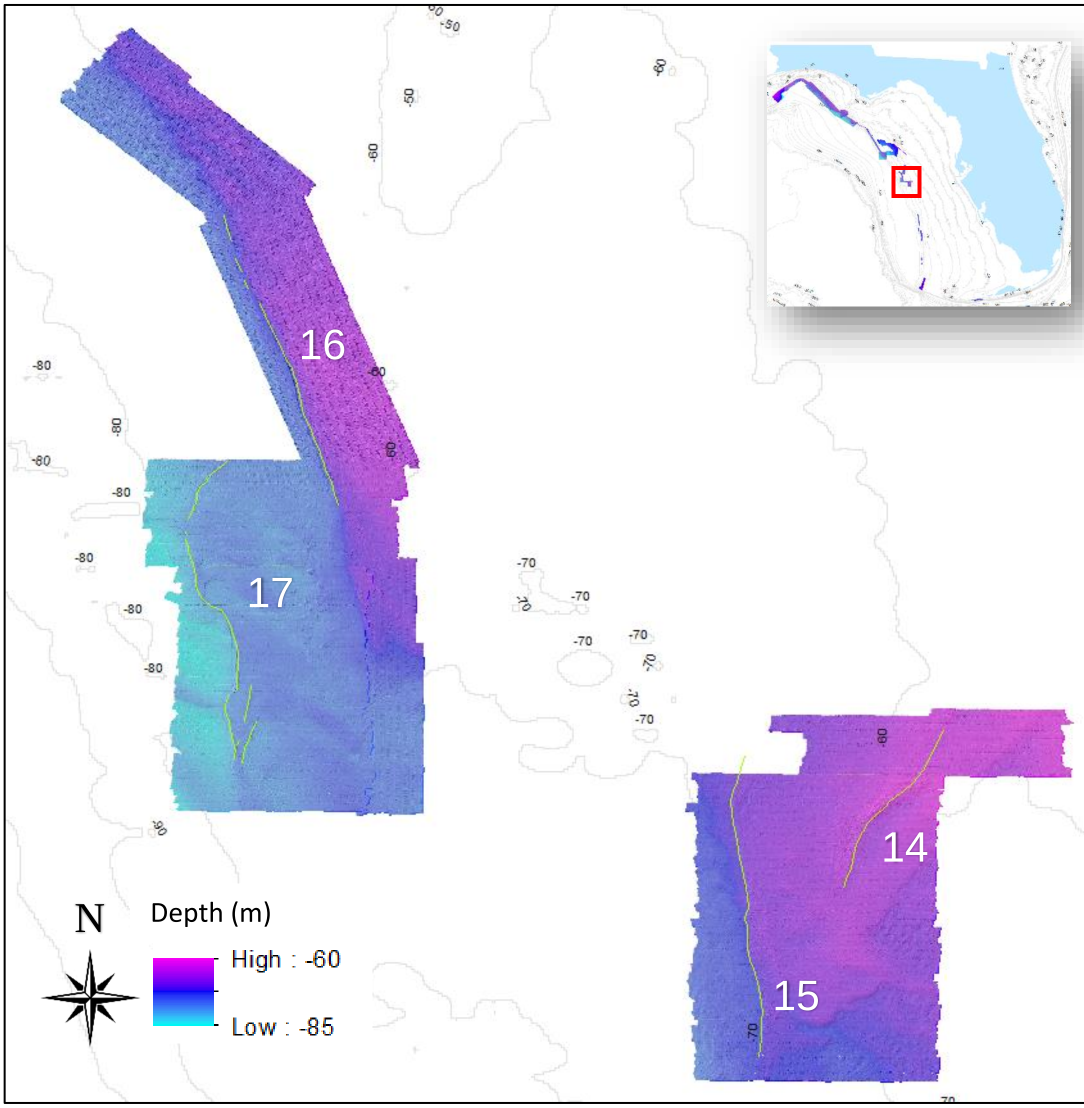

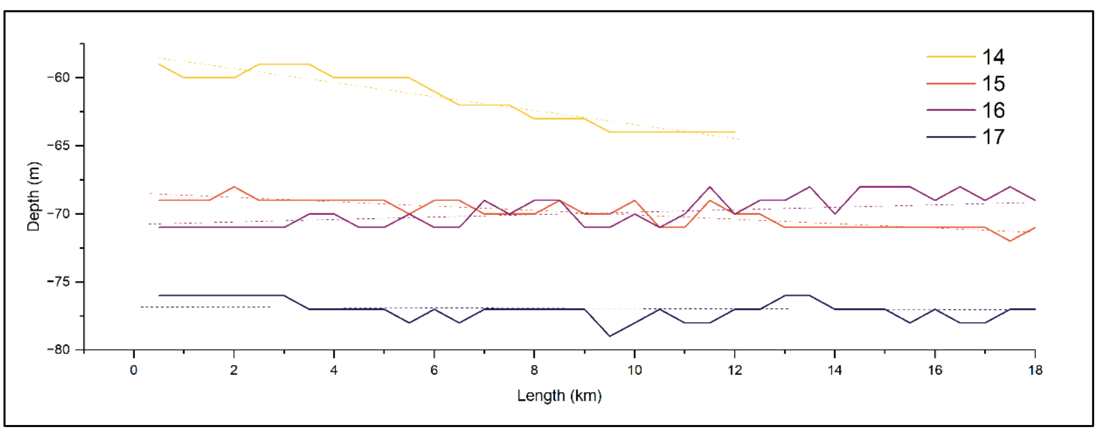

Shorelines 18 - 21

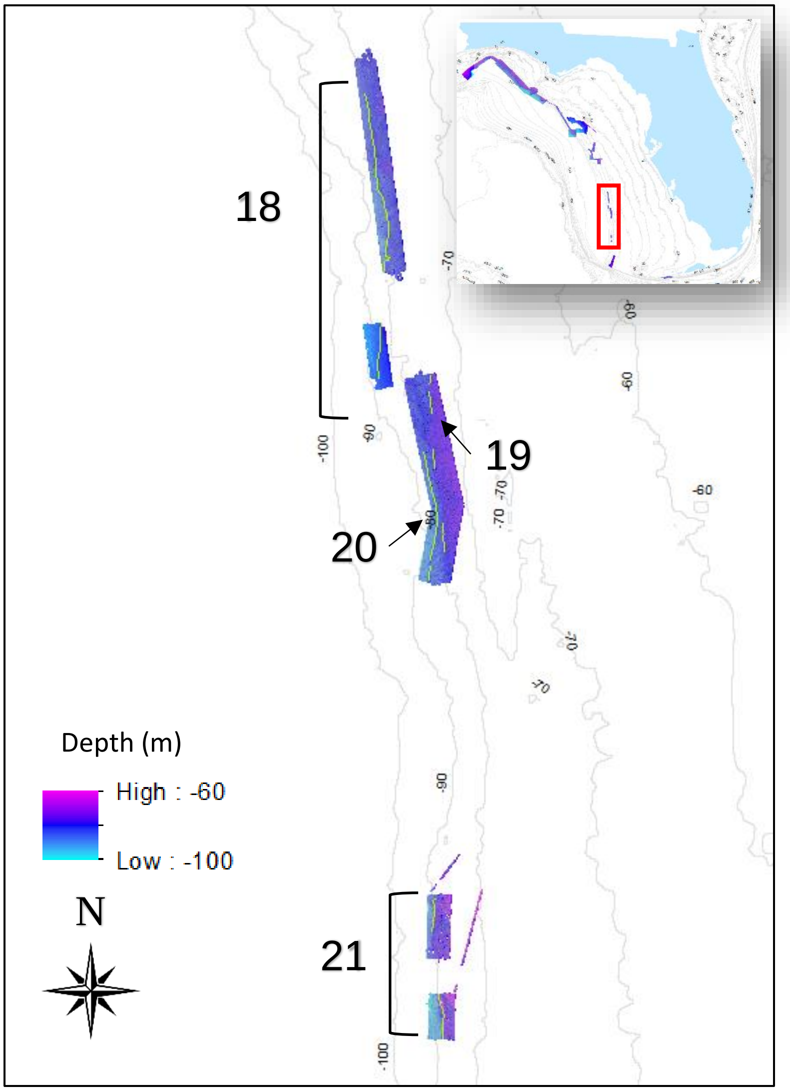

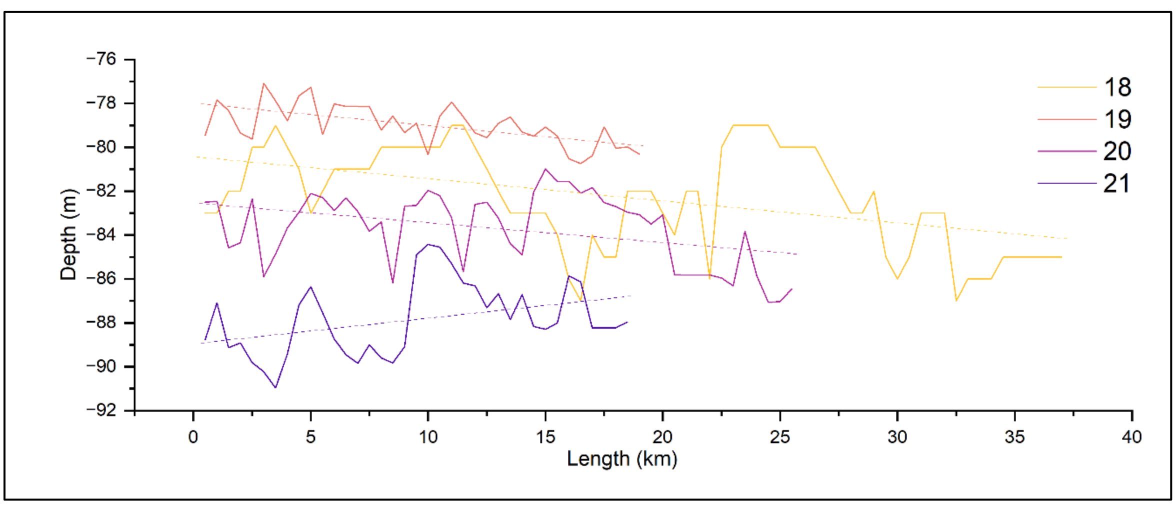

Shorelines 22 - 24

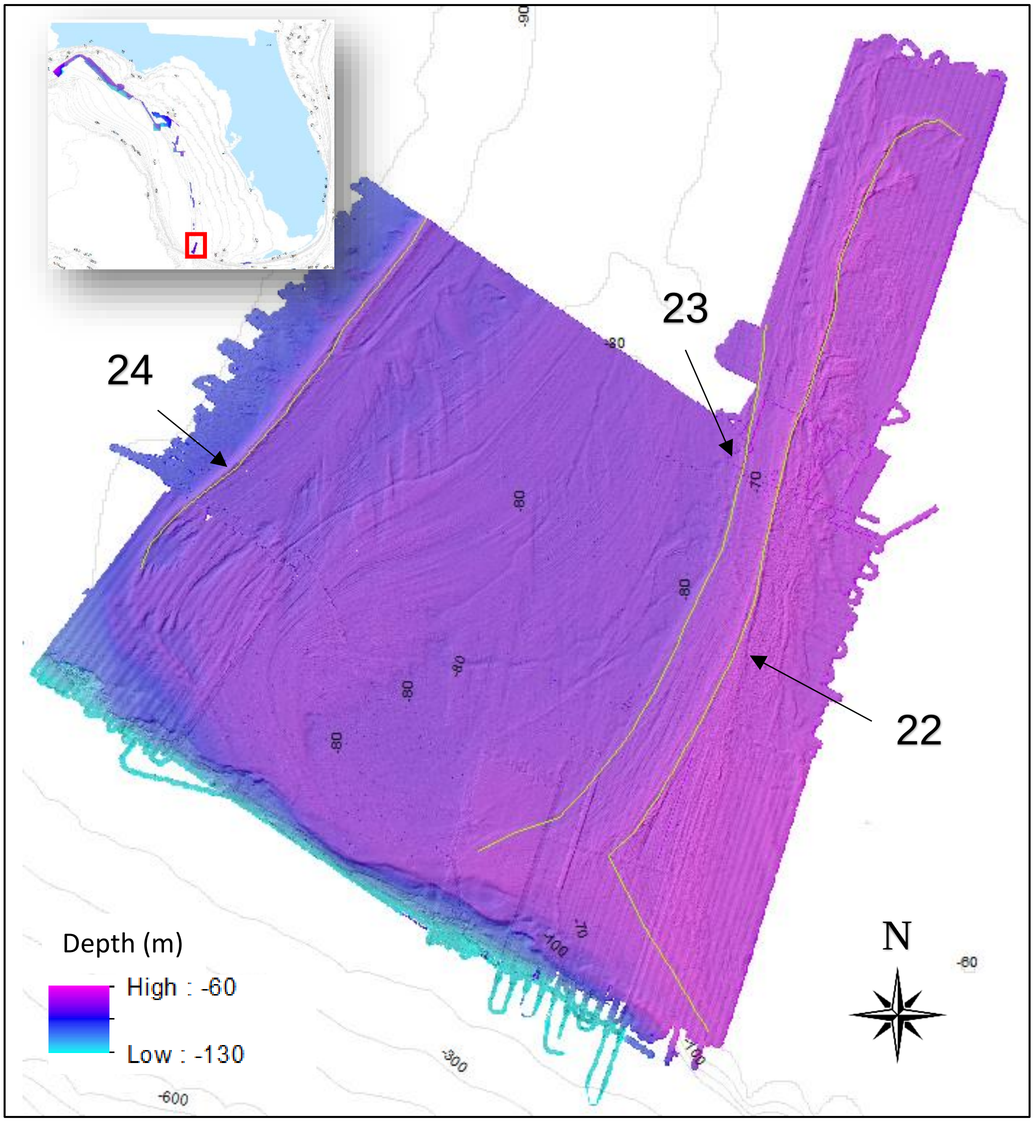

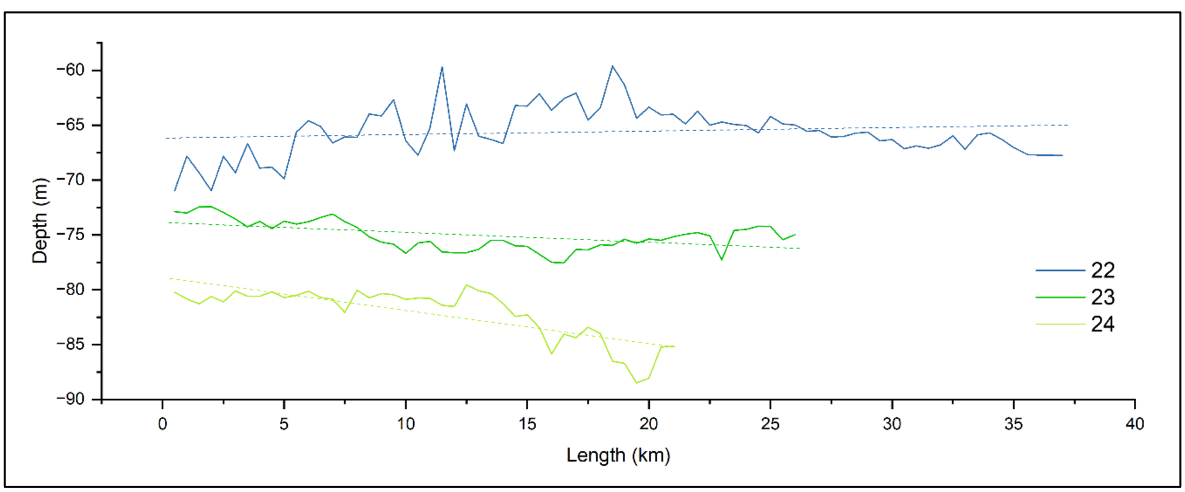

Shorelines 25 - 27